AN EVALUATION OF THE PERFORMANCE OF PROTOTYPE INSTRUMENTED SOIL COVERS AT THE REGINA MUNICIPAL LANDFILL

A Thesis Submitted to the College of

Graduate Studies and Research

In Partial Fulfillment of the Requirements

For the Degree of Masters of Science

In the Department of Civil Engineering

University of Saskatchewan

Saskatoon

By

Randi Lynn Strunk

Permission to Use

In presenting this thesis in partial fulfilment of the requirements for a Postgraduate degree from the University of Saskatchewan, I agree that the Libraries of this University may make it freely available for inspection. I further agree that permission for copying of this thesis in any manner, in whole or in part, for scholarly purposes may be granted by the professor or professors who supervised my thesis work or, in their absence, by the Head of the Department or the Dean of the College in which my thesis work was done. It is understood that any copying or publication or use of this thesis or parts thereof for financial gain shall not be allowed without my written permission. It is also understood that due recognition shall be given to me and to the University of Saskatchewan in any scholarly use which may be made of any material in my thesis.

Requests for permission to copy or to make other use of material in this thesis in whole or part should be addressed to:

Head of the Department of Civil Engineering
University of Saskatchewan
Saskatoon, Saskatchewan (S7N 0W0)

ABSTRACT

The City of Regina Fleet Street landfill, north-east of Regina, Saskatchewan, is approaching its maximum capacity after a 47-year operating life and plans are now being made for its closure. As part of closure planning work, four test plots encompassing two different cover designs (a capillary break cover and a store-and-release cover) were constructed on the landfill in the summer of 2004. One cover of each design was constructed on both the north facing and the south facing slopes.

The overall objective of this thesis is to evaluate the preliminary performance of the four test plots on the City of Regina landfill with regards to net percolation, gas flux, water balance and vegetation. To meet this overall objective three specific objectives were developed as follows:

- Evaluate the performance and integrity of the monitoring scheme.
- Characterize the properties of the soil covers on the four test plots.
- Develop a preliminary water balance using the monitoring field data.

A field instrumentation program was carried out which included detailed monitoring of gas composition, volumetric water content, matric suction and temperature within the cover profile as well as measurements of interflow, runoff and site-specific meteorology. Generally, the instrumentation performed well with the exception of the tipping bucket which did not accurately measure precipitation.

Evaluation of the covers revealed that the slope aspect exerts greater influence over the water balance than that exerted by cover design itself. The south test plots were drier than the north, experienced more net radiation, and generally had more abundant vegetation. A water balance was conducted for each test plot at the upper, mid and lower slope. It is clear that a capillary break was not maintained on the north slope for the entire monitoring period and the percolation from the store-and-release cover was less than that of the capillary break cover. The south test plots were very dry and net percolation was nearly the same for both test plots. Therefore, it is believed that the store-and-release covers are performing better than the capillary break covers.

ACKNOWLEDGMENTS

I'd like to express my gratitude to my supervisor, Dr. Lee Barbour. Your vast knowledge of the subject matter has been invaluable to me, as has your willingness to share your wisdom and enthusiasm. Your patience through my various degrees of focus is greatly appreciated.

The completion of this thesis would not have been possible without funding and support from NSERC, O'Kane Consultants, Golder Associates, NRC and the City of Regina. Thanks in particular O'Kane Consultants for allowing me to blur the line between work and school. Appreciation is also extended to my co-supervisor Dr. Ian Fleming, as well as my advisory committee members, Dr. Jitendra Sharma, Dr. David Hubble and Dr. Kerry Mazurek. My thanks to Alex Kozlow for his technical support in the lab, as well as for providing the perfect mixture of reassurance and motivation when discussing my thesis.

I owe a special thanks to Heather Rodger, Dana Fenske, Adam Meier and Sophie Kessler. Your assistance with various aspects of my thesis not only made my work easier, but more enjoyable as well.

Finally, I would like to thank my family for their encouragement and support. I appreciate all attempts to try and understand what I was doing even if it meant discussing garbage dumps and dirt. In particular I would like to thank my husband Chris for his understanding and patience throughout this process.

TABLE OF CONTENTS

LIST OF TABLES

LIST OF FIGURES

CHAPTER 1
INTRODUCTION

The Fleet Street landfill in Regina, SK is approaching capacity. A closure study conducted in 1993 (Reid Crowther & Partners Ltd, 1993) recommended a multi-layered barrier cover for final decommissioning of the landfill mound. In 2003, a second study was initiated to investigate alternative capping options for the Fleet Street landfill (GAL and OKC, 2005b). As a result of this second study, test covers were proposed to assess the performance of different cover alternatives in different areas of the landfill. This thesis focuses on the characterization of these test soil covers along with a preliminary interpretation of the water balance associated with each prototype cover.

The purpose of a landfill cover is to reduce the risk posed by the landfill to human health and the environment to acceptable levels. The principal functions of a landfill final cover in order to achieve this reduction of risk may include the following (Othman et al., 1995):

- Minimize water infiltration into the landfill;
- Minimize gas migration out of the landfill;
- Control odors, blowing waste and other nuisances; and
- Allow the area to be used for other applications.

Guidelines in Saskatchewan pertaining to landfill cover systems are limited. Saskatchewan Environment, the governing body, has draft guidelines that require a range of monitoring from no monitoring for low risk sites to a monitoring program designed by an engineer for high risk sites (SERM, 1988). The final responsibility for the landfill and any pollution resulting from it are the responsibility of the owner.

1.1. General Site Background

The Fleet Street landfill is a municipal solid waste (MSW) landfill located northeast of the City of Regina (COR) along Fleet Street, north of Highway No. 46, in the west half of Section 3 of TP18, Rng 19, W2M (Figure 1). The landfill occupies approximately 60 hectares and rises to approximately 35 m above the surrounding ground surface.

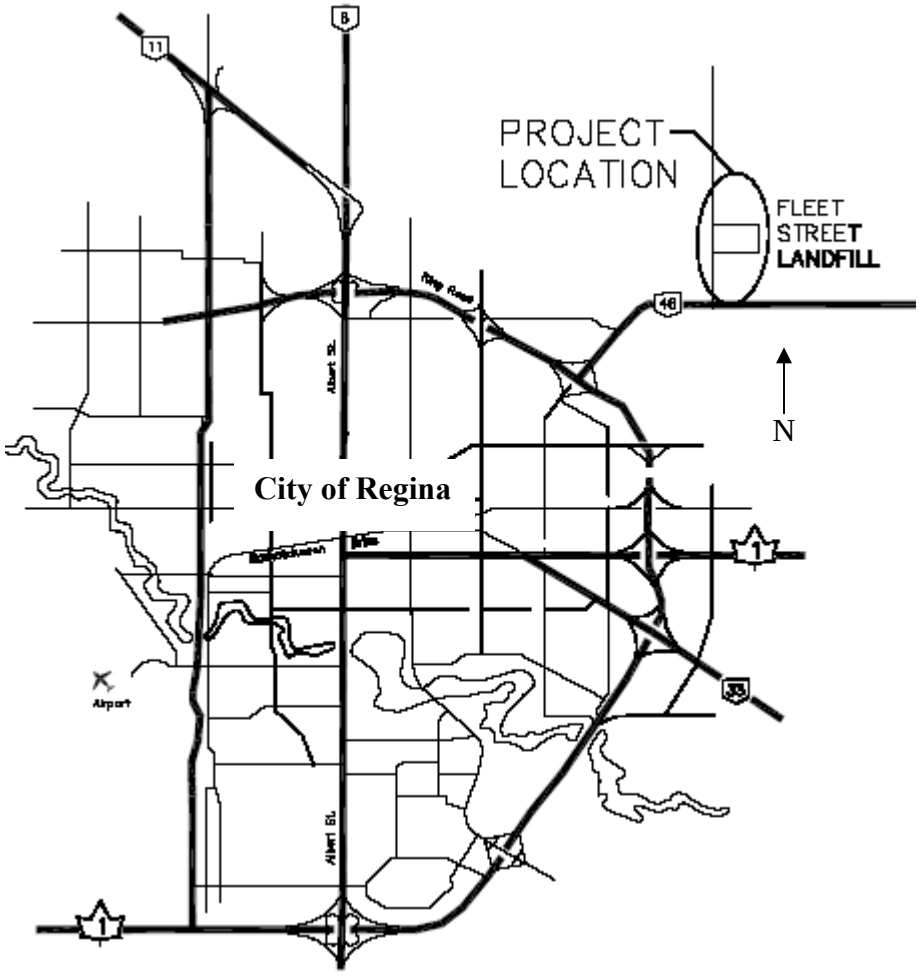

Figure 1-1 Map of the City of Regina showing project location (from GAL-OKC 2004)

The Fleet Street landfill began accepting waste following the closure of the Mount Pleasant landfill site in 1961 (Reid Crowther & Partners, 1993). The landfill accepts a variety of waste material including residential, commercial and industrial garbage, fill dirt, and rubble, including building demolition materials, recyclable asphalt and concrete, manure, special wastes such as asbestos, confidential papers, and other materials.

All material brought to the landfill must pass through the scales at the entrance to the site. All material, except for recyclable asphalt and concrete, are hauled onto the disposal area. The landfill is a raised disposal area and the current active tipping area is 35 m above the overall grade. Recyclable asphalt and concrete are hauled to either the "Asphalt/Concrete Area" north

of the landfill or to the crushing area at the southwest corner. Fill dirt is either hauled to the hill or to the fill dirt stockpile north of the hill. Grit and sludge have not been accepted on the site since 1995 (GAL and OKC, 2005(b)).

The topography in the Regina area is generally flat to gently undulating with local relief rarely exceeding 3 m. The landfill is located on a former lake basin consisting of lacustrine deposits known as Regina Clay underlying the waste mound. The clay is underlain by a lacustrine silt. The total thickness of the clay and silt strata is between 3.5 m and 6.5 m in the immediate vicinity of the landfill (GAL and OKC, 2005(b)). The Condie Moraine is below the silt and is 15 m to 20 m thick, consisting of ice contact sands and gravely sands with occasional interbedded silt and clay lenses. The Condie Moraine is underlain by Floral Formation till. The Floral Formation consists of an upper 25 m to 30 m of unoxidized sandy clay till and a lower 12 m to 22 m of medium to coarse sand. The Floral Formation is underlain by till from the Sutherland Formation, which in turn is underlain by Empress Group silt. The Empress group sediments overlie silt and clay of the Bearpaw Formation that is the bedrock in the Regina Area.

Aquifers in the immediate vicinity of the Fleet Street landfill are located within the Condie Moraine sand (approximately 18.5 m to 26.5 m below surface) and within the sand of the lower Floral Formation (approximately 43.5 m to 46.5 m below surface). The COR currently draws a portion of its water supply from the lower Floral Formation sands. The 1993 Fleet Street landfill Closure study identifies potential contamination of the Condie Moraine aquifer attributed to landfill activities, but no impacts were identified in the lower Floral sands. Because of the potential threat of contamination to the aquifer, the cover design was focused on minimizing water ingress.

1.2. Study Objectives and Scope

The overall objective of this thesis is to evaluate the preliminary performance of the four test plots on the Fleet Street landfill with regards to net percolation, gas flux, water balance and vegetation. To meet this overall objective, three specific objectives were developed as follows:

- Characterize physical properties of the soil covers on the four test plots.
- Evaluate the performance and integrity of the monitoring scheme.
- Develop a preliminary water balance using the monitoring field data.

The preliminary water balance refers to a water balance representing early behaviour in the operation of the cover. The activities undertaken to achieve these objectives included the following: a review of background data and literature; field monitoring, field testing and sampling; laboratory testing; and data interpretation and analysis. The design and construction of the test plots and the installation of most of the instrumentation was completed separate from this thesis by consultants contracted by the COR.

1.3. Overview of Thesis

The required literature review and theoretical background are presented in Chapter Two. Chapter Three describes the methods used in the field instrumentation program, the *in situ* testing program and the laboratory testing program. Chapter Four presents and discusses the data collected during this study. Chapter Five presents the analysis and interpretation of the dataset. Chapter Six provides conclusions and recommendations developed from this study.

CHAPTER 2
LITERATURE AND THEORETICAL BACKGROUND

This chapter provides the necessary theoretical background required for this thesis. This includes addressing the need for covers and some case studies investigating soil cover alternatives. Instrumentation available for monitoring soil covers is also described.

2.1. Introduction and the Need for Covers

The placement of municipal solid waste into landfills has been a widely accepted method of disposal for many years (Shafer et al., 1984). Natural processes occur within the buried waste allowing it to decompose; however, these processes can also create a contaminant laden liquid effluent called leachate (Shafer et al., 1984). Water infiltration can compound the problem and help to mobilize the leachate that may eventually reach the groundwater (McCartney and Zornberg, 2006). Landfill gas produced by these processes can also be potentially harmful. Berger et al. (2005) suggest that a secondary role of landfill covers is to aid in the collection and treatment of any landfill gases before they reach the atmosphere.

The purpose of a landfill cover is to isolate the landfill waste from the surrounding environment, (Blight and Fourie, 2005). Shafer et al. (1984) described a cover as a natural or synthetic barrier placed on top of a landfill in order to keep contaminants in and precipitation out. They break surface covers into three types: daily, intermediate and final. Daily covers are used to control litter, odor, fire, and moisture until additional waste is placed. These are typically placed at the end of a working day and are the thinnest type of cover, consisting of any readily available material. Intermediate covers are placed to meet the same requirements as a daily cover; however, intermediate covers are thicker and can be left exposed for a longer period of time than a daily cover, anywhere from a few days to several years. Final covers are placed after the landfill is complete and have various requirements as defined by final site use. Final cover designs require the most planning and design with respect to infiltration, gas egress, erosion and vegetation.

Natural or synthetic materials can be used in the construction of final covers, each having its own advantages and disadvantages. Soils are the most commonly used natural material. Synthetic membranes are made of a variety of materials including polyethylene, polyvinyl chloride and others. Landfill covers combining natural and synthetic materials are also common.

There are two main approaches to the storage of municipal solid waste in landfills. The first is the "dry tomb" approach, which attempts to prevent all moisture from entering the landfill (Blight and Fourie, 2005). This will significantly reduce the amount of landfill gas and leachate that could potentially harm the surrounding environment. However, a completely dry landfill will never fully decompose and stabilize, as a supply of moisture is necessary for the decomposition of the waste. The stabilization of a "dry tomb" landfill will likely require many years, thus extending the waste production phases of decomposition over long periods of time (Vesilind et al., 2002).

The second approach is that of a bioreactor. This option encourages rapid stabilization of the landfill by controlling the moisture, temperature, pH, nutrients and other properties. Generally, in arid climates, moisture must be added to the landfill. Leachate recycling, which entails recycling collected leachate back into the landfill, is often used to promote faster stabilization than that achieved using precipitation as the sole moisture provider. This leachate recycling will also produce landfill gas at a higher rate that may be collected for other purposes. In order to use this type of cover, there must be a system in place to allow for the collection of leachate. This system is usually included in a landfill liner system. According to Khire and Haydar (2007), the benefits of rapid stabilization include: reducing the leachate treatment and disposal costs; accelerated decomposition and settlement of the waste; an increased rate of gas production; and, potential reduction in the post-closure care period and maintenance costs. Associated risks include an increased potential for slope instability, and the potential for increased leachate head at the base of the landfill if the collection system does not function properly.

Since the Fleet Street landfill does not have a liner or a leachate collection system, and has associated risk of aquifer contamination, the dry tomb approach was used.

Traditional landfill covers, also known as barrier covers, attempt to minimize the amount of water entering the waste. The main components of a traditional cover are: a leveling soil layer immediately above the waste; a gas venting system; the sealing layers; a drainage system; and, the vegetative soil (Gartung, 1996). A traditional landfill cover requires low hydraulic

conductivity, no greater than 1 x 10^{-7} cm/s (Dwyer, 1995). These covers are generally effective in wet climates, where precipitation exceeds potential evapotranspiration. Traditional compacted clay covers have inherent problems in cold, arid or semi-arid locations where the barrier layers are subject to desiccation cracking as well as increased hydraulic conductivity due to freeze/thaw cycles (Boese, 2003).

Evapotranspiration (ET) covers, or store-and-release covers, are rapidly becoming the preferred alternative to traditional barrier type covers for landfills in arid and semi-arid regions (Somasundaram et al., 2005; and McCartney and Zornberg, 2006).

An ET cover (or store-and-release cover) is a simple system that involves a monolithic soil layer with a vegetative cover (McCartney and Zornberg, 2006). Moisture storage and evapotranspiration play significant roles in the performance of this type of cover. The cover does not act as a barrier, but as a reservoir that stores moisture during precipitation events and subsequently returns it to the atmosphere as evapotranspiration. There is potential for net percolation into the landfill over a period of years to be zero if infiltration during the wet season or from snowmelt is completely evaporated during the ensuing dry season, particularly in arid and semi-arid climates (Blight and Fourie, 2005). ET covers are relatively simple to construct, require little long-term maintenance and can provide significant cost savings (Zornberg et al. 2003). These are typically approved by the regulatory agencies based on a demonstrated equivalent performance to the prescribed barrier cover. Such equivalencies are demonstrated usually by numerical modelling of cover percolation followed by field verification with demonstration test plots.

A capillary break cover is a variation of an ET cover. It consists of a finer grained soil layer placed above a coarser grained soil layer constructed on a slope (Kampf et al., 2001). Under unsaturated conditions, the textural contrast delays the vertical drainage of the fine-grained soil by capillary forces. The suction in the bottom layer remains low due to its coarser texture and at this level of suction the finer soil layer can retain water up to levels of full saturation. This allows infiltrating soil water to be stored in the finer soil above the interface. The soil water in the finer soil may flow downslope laterally along the sloped interface due to gravitational forces. At a certain distance downslope, the suction in the finer soil may be reduced sufficiently so that capillary forces no longer prevent water from moving vertically into the coarser layer. The point

where there is no longer diversion along the interface, but rather vertical flow into the coarser material is known as the breakthrough point.

2.2. Case Studies Investigating Soil Cover Alternatives

There are several examples of using store-and-release covers on landfills as opposed to traditional, low conductivity barrier type covers. Several case studies are described in the following paragraphs on the use of these non-traditional covers for landfills.

Lee (1999) discusses the types of covers available for different climatic conditions. In climates where potential evaporation is less than precipitation, covers constructed with a compacted clay layer with a low saturated hydraulic conductivity can be used to limit infiltration. In climates where the potential evaporation exceeds precipitation, this type of cover might desiccate and crack, thus increasing the hydraulic conductivity and allowing increased rates of percolation into the underlying waste. Consequently, store-and-release type covers are often used in drier climates to take advantage of the use of ET to remove stored water from the cover.

The Alternative Landfill Cover Demonstration (ALCD) was a large-scale field test in New Mexico to evaluate the performance of alternative landfill cover technologies in arid or semi-arid environments (Dwyer, 1995). The ALCD included two traditional covers as a base or control case. The two traditional covers include compacted barrier layers with a low hydraulic conductivity including a Resource Conservation and Recovery Act (RCRA) subtitle C compacted clay layer and a conventional RCRA subtitle D cover (see Dwyer 1998 for specific details of these covers). Four alternative covers were also constructed: a geosynthetic clay liner (GCL) cover, a capillary barrier cover, an anisotropic barrier cover and an ET cover.

The conventional subtitle C compacted clay cover consisted of a geomembrane placed over the waste, overlain by a geotextile, then a 45 cm thick compacted soil barrier with a maximum saturated hydraulic conductivity of 1×10^{-7} m/s and finally a top vegetation layer. The conventional subtitle D cover consisted a geomembrane on top of the waste, overlain by a geotextile, then a 60 cm thick clay barrier layer mixed with bentonite to meet the saturated hydraulic conductivity requirement of less than 1×10^{-9} m/s, a polyethylene geomembrane placed above this layer and then a top vegetation layer. The GCL test cover is identical to the conventional clay cover with the exception that the clay barrier was replaced by a thin GCL. The capillary barrier cover was constructed without any geosynthetic materials. The anisotropic

barrier consisted of a layered capillary barrier. The ET cover was engineered to encourage water storage and enhance ET. It consisted of a thick layer of native soil and a topsoil layer.

Monitoring at the ALCD included meteorological and water balance data such as precipitation, surface runoff, lateral drainage, soil water storage and percolation. All measurements were automated. There were also periodic measurements of biomass, vegetation cover, leaf area index and species composition.

The conventional clay cover performed poorly, with an increasing percolation rate over time. Dwyer (1998) attributes this to desiccation cracking, freeze/thaw cycles, root penetration and earthworm and insect activity causing an increase in hydraulic conductivity. This cover experienced the most percolation. The conventional cover D had little percolation in the first year; however Dwyer (1998) believes that as additional moisture infiltrated the barrier layer it will eventually create percolation. The compacted layer cannot dry as a result of evaporation because the geomembrane is protecting it from moisture loss.

The GCL cover experienced problems due to defects in the geomembrane. Dwyer (1998) hypothesized that moisture moved through the geomembrane via defects and penetrated the GCL seams. This cover experienced the third highest percolation.

The capillary barrier cover showed a very high net percolation in the first year, but Dwyer (1998) claimed that the rate was slowing significantly as surface vegetation thickened. This was the second worst cover in terms of percolation.

The anisotropic barrier and the ET cover, both performed well in terms of net percolation. As these covers cost less than half that of the compacted clay cover and the long-term performance is expected to be better, Dwyer (1998) concluded that they were likely the best covers for municipal solid waste landfills in arid or semi-arid climates.

Blight and Fourie (2005) describe two large-scale field experiments in semi-arid climates where the behavior of “infiltrate-stabilize-evapotranspire”, or ISE covers was investigated. These covers are designed similar to store-and-release covers, absorbing the annual rainfall and then allowing it to re-evaporate through the surface. However, this type of cover would allow part of the water to penetrate into the waste, thus accelerating the decomposition process and allowing stabilization of the waste, before allowing it to evapotranspire. The experimental covers functioned as a store-and-release cover during drier periods; however, in wetter periods, water

infiltrated through the cover, and later was drawn up from the waste within the landfill to evaporate. It was unclear what conditions were necessary in the waste to ensure that an upward gradient could be established to move water back up out of the waste.

Blight et al. (2005) describes one of these landfills further and investigates whether the moisture storage in the landfill could be increased sufficiently through raising the height of the landfill to eliminate the net percolation. While the net percolation was not eliminated at the completion of the experiment, the percolation rate had decreased and appeared likely to continue decreasing. Essentially, the landfill waste itself is being used as part of the store-and-release cover, with evaporation moving water out of the landfill from as deep as 15 m.

Berger et al. (2005) investigated the methane oxidation potential of a capillary break landfill cover in a laboratory simulation. Microbial activity in the top 30 cm of the cover was able to oxidize between 57% and 98% of methane from the waste. After irrigation, the location of greatest oxidation moved closer to the surface where more oxygen was present. They found that the degree of saturation played a large role as the oxygen was required in the soil to oxidize the methane. However, a property of capillary break covers is that they increase the saturation in the finer grained material, therefore reducing oxygen availability. Berger et al. (2005) concluded that a capillary barrier can perform both primary functions of a landfill cover (reducing net percolation to the waste, and treating methane before it reaches the atmosphere), and may be a cost-effective alternative to other landfill covers.

Albright et al. (2004) conducted a study comparing the ability of different landfill covers to control percolation to the underlying waste. They investigated barrier covers as well as store-and-release covers. Several capillary break barrier covers employing layers of fine-grained soils over coarse-grained soils were investigated, as well as some monolithic covers consisting of a thick layer of fine-grained soil covered by topsoil. The primary focus of the study was on the water balance within the cover with emphasis on percolation rates. Large, instrumented, pan-type lysimeters were used to evaluate the percolation on all test plots. Time domain reflectometry (TDR) probes and thermal dissipation sensors were used to measure water content and suction. The study found that store-and-release covers in arid and semi-arid climates limit percolation as effectively as conventional covers with a composite barrier, allowing percolation rates of less than 1.5 mm/year or 0.2% of precipitation on average.

Hauser et al. (2001) studied a store-and-release cover, describing it as a vegetated cover or ET cover. The paper offers recommendations for the design of ET covers in arid and semi-arid climates, based on the evaporation to precipitation ratio. It recommends using evapotranspiration covers wherever applicable since they are natural, self-renewing and more economical than conventional, low hydraulic conductivity, barrier covers.

Nyhan et al. (1997) conducted a water balance study on four landfill cover designs in semi-arid regions paying particular attention to the influence of slope. They tested two capillary break covers; an Environmental Protection Agency (EPA) recommended cover consisting of loam over medium sand over clay; and, a "conventional" design consisting of a loam surface layer over a layer of crushed tuff. These covers were tested in fabricated boxes rather than test plots. They found that the greater the slope angle, the greater the evapotranspiration because of the increased shortwave radiation on the east facing site. This study, and a similar study by Albright et al. (2004), found that runoff accounted for about 2 to 3% of precipitation. The design that had the lowest percolation through the cover was the EPA cover, followed by the capillary break designs, with the conventional design showing the most percolation. It was found that net percolation decreased with increasing slope angle. Nyhan et al. (1997) state that the best landfill cover must be designed specifically for each site based on the types of waste, risks, costs and pertinent regulations. They also describe the use of the computer models to justify the validity of the proposed landfill cover design.

Young et al. (2006) investigated the relationship between cover thickness, vegetation coverage and deep percolation through a landfill cover. They performed numerical simulations to compare various cover thickness and plant coverage relationships. They found that the increasing cover thickness reduced percolation because of the increased storage capacity. After the cover is sufficiently thick to store the largest annual infiltration (whether through a rainy season or snowmelt infiltration), further increases in thickness are not necessary. They also found that no combination of cover thickness and soil type reduced net percolation estimates to below the desired limit without vegetation. The greatest increase in performance occurred by increasing plant cover from 0 to 10%, which the authors characterized as threshold vegetation, though net percolation did continue to decrease with greater vegetative cover.

These and other studies support the use of both capillary break and store-and-release type covers for use as landfill final covers in semi-arid climates. Both types of covers use the climate

to remove stored water through evapotranspiration. Conventional barrier type covers are susceptible to failure through increases in hydraulic conductivity in semi-arid climates. A key aspect in improving the performance of capillary break and store-and-release covers is the presence of vegetation capable of removing water from a greater depth than evaporation alone.

2.3. Instrumentation Available for Field Monitoring

2.3.1. Water Balance

Understanding the flow of water across the soil-atmosphere boundary is critical in the evaluation of many geotechnical engineering problems (Wilson et al., 1991). Several fluxes exist at the soil-atmosphere interface and are important in creating a surface water balance as shown in Figure 2-1. Barbour et al., (2001) describe a surface water balance in the following equation:

$$\Delta S = PPT - R - DP - I - AET \qquad \text{Equation 2.1}$$

where, ΔS represents change in soil moisture storage (S), PPT is precipitation, R is runoff, DP is deep percolation, I is interflow and AET is actual evapotranspiration, all expressed as depth of water (in mm).

This relatively simple equation is often difficult to quantify as measurement of one or more of the components are often lacking in many studies, leaving some of the main components to be calculated as a residual value or eliminated completely (Flerchinger et al., 1998). The instrumentation available to monitor the parameters in the above equation are described by O'Kane (1996) and Ayres (1998) in detail and are also reviewed briefly in this section.

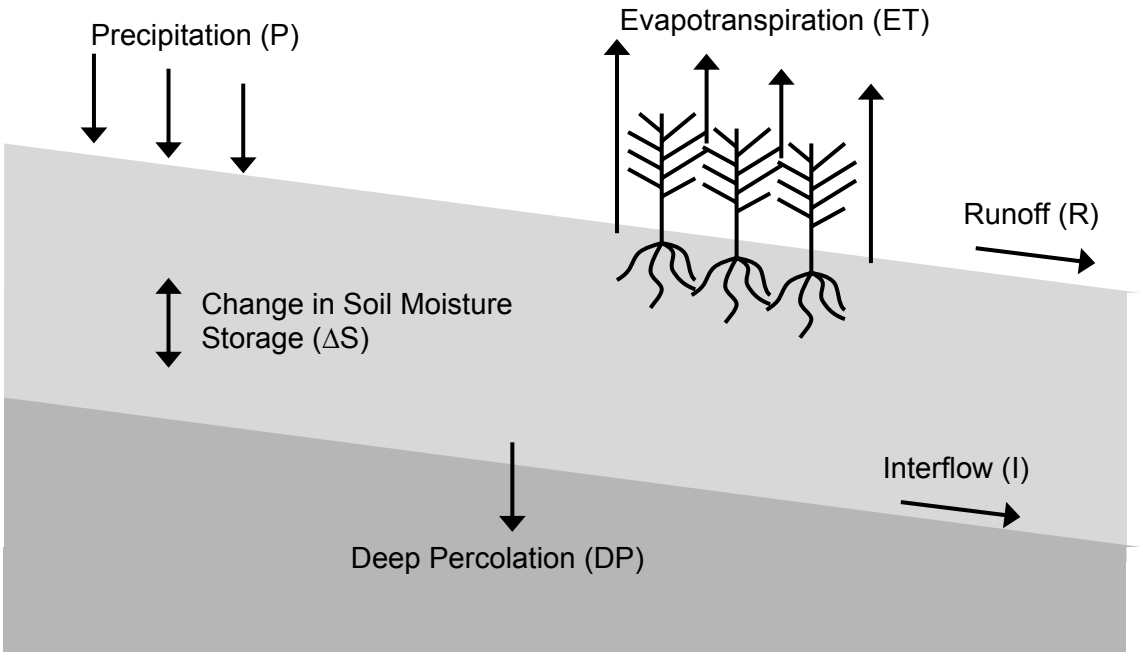

Figure 2-1 Water balance components of a sloping soil system.

2.3.2. Soil Moisture

Soil moisture is the amount of water in a given volume of soil. Soil moisture measurements can be made using disturbed samples or by *in situ* instrumentation. The most common methods are the gravimetric method, time domain reflectometry (TDR), capacitance and the neutron probe method. Each of these methods is briefly discussed below.

Gravimetric Method

The gravimetric method of obtaining soil moisture is described in ASTM D2216-92 (ASTM, 1992). A sampling device is used to obtain soil samples at various depths and then these samples are taken to a laboratory to obtain the gravimetric water content. The laboratory procedure is easy and straightforward and provides an accurate value; however, obtaining the samples at various depths makes this method time consuming and it cannot be automated. Another downfall of the gravimetric method is that the gravimetric water content does not directly correlate to the volume of stored water unless the dry bulk density of the soil is known. Provided the dry bulk density is known, the gravimetric samples provide an accurate data point to which automated instrumentation can be calibrated.

Time Domain Reflectometry

Time domain reflectometry (TDR) is used in many different types of instrumentation. TDR is reliable, easy to use, provides an immediate response and is capable of continuous and remote monitoring (Boese, 2003). These traits have made TDR attractive for field monitoring in many different applications including agriculture, geotechnical engineering and environmental engineering (Topp et al. (1980); Look and Reeves, 1992; Benson et al., 1994; O'Kane, 1996; Ayres, 1998). It is an attractive option because it measures volumetric soil water content in a non-destructive manner and provides an immediate response.

The principles behind TDR have been described in detail by Topp et al. (1980) but are reviewed briefly here. In TDR a very fast time-rise voltage pulse is propagated down a cable, through soil, and reflected back. The travel time is measured and is related to an apparent dielectric constant of the soil. The dielectric constant of water is much greater than that of soil and air, therefore, the apparent dielectric constant measured by the TDR can be related back to volumetric water content. One important note about the use of TDR is that it measures only liquid water content, as the dielectric constant of ice is approximately the same as that of soil.

Capacitance Sensors

Capacitance sensors also measure the dielectric constant of the soil and have the ability for continuous monitoring and connection to data acquisition systems. The difference between TDR and capacitance sensors lies in the electronic means employed to measure the dielectric constant. The TDR measures the time for an electromagnetic wave to propagate along a transmission line within the soil. A capacitance sensor measures the time it takes to charge a capacitor using the soil as the dielectric (Soilmoisture Equipment Corp. 2007). Like the TDR, the time is related to an apparent dielectric constant of the soil and is then related to volumetric water content. As with TDR, capacitance sensors can only measure liquid water content.

Neutron Moisture Probe

The neutron moisture probe was first used in the agricultural industry for measuring soil water content in drainage and irrigation studies (Gardner and Kirkham, 1952). In recent years it has been used in hydrologic modelling, environmental monitoring projects and soil cover evaluations

(Boese, 2003). Although this method has been used for more than fifty years in many applications, it continues to have problems associated with the probe calibration curve and the interpretation of the calibration results (Lee, 1999).

The neutron probe emits high energy, fast neutrons from radioactive sources, which are slowed down by colliding with surrounding hydrogen atoms (O'Kane, 1996). In soil, nearly all of the hydrogen atoms are found in water; therefore, the slowed neutrons indicate the volume of soil water. A neutron detector on the neutron probe the measures a count of the slowed neutrons and correlates this count using a material specific calibration curve to volumetric water content.

2.3.3. Precipitation

Precipitation can occur as either rainfall or snowfall. Several methods have been developed for measuring precipitation either as rainfall or snowfall. Rainfall can be measured by either recording gauges or non-recording gauges. Snowfall can be measured either by adapting a rainfall gauge or using a snow survey.

Non-recording gauges are the most simple and inexpensive. While they may take different forms, they are all essentially a container to collect and store rain or snow and a calibrated measuring stick. The drawback of this type of instrument is that it requires human intervention on a regular basis to record and empty the gauge.

Recording gauges eliminate the need for human intervention but are more expensive and complex. Again, recording gauges may take various forms, but the most common is the tipping bucket (Bras, 1990). A tipping bucket uses two balanced buckets that tip back and forth as they are filled by precipitation entering via a funnel. Each bucket tip is counted, and by knowing the volume of the bucket and the diameter of the funnel the recorded number of tips can be converted to volume or depth of precipitation. This also allows rainfall intensity to be recorded using the frequency of bucket tips.

To measure snowfall in the winter months, a snowfall adaptor can be added to many automated rain gauges. The adaptor consists of a catch tube, an overflow hose and a reservoir filled with antifreeze. The snow is captured in the catch tube and slowly melts into the antifreeze reservoir causing a mixture of antifreeze and water to flow through the overflow tube into the tipping bucket funnel. A delay of several hours is expected before the snow will completely melt

in the antifreeze. Regular maintenance is required to ensure the antifreeze reservoir remains full. A disadvantage of the snowfall adaptor is the possibility of snow capping or bridging occurring over the gauge (Boese, 2003).

The snow survey method can also be used to determine the snow water equivalent (SWE) of the snow pack (Gray, 1970; Woo, 1997). In this method, several snow samples are taken across the area of interest to determine the overall density and depth of snow cover. This method is generally regarded as the best approximation of SWE for the snow cover, but it is labour intensive and time consuming (Boese, 2003).

2.3.4. Runoff

Surface runoff is difficult to measure accurately from a natural soil system as it is a complex process (Ayres, 1998). Several mechanisms are involved in creating runoff and have been reviewed thoroughly by Lee (1999). Two examples of runoff measurement were reviewed by O'Kane (1996) and Lee (1999) and are mentioned briefly here.

O'Kane (1996) attempted to measure surface runoff from an engineered cover system in British Columbia at Equity Silver Mines Ltd. A system of PVC gutters and collection reservoirs were installed at two locations on the cover to measure runoff from storm events during non-freezing conditions. The volume of water collected was manually measured and recorded and was then used to compute the runoff from the areas contributing to the reservoirs. O'Kane (1996) reported that data collection and installation problems led to unreliable measurements.

Lee (1999) measured surface runoff at the Cameco mine in Key Lake, Saskatchewan from a non-vegetated prototype soil cover. A half culvert was set into the ground to collect runoff and berms were constructed on the edges of the soil cover to contain the runoff originating on the soil cover. The culvert emptied water into a containment area where water depth was measured by a sonic wave sensor. Lee (1999) encountered difficulties estimating low flow conditions and modified the measuring system by installing a 60^{o} V-notch weir at the end of the runoff collection culvert. A tipping bucket rain gauge was added on the downstream side of the weir to activate the sonic sensor to record depths only when water was flowing. These modifications enabled measurement of low flow conditions and improved the accuracy of the runoff measurements.

Flow volumes for V-notch weirs are calculated using the following equation from Smith (1995):

$$Q = C_d \cdot \frac{8}{15} \cdot \sqrt{2g} \cdot \tan\left(\frac{\theta}{2}\right) \cdot h^{\frac{5}{2}} \qquad (m^3/s) \qquad \text{Equation 2.2}$$

where,

Q = flow rate (m^3/s)

C_d = coefficient of discharge

θ = angle of V-notch

h = height of water (m)

The coefficient of discharge is dependent on the angle of the V-notch as well as the head over the weir; the relationship is shown in Figure 2-2. This relationship was developed for a condition in which the upstream water depth below the notch is not less than the head above the V-notch and is not less than 0.15 m.

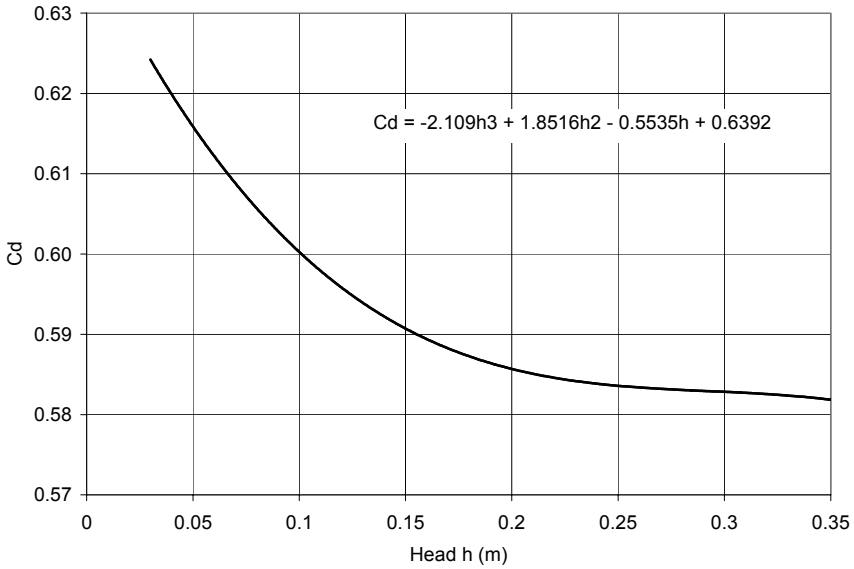

Figure 2-2 Coefficient of discharge for a 60° V-notch weir (after Smith, 1995)

2.3.5. Interflow

Water that flows laterally within the shallow subsurface soil horizons without entering the general groundwater table is known as subsurface flow (Hewlett, 1982). Interflow, or through flow, is subsurface flow occurring when infiltrating waters move laterally through the upper horizons of the soil unit until returning to the to surface some point downslope, either

reappearing as surface runoff or stream flow (Gray, 1970). This typically occurs where a relatively permeable soil overlies a less permeable layer, promoting the development of a perched water table and flow parallel to the upper surface of the confining layer (Hutchinson and Moore, 2000). It could also occur in the situation of a capillary break in which water moves downslope within the fine-grained soil layer overlying a coarse layer under the influence of gravitational gradients (Bussiere et al., 2003; Parent and Cabral, 2006).

Several studies have been undertaken to better understand the mechanisms of interflow and to quantify its contribution to the overall water balance. Anderson et al. (1997) used tracers while Bosch et al. (1994) and Jordan (1994) all used tensiometers and monitoring standpipes to try and characterize interflow. Hutchinson and Moore (2000) monitored a small, forested hill-slope and were able to quantify the interflow at a logging road cut across the base of the hill-slope. Concrete troughs were anchored to the face of the cut along the cut to intercept flow from the soil above a compacted till layer. A funnel set into the concrete at the lowest point was used to collect and measure the flow and tarpaulins were erected over the road cut to prevent rainfall entering the troughs. Flows were measured manually with a stopwatch and graduated cylinder. Hutchinson and Moore (2000) reported that maximum uncertainty for the trough flow was +/- 10%.

Bussiere et al. (2003) discussed the hydraulic behaviour of inclined capillary break covers. They noted that the degree of saturation in the finer, storage layer reduced as the distance from the toe of the slope increased. This indicates interflow within the finer layer above the capillary break layer. Stormont (1996) also discussed lateral flow of water above the capillary break layer in sloping covers. He discussed how water could drain laterally in unsaturated conditions reducing the amount available to percolate into the underlying soil compared to a uniform soil cover.

Boese (2003) installed an interflow collection system at the base of prototype covers to collect water flowing downslope along a soil material interface. The system consisted of a geomembrane cutoff located at the soil interface and a weeping tile collection system to gather water into a catchment barrel. The water in the barrels was monitored regularly and water was pumped out as it accumulated. Boese (2003) reported that the system captured interflow from along the soil material interface but it was unclear whether the entire cover was contributing to the interflow system or whether the water was merely from a small saturated zone at the toe.

2.3.6. Soil Matric Suction

Feng (1999) states that field measurements of matric suction are necessary to monitor the moisture fluxes through a soil cover. Lee (1999) states that changes in soil water content are a result of soil matric suction changes caused by infiltration and evaporation. Though several devices are available for measuring soil matric suctions, tensiometers and thermal conductivity sensors are the most common. Both of these techniques are described in detail by Fredlund and Rahardjo (1993) and are reviewed briefly here.

Tensiometers

Tensiometers give a direct measurement of the negative pore pressure, or matric suction in a soil when the pore-air pressure is atmospheric. The maximum suction that a tensiometer can measure is approximately 90 kPa (Soilmoisture Equipment Corporation, 1997). The tensiometer consists of a high air entry, porous ceramic cup connected by a small bore tube to a vacuum gauge, or other pressure measuring device. The tube and cup are filled with de-aired water and are then inserted into a predrilled hold, ensuring good contact with the soil. The water in the tensiometer will come into equilibrium with the surrounding soil and the matric suction will be indicated on the gauge.

Tensiometers require regular maintenance as air bubbles will accumulate within the tensiometer. The water pressure in an unattended tensiometer will eventually increase towards zero. There are several types of tensiometers available of which the jet-fill tensiometer provides the most efficient way to remove the air from the tensiometer. The jet-fill tensiometer has a reservoir at the top of the tube for removing air bubbles. O'Kane (1996) and Ayres (1998) successfully used a nest of jet-fill tensiometers to verify the performance of adjacent thermal conductivity sensors.

ASTM D3404-91 (ASTM, 1991) provides guidelines for tensiometer selection, installation and operation. Advantages of tensiometers are that they are simple to install and operate, no field or laboratory calibration is necessary and they are relatively inexpensive. However, the tensiometer requires human intervention to record data and remove air bubbles from the system.

Thermal Conductivity Sensors

Thermal conductivity sensors measure soil matric suction indirectly over a range of 5 to 500 kPa (Fredlund and Rahardjo, 1993). These sensors consist of a porous ceramic cylinder containing a temperature sensing element and miniature heater. The pores of the ceramic cylinder allow water to flow in and out of the sensors, allowing the matric suction to come to equilibrium with that of the soil. A suction water content relationship for each thermal conductivity sensor is measured in a laboratory prior to use. By measuring the change in temperature after a fixed time period the suction can be determined. Thermal conductivity sensors have gained acceptance as they are easy to use, relatively insensitive to temperature and salinity changes, have a wide measurement range, and are easily connected to data acquisition systems for continuous monitoring. Applications have been described by Curtis and Johnson (1987) for a groundwater recharge study, and by O'Kane (1996), Wilson et al. (1995), Ayers (1998) and Boese (2003) for the evaluation of engineered soil cover systems.

One limitation of thermal conductivity sensors is the elaborate process required to calibrate the sensors to various suctions. Fredlund et al. (1991) also observed that as temperatures drop to below freezing the suction readings drop sharply, related to water freezing within the soil. Errors due to hysteresis are also possible at matric suctions less than 20 kPa (Feng, 1999).

2.3.7. Evapotranspiration

Evaporation is defined as the loss of free water as vapour from open water or bare soil. Soil evaporation is a coupled process, depending on both atmospheric conditions and soil properties. This process is described more thoroughly in Ayres (1998). Transpiration occurs when soil water is drawn up by plant roots and discharged through the leaf system in the form of water vapour (Strahler and Strahler, 1983). Evapotranspiration (ET) is the combination of these two processes and is the cumulative sum of bare soil evaporation and plant transpiration (Granger, 1989). Potential evapotranspiration (PET) is the evapotranspiration that would occur from an area with sufficient water supply to permit the maximum quantity of water to evaporate and/or transpire based on climatological demand. The rate of actual evapotranspiration (AET) slows during dry periods as soil water supply becomes depleted and the plants reduce transpiration.

Numerous methods have been developed to estimate potential evaporation (Wilson, 1990). One of the most popular and widely accepted methods was developed by Penman (1948). The Penman method assumes the surface to be fully saturated at all times, therefore providing an estimate of potential evaporation. The estimation is based on the climatic parameters of net radiation, air temperature, relative humidity and wind speed. Wilson (1990) modified the Penman method to calculate evaporation from unsaturated soil surfaces.

2.3.8. Instrumentation Used at the Fleet Street Landfill

In order to calculate the water balance in each cover for this project, various water balance components were measured. Precipitation was measured with a rainfall tipping bucket and snowfall through snow surveys. Water fluxes and soil moisture were measured with thermal conductivity suction sensors and capacitance sensors, respectively. Runoff was measured with a geomembrane lined collection channel and a zero-depth V-notch weir. Interflow on the capillary break covers was measured with an interflow collection channel diverted into a tipping bucket. Evapotranspiration was not measured directly, but PET can be estimated using measured climate data such as net radiation, wind speed, air temperature, and relative humidity. Further details about the installation of all of these instruments can be found in Chapter 3.

CHAPTER 3
FIELD AND LABORATORY PROGRAM

The initial study conducted by GAL and OKC for the COR included a literature review, borrow material investigation study, laboratory testing, and numerical modelling. Based on this study, two systems were evaluated: a moisture store-and-release homogenous soil cover and a layered capillary break cover.

To further investigate the effects of delayed snowmelt and net radiation, it was decided to construct the cover options on both the north and south facing slopes for a total of four cover trials in the summer of 2004. Details regarding the design and construction of the test plots can be found in GAL and OKC, 2005(b). Test plot dimensions were 20 m wide by 60 m long, except for the north facing capillary break cover (TP2N) which was made 120 m long, in order to try and capture break-through of interflow through the liner.

Soil and meteorological conditions on the test plots at the Fleet Street landfill were monitored from 2004 to 2006. The soil monitoring program consisted of detailed monitoring of matric suction, volumetric water content, gas pressure and composition, and soil temperature within the soil profile as well as measurements of runoff, and interflow on each test plot. Meteorological monitoring includes wind speed and direction, air temperature, relative humidity, net radiation, and precipitation. *In situ* testing, soil sampling and laboratory testing was undertaken to help characterize the soils and vegetation on the test plots. Laboratory tests included grain size distribution, Atterberg limits, moisture retention, dry density, and root density. The field testing included Guelph permeability measurements and density testing using a nuclear densometer. The methods and procedures used in these field and laboratory programs are presented in this chapter.

3.1. Test Plot Description

The test plots were constructed in the summer of 2004. The field trial comprised of four test plots demonstrating two different cover designs: a capillary break cover and a store-and-release

cover. The test plots were constructed on both the north and south facing slope to evaluate the effect of delayed snowmelt and different net radiations associated with different slope aspects.

The construction of test plots began in May 2004 and was substantially completed by June 2004. Each of the test plots was constructed directly on the existing cover material, which was nominally 0.3 m thick. Each test plot was rectangular in shape with a 20 m width, and with different lengths. Each test plot generally followed the contours of the existing slope. A 0.3 m high ridge ran lengthwise down the edges of each test plot to help direct water downslope to the toe of the test plot rather than off the side.

Till material from a borrow area north of the Tor Hill Golf Course was used for constructing the test plots. GAL and OKC (2005(b)) contain more details about the location and properties of the borrow material.

3.1.1. Store-and-Release Test Plot Covers

Table 3-1 summarizes the composition and nomenclature of all the test plots. Each test plot was 60 m in length and constructed from 2 m of uncompacted till overlain with 0.2 m of topsoil. The store-and-release test plot on the north slope (TP1N) has a slope of approximately 4.2H:1V. The south store-and-release test plot constructed on the south slope (TP1S) has a slope of approximately 3.2H:1V. The edges of each test plot were constructed at a 2H:1V slope. Till placement at the start of construction is shown in Figure 3-1. GAL and OKC (2005(b)) provide further details of the store-and-release test plot covers.

Figure 3-1 Till Placement at the Start of Construction of TP1N

Table 3-1 Summary of test plot nomenclature and composition

Test Plot	Type	Composition	Slope
TP1N	Store-and-release	0.2 m topsoil 2.0 m till	4.2:1 north facing
TP1S	Store-and-release	0.2 m topsoil 2.0 m till	3.2:1 south facing
TP2N	Capillary Break	0.2 m topsoil 1.3 m till 0.3 m sand	4.3:1 north facing
TP2S	Capillary Break	0.2 m topsoil 1.3 m till 0.3 m sand	3:1 south facing

3.1.2. Capillary Break Test Plot Covers

One capillary break test plot was constructed on each of the north and south slopes of the landfill. Each test plot was constructed from 0.3 m of sand, overlain with 1.3 m of uncompacted till, which was overlain by 0.2 m of topsoil. The north capillary break test plot (TP2N) was 120 m in length and had a slope of approximately 4.3H:1V. The south capillary break test plot

(TP2S) was 60 m in length and had a slope of approximately 3.1H:1V. The edges of each test plot were constructed at a 2H:1V slope. Till placement is shown in Figure 3-2. Table 3-1 summarizes the nomenclature and composition of the covers. Further details of the capillary break test plot covers are given in GAL and OKC (2005(b)).

The monitoring phase of the project involved collecting and managing data from the various instrumentation installed on the site. This also involved maintenance of the test plots and instrumentation as well as preparing annual monitoring reports for COR. The detailed instrumentation program developed for each test plot is described in Chapter 3.

Figure 3-2 Till placement over sand on TP2S

3.2. Field Instrumentation

3.2.1. Components of the Field Instrumentation Program

Each of the four test plots was constructed directly over the existing cover material, which was a general fill used by the COR as a temporary cover to limit odors and debris and to provide a working surface. The temporary fill is nominally 30 cm thick and is composed of various readily available soils.

Details on the installation and calibration of field instrumentation is discussed in GAL and OKC (2005(a); 2005(b)) but will be briefly reviewed here. Instrument manuals are included in GAL and OKC 2005(a). A summary of each of the four test plots and the instruments installed on each test plot are shown in Table 3-2. A plan showing the location of all the instrumentation is shown below in Figure 3-5. Cross sections of the store-and-release test plots and the capillary break test plots are shown in Figure 3-3 and Figure 3-4, respectively.

The majority of instruments were installed as the test plots were constructed. The locations of various instruments on each test plot are shown in Figure 3-5. The following instruments were installed by OKC during test plot construction: a total of twelve soil monitoring stations were installed on the test plots; a weather station installed on the north slope and an additional net radiometer on the south slope; a runoff collection system installed on each test plot with each capillary break test plot also having an interflow monitoring station. Sixteen soil gas monitoring stations along with an additional 4 access tubes for measuring water content were installed in the summer of 2005 by the author.

Each test plot had a soil monitoring station installed at the top, middle and bottom of the slope. Each station included ten automated volumetric water content sensors. The station at the midslope of each test plot also had twelve matric suction sensors. All sensors were connected to a Data Acquisition System (DAS) located in the center of each test plot. Access tubes were also installed along a center transect of the test plot between the soil monitoring stations for measurements using a portable soil moisture probe called the Diviner 2000. An additional access tube was installed midslope on the right side of the test plot to monitor edge effects.

Table 3-2 Summary of test plots and instrumentation

Cover	Description	Instrumentation by OKC	Instrumentation by U of S researchers
TP1N	Store-and-release on north slope	3 soil monitoring stations (each with 10 automated water content sensors and 12 matric suction sensors) Runoff collection system Weather station 9 Diviner water content access tubes	4 gas monitoring stations 1 manual water content access tube
TP2N	Capillary break on north slope	3 soil monitoring stations Runoff collection system Interflow collection system 5 standpipes for monitoring saturation 14 Diviner water content access tubes	4 gas monitoring stations 1 manual water content access tube
TP1S	Store-and-release on south slope	3 soil monitoring stations Runoff collection system 9 Diviner water content access tubes	4 gas monitoring stations 1 manual water content access tube
TP2S	Capillary break on south slope	3 soil monitoring stations Runoff collection system Interflow collection system 5 standpipes for monitoring saturation Net radiometer 9 Diviner water content access tubes	4 gas monitoring stations 1 manual water content access tube

The weather station was located at the top of TP1N. The weather station recorded wind speed and direction, air temperature, net radiation, and precipitation. Precipitation was recorded as it occurred and a daily maximum, minimum and average value was recorded for all other parameters.

Runoff from each test plot was collected in a runoff collection channel at the bottom of the slope. The channel ran the entire width of the test plot and directed surface runoff into a monitoring hut for automated monitoring of the volume of surface runoff with a zero-height V-notch weir.

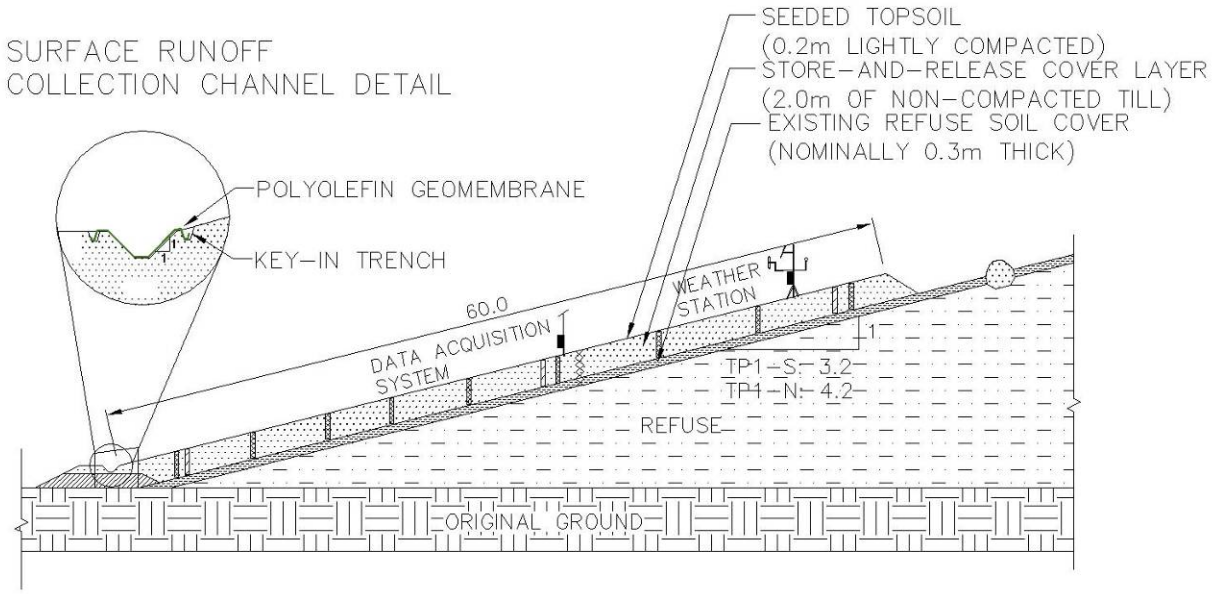

Figure 3-3 Cross section of store-and-release test plots (from GAL-OKC 2005(b))

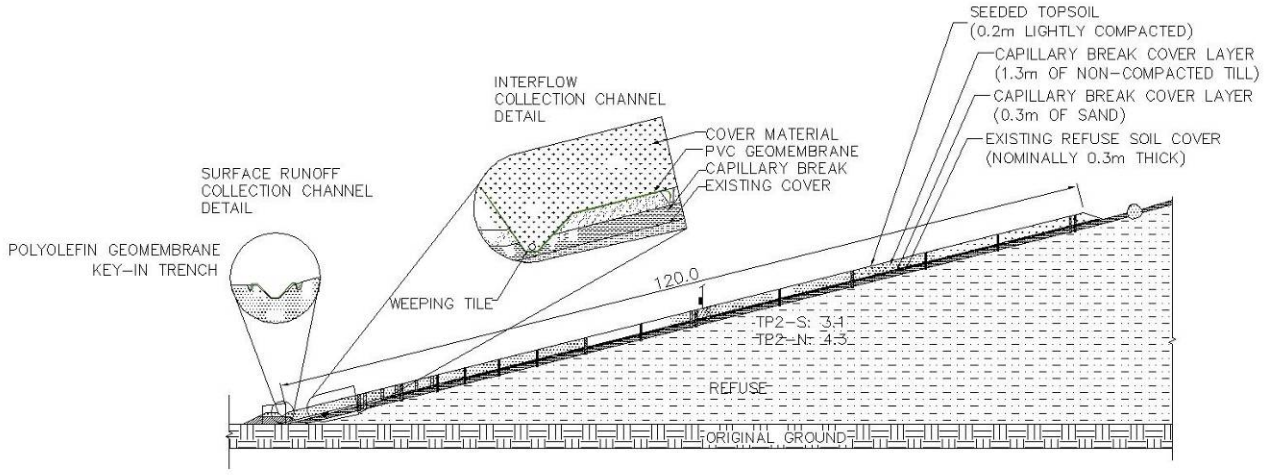

Figure 3-4 Cross section of capillary break test plots (from GAL-OKC 2005(b))

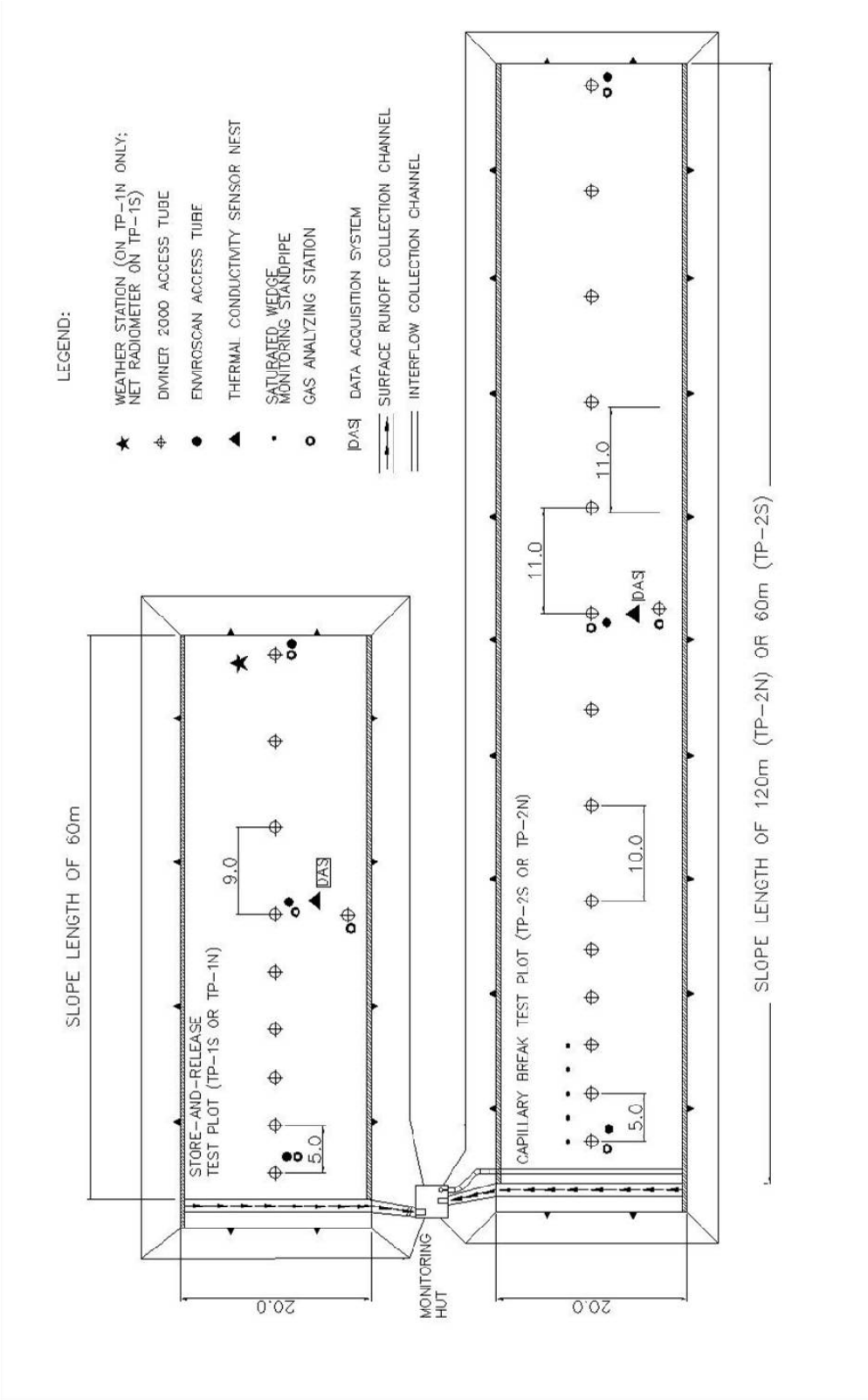

Figure 3-5 Plans of test plots (from GAL-OKC 2005(b))

The weir was equipped with a sonic ranging probe that reads the depth of water passing through the weir. The readings from the sonic sensor were sent to a DAS located in the hut. Details of the runoff collection channel can be found in GAL and OKC, (2005(b)).

An interflow drainage channel was also constructed near the base of the slope on the capillary break test plots above the sand layer in order to collect subsurface water diverted by the capillary break sand layer (interflow). The channel ran the entire width of the test plot and directed subsurface water to a monitoring hut where the volume of interflow was measured with a tipping bucket flow gauge. Construction of the interflow channel involved excavating a channel and key-in trench, installing a PVC liner and weeping tile, backfilling the channel with sand and connecting the weeping tile to a solid drainpipe. Further details can be seen in GAL and OKC, (2005(b)).

Gas monitoring stations were installed adjacent to the soil monitoring stations. An additional gas monitoring station was installed midslope at the right edge of each test plot to evaluate potential edge effects. Each gas monitoring station had several ports at various depths to test for composition.

3.2.2. Data Acquisition System (DAS)

The data acquisition system is a central component to the automated monitoring scheme. The DAS allows for automated readings, reducing the need for human intervention, and in particular, the time required for manual monitoring by site personnel (Ayres, 1998). The DAS controls the frequency of automated readings, performs necessary calculations, and records the data to be saved until retrieved by those monitoring the site. Details about the DAS can be found in Appendix A.

3.2.3. Thermal Conductivity Sensors

Thermal conductivity sensors were selected to continuously monitor the *in situ* matric suction and temperature. Model 229 thermal conductivity sensors, manufactured by Campbell Scientific Inc. (CSI) were used in this study. Further details about these sensors can be found in Appendix A.

A laboratory calibration curve for each Model 229 thermal conductivity sensor installed in the cover field trials was measured in the laboratory by OKC. Individual calibration curves are important as the response of each sensor is dependent on the insertion of the temperature sensor and heater in the ceramic at the factory, which varies from sensor to sensor. Calibration curves can be found in Appendix B.

Thermal conductivity sensors were installed in a single nest at the midslope soil station on each test plot. Installation of the Model 229 sensors involved excavating a narrow trench and drilling small holes into the face of the trench at the desired depths to allow the thermal conductivity sensors to be installed into undisturbed material. The trench was backfilled after all the sensors were installed. Figure 3-6 and Figure 3-7 show the depths of installation for the thermal conductivity and water content sensors on each test plot.

3.2.4. Water Content Sensors

EnviroSCAN® sensors and the Diviner 2000® system, electrical capacitance sensors manufactured by Sentek Pty Ltd., were used in this study. EnviroSCAN® sensors are at a various depths on each test plot (shown in Figure 3-6 and Figure 3-7). They are automated sensors that take readings every two hours. The Diviner 2000® uses the same technology, but is a single sensor installed on a probe that is manually lowered into access tubes to take readings every 10 cm. Further details about the instruments can be found in Appendix A.

Sentek Pty Ltd. has developed standard "default" calibration equations using sand, loams, and clay loam for the EnviroSCAN® and Diviner 2000® system. While this is suitable for assessing relative changes in the *in situ* moisture conditions, material-specific calibration curves are required to quantitatively assess *in situ* volumetric water content within the system. Material specific calibration curves were developed by OKC in the laboratory for the EnviroSCAN® system and can be found in Appendix B.

A specialized installation kit supplied by Sentek Pty Ltd. was used to install the vertical tubes for both the EnviroSCAN® and Diviner 2000® system. This method involves repeatedly driving the 2.5 m long PVC access tube with a cutting ring attached vertically into the cover material with a sledgehammer and augering out the soil from inside the tube until it reaches the required depth. A double ring stopper was installed to seal the base of the access tube. The sensor rail was then installed in the access tube and connected to the DAS.

EnviroSCAN® access tubes were installed at an upslope, midslope and downslope location on each test plot. Figure 3-5 shows the locations and Figure 3-6 and Figure 3-7 show the depths of the sensors. Portable Diviner 2000® access tubes were installed along a central transect of each test plot. A total of ten, 2.0 m long, 50 mm diameter, PVC access tubes were installed on the 60 m long test plots (TP1N, TP1S, and TP2S), and fifteen were installed in the 120 m test plot (TP2N). Figure 3-5 shows the locations. All access tubes provided manual monitoring of the *in situ* water content to a depth of 1.5 or 1.6 m. Table 3-4 lists the profile number and the corresponding access tube installed in this study.

3.2.5. Gas Monitoring

Gas pressure and composition monitoring stations were installed along the center of each test plot, at the same location as the automated water content sensors, and next to the Diviner water content access tube installed on the right edges of the test plots for a total of four nests per test plot. Each station consisted of multiple gas ports at various depths in each material layer. A gas port consisted of a small filter surrounded by a screen to keep soil particles from clogging the filter. The filter was connected to a thin HDPE tube connecting the port to the surface, where a valve sealed the port until readings were to be taken. Various manometers or sampling devices could be connected to the port to measure gas pressure within the test plot.

A small hole was augered by hand as deep as physically possible for each nest of gas ports. The ports were connected to the outside of a small PVC tube to maintain the proper depths. The system was then placed in the hole and the hole was backfilled using sand adjacent to each gas port and bentonite pellets as a seal between ports. Four or five ports were installed in each hole. The depths and locations are listed in Table 3-2.

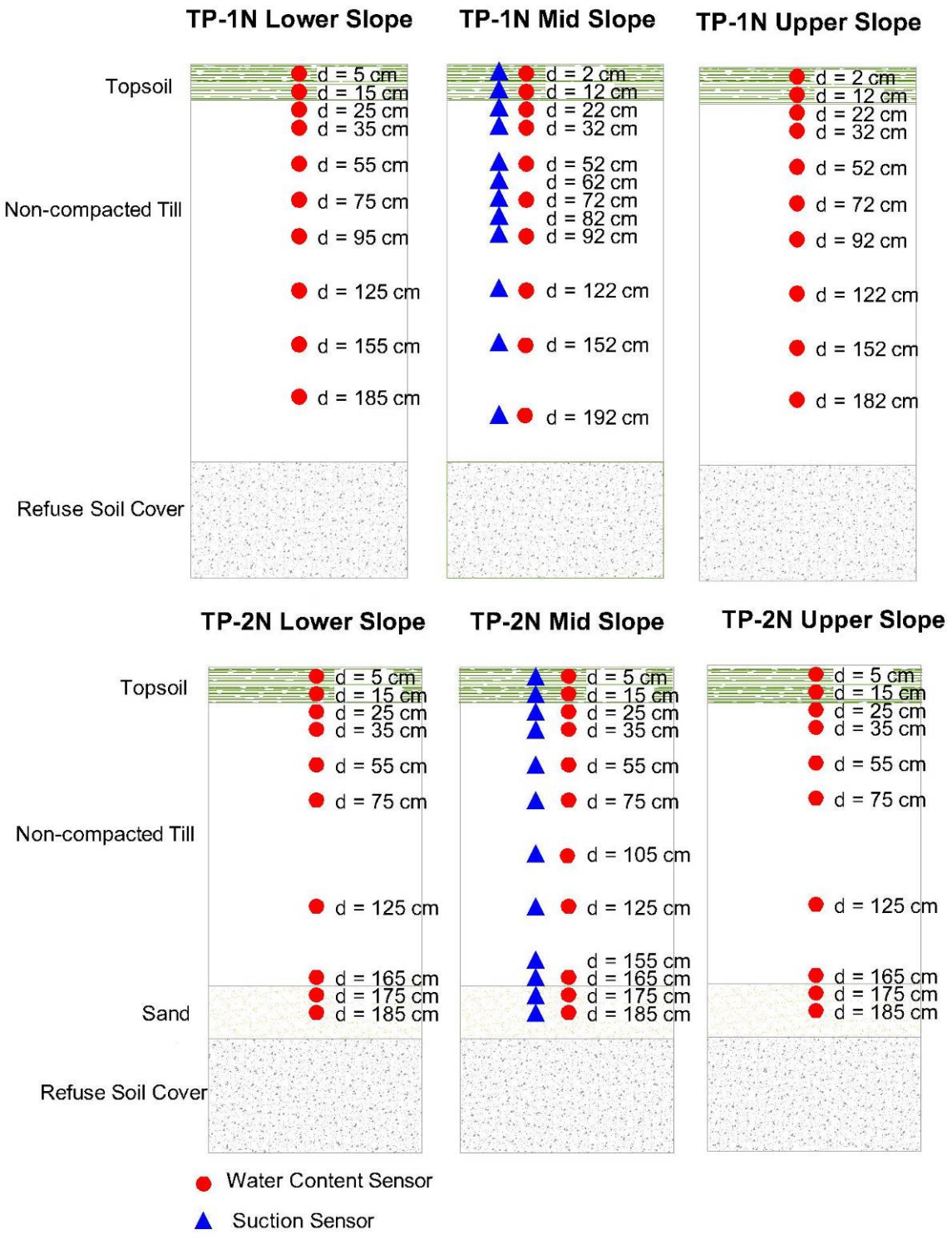

Figure 3-6 Locations of soil sensors on the north slope, from GAL and OKC, 2005(b)

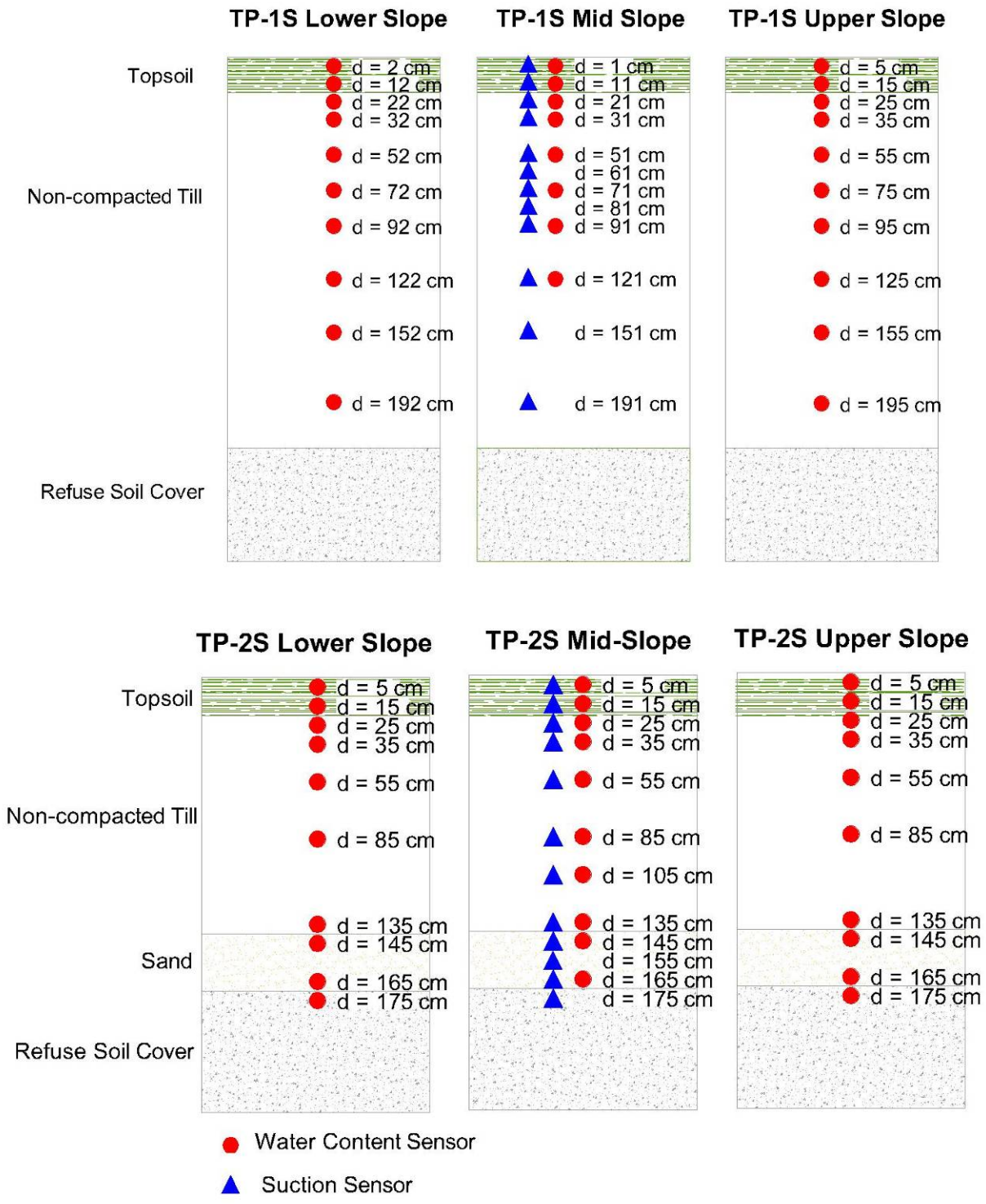

Figure 3-7 Depths of soil sensors on the south slope, from GAL and OKC, 2005(b)

3.2.6. Soil Temperature Monitoring

Soil temperature was monitored in two ways in this study; first, using the thermal conductivity sensors that also measure matric suction, and, second, using thermocouples installed with the gas monitoring systems at the upper and lower slope locations. The thermal conductivity sensors measure temperature as part of the procedure for measuring matric suction. Details about installation are found above in Section 3.2.3. The thermocouples were installed at the same depths as the gas monitoring ports but inside the small PVC tube to which gas ports are connected. The tube was then filled with oil to better conduct the temperature of the soil to the thermocouple. The locations and depths were the same as those for thermal conductivity sensors and upper and lower gas monitoring stations as summarized in Figure 3-6 and Figure 3-7 and Table 3-3.

Table 3-3 Depths of gas ports for each monitoring nest (m).

Test plot /Location	Bottom	Mid	Side	Upper
TP1N	0.69	0.64	0.71	0.76
	1.37	1.27	1.45	1.52
		2.21	2.16	2.29
		2.46	2.59	
			2.90	
TP2N	0.58	0.58	0.51	0.64
	1.17	1.78	1.02	1.27
	1.91	2.21	1.42	2.24
	2.29			2.41
TP1S	0.64	0.76	0.66	0.91
	1.27	1.52	1.32	1.93
	2.49	2.21	1.98	2.69
		2.57	2.41	2.92
		2.79		
TP2S	0.58	0.46	0.46	0.56
	1.17	0.91	0.91	1.68
	2.24	1.35	1.37	2.39
	2.54	1.55	1.57	2.67
		2.21	1.83	

3.2.7. Weather Station

Accurate weather data are necessary for the estimation of water balance. Therefore, a fully automated weather station was installed at the top of TP1N to provide site-specific measurements of air temperature, relative humidity (RH), wind speed, net radiation and precipitation. All components were supplied by Campbell Scientific Inc. Further details about the various instrumentation can be found in Appendix A. The weather station was operational year round. Data from the site was recorded on its own data acquisition system (DAS). Figure 3-8 shows the weather station on the top of TP1N.

Snow surveys were completed in early March 2005 and late February 2006 to aid in calculating total precipitation. Two or three transects were made on each test plot with depth measurements made at regular intervals of approximately 5 m or closer when the snow depth was more variable. Several snow samples were also taken to determine the snow density.

3.2.8. Runoff Monitoring

A channel at the base of each test plot was installed during construction and lined with a geomembrane. The channel directs the flow into a monitoring hut installed between the test plots on both the north and south slope. The runoff flowed into the hut through a V-notch weir. The design of the zero-height V-notch weir had to accommodate the peak design flow rate for the surface runoff collection system. This was calculated to be a peak design flow rate of 0.033 m^3/s for the 60 meter test plots and 0.066 m^3/s for the 120 m long test plot (TP2N) (GAL and OKC, 2005b).

Table 3-4 Location of Diviner 2000® access tubes

Diviner 2000® profile number	Approximate location of the Diviner 2000® access tube
01	25 m downslope of DAS on TP-1N
02	20 m downslope of DAS on TP-1N
03	15 m downslope of DAS on TP-1N
04	10 m downslope of DAS on TP-1N
05	5 m downslope of DAS on TP-1N
06	Adjacent to the DAS on TP-1N
07	9.5 m upslope of DAS on TP-1N
08	19 m upslope of DAS on TP-1N
09	28.5 m upslope of DAS on TP-1N
10	49 m downslope of DAS on TP-2N
11	44 m downslope of DAS on TP-2N
12	39 m downslope of DAS on TP-2N
13	34 m downslope of DAS on TP-2N
14	29 m downslope of DAS on TP-2N
15	24 m downslope of DAS on TP-2N
16	16 m downslope of DAS on TP-2N
17	8 m downslope of DAS on TP-2N
18	Adjacent to the DAS on TP-2N
19	10 m upslope of DAS on TP-2N
20	20 m upslope of DAS on TP-2N
21	30 m upslope of DAS on TP-2N
22	40 m upslope of DAS on TP-2N
23	50 m upslope of DAS on TP-2N
24	25 m downslope of DAS on TP-1S
25	20 m downslope of DAS on TP-1S
26	15 m downslope of DAS on TP-1S
27	10 m downslope of DAS on TP-1S
28	5 m downslope of DAS on TP-1S
29	Adjacent to the DAS on TP-1S
30	9.5 m upslope of DAS on TP-1S
31	19 m upslope of DAS on TP-1S
32	28.5 m upslope of DAS on TP-1S
33	25 m downslope of DAS on TP-2S
34	20 m downslope of DAS on TP-2S
35	15 m downslope of DAS on TP-2S
36	10 m downslope of DAS on TP-2S
37	5 m downslope of DAS on TP-2S
38	Adjacent to the DAS on TP-2S
39	9.5 m upslope of DAS on TP-2S
40	19 m upslope of DAS on TP-2S
41	28.5 m upslope of DAS on TP-2S

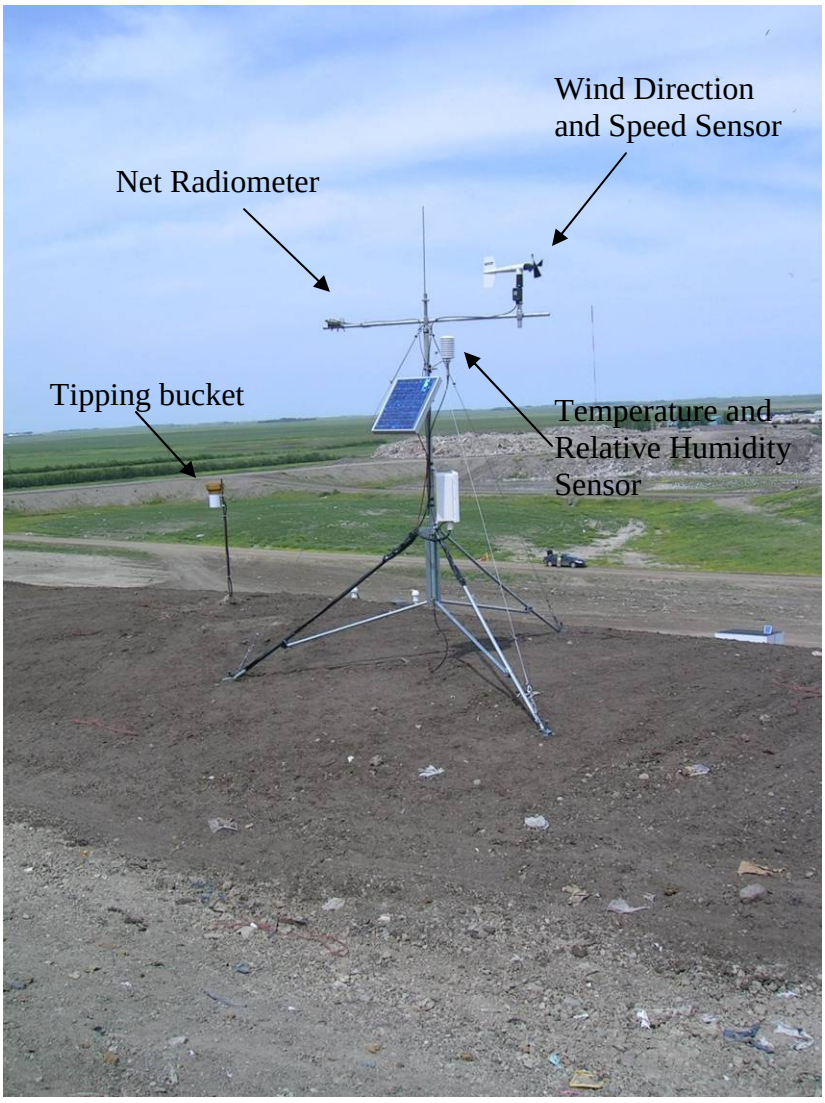

Figure 3-8 Weather station located at the top of TP1N

The weir plate and weir box were fabricated from a 3-mm-thick stainless steel plate and pressure-treated wood respectively. Flow can be calculated by knowing the height of water behind the weir. A CSI SR50 sonic ranging probe measures the water height. Readings required a temperature correction so a CSI 107F air temperature probe was also installed in the weir box. The SR50 was mounted using 2” x 4” bracing attached to posts on either side of the V-notch weir. The sonic ranging probes were each calibrated to read zero depth when the weir box was empty. All of the sensors for surface runoff monitoring were connected to a CSI CR510 datalogger mounted inside the monitoring hut. A 12-volt battery is charged by a 20 W solar panel mounted on top of the monitoring hut. CSI supplied all the surface monitoring and DAS equipment used in this study.

Due to the lack of established vegetation, erosion was a problem with sediment flowing through the weir with the runoff. This sediment then built up beneath the sonic ranging probe, providing false readings of runoff. Debris from the landfill would also enter the hut and block the sonic ranging probe, again providing falsely high readings of runoff. In early summer of 2005, after the first snowmelt, modifications were made to better record accurate runoff readings. A coarse-meshed screen was installed at the entrance to the hut to capture large debris. More rigorous monitoring and cleaning of the weir boxes during periods of expected runoff was also established. The readings for the spring melt of 2005 were also compromised because the heaters used to heat the monitoring huts to ensure runoff does not freeze inside the hut were not turned on in time to capture the entire melt. This allowed ice to build up in the channel, which produced false readings of runoff.

3.2.9. Interflow Monitoring

Interflow is soil water that moves laterally down slope within the soil cover. A drainage channel was constructed near the toe of the capillary break test plots (TP2N and TP2S) above the sand layer. The channel ran the entire width of the test plot and directed subsurface water diverted by the capillary break sand into a monitoring hut for automated monitoring of the volume of interflow. A tipping Rainwise Model RGP tipping bucket flow gauge, distributed by Hoskins Scientific Ltd. was used to measure interflow volumes. The channel was lined with a geomembrane fabricated from 40 mil PVC liner material and is approximately 0.4 m deep and 0.2 m wide at the bottom with 1H:1V side slopes.

Construction of the interflow channel involved excavating a channel and a key-in trench, installation of the PVC liner and weeping tile, backfilling the channel with sand and connecting the weeping tile to a drainpipe. The PVC liner was keyed-in to the underlying sand upslope of the channel and pinned on the downslope side. The weeping tile was fed into a 100 mm diameter drainpipe that fed into the tipping bucket inside the monitoring hut. The tipping bucket was connected to the CR510 data logger inside the monitoring hut. A bucket was placed beneath the tipping bucket to provide a sample of the interflow water for water quality analysis. The sensitivity of the tipping bucket was 0.254 mm and readings were recorded only recorded when tips are made.

3.2.10. Saturated Wedge Monitoring

Five 51 mm diameter PVC tubes were installed in the sand layer of each capillary break test plot (TP2N and TP2S). The bottom 150 mm of the tubes was slotted to allow any water table developing above the capillary break to enter the tube and be monitored.

3.3. In Situ Testing

3.3.1. Gas Composition

Pore gas samples were obtained from gas ports using gas-tight syringes. These samples were then analyzed using a portable Agilent M200 Micro Gas Chromatograph. Gas chromatography is an analytical technique used for separating a gas sample into components. Details on the equipment and procedures can be found in Agilent Technologies, Inc. (2000).

3.3.2. Soil Sampling

Soil samples were collected during the installation of the gas monitoring equipment. Auger cuttings were collected and brought to the lab for grain size analysis, root density testing, and Atterberg limits laboratory tests. Further soil sampling was completed during the summer of 2005 when undisturbed soil samples were collected for density and moisture retention measurements.

3.3.3. Vegetation Sampling

In the summer of 2006 vegetation samples were taken from the site for biomass calculations. A 1 m^2 area was marked off, and all plant material inside the area was collected and weighed, providing an approximate value for biomass/m^2. Several samples were taken from various areas of vegetation.

3.3.4. *In Situ* Density Measurement

A CPN 501DR Depthprobe was used to determine the distribution of density with depth at various locations on all test plots. The Depthprobe is a standard nuclear densometer, however

instead of aluminum casing for which it was designed and calibrated, the plastic Diviner 2000® access tubes were used. Because the instrument was not calibrated for these tubes, raw readings were matched with densities obtained from field samples taken at similar locations and depths. Further details about the Depthprobe can be found in Appendix A.

3.3.5. Hydraulic Conductivity Testing

A Model 2800K Guelph Permeameter (GP) from SoilMoisture Equipment Corp was used to measure saturated hydraulic conductivity. The GP measures the steady state infiltration rate necessary to maintain a constant depth of water in a cylindrical augered hole. The time required for the GP to reach steady state flow is a function of the permeability of the material. Further details are in Appendix A and Meiers, (2002).

3.4. Laboratory Testing

3.4.1. Grain Size Distribution

The procedure for determining the grain size distribution of a soil is specified in ASTM D422-63 (ASTM, 1990). Four grain size distributions were completed on samples of the uncompacted till.

3.4.2. Atterberg Limits

Liquid and plastic limit tests were completed on four soil samples of the uncompacted till. Testing was carried out according to procedures outlined in ASTM D4318-93 (ASTM, 1993).

3.4.3. Moisture Retention Curve

The measurement of the moisture retention relationships is used to establish the relationship between matric suction and volumetric water content for the uncompacted till from the test plots. ASTM D6836-02 (ASTM, 2003) Method C was used to measure the moisture retention curve for six undisturbed soil samples with pressure increments from 0 to 500 kPa. This method involves the use of a pressure chamber to apply a matric potential and then taking gravimetric measurements of water content.

Testing was also attempted with a Dewpoint PotentiaMeter (Decagaon Devices, Inc., 1998-2003). The procedure involves drying small samples to known water contents and a using the Dewpoint PotentiaMeter to read the suction. Several samples were measured, however it was later discovered that the machine had a cracked mirror and was not operating properly at the time of measurements. Therefore the results obtained are inaccurate and are not presented.

3.4.4. Dry Bulk Density

Undisturbed samples collected in Shelby tubes were used to calculate dry bulk density. The samples were trimmed to a known volume, weighed, dried in an oven and weighed again. Dry bulk density was calculated as dried mass divided by volume of sample.

3.4.5. Root Mass Density

Auger cuttings were collected at approximately 15 cm depth increments in September 2005 at various locations based on vegetation quality. The roots were sorted from the soil by massaging the sample held within a fine meshed screen in a pool of water until the majority of the soil was washed away. Then roots were picked out individually and weighed. The roots from each depth interval were weighed providing a distribution of root mass.

CHAPTER 4
PRESENTATION OF DATA

The laboratory tests, *in situ* tests, and field monitoring data are presented and discussed in this chapter. This chapter is divided into two main sections. The results from the laboratory and *in situ* testing are presented and discussed first in an attempt to characterize the properties of the soils in the test plots. Next, the data collected from the monitoring instrumentation installed in the test plots are presented and discussed. The field instrumentation program generated a large amount of data; therefore, this section summarizes this data in graphical form only. The entire monitoring data set is provided in the CD enclosed with this thesis. The reporting period for this data is from June 2004 to November 2006.

4.1. Laboratory testing

4.1.1. Grain Size Distribution

The grain size distribution of the till samples, one sample from each test plot, are presented in Figure 4-1. Golder Associates also obtained grain size distributions from the source pit for the till used in constructing the test plots and these are also included in Figure 4-1 (from GAL and OKC, 2005(b)).

The grain size distributions indicate that the till was well graded and contained approximately 50 to 60% fines (smaller than 0.075 mm) and 25 to 35% clay-sized particles (smaller than 0.002 mm). The distributions from the samples obtained from each test plot were comparable with the distributions obtained by Golder Associates.

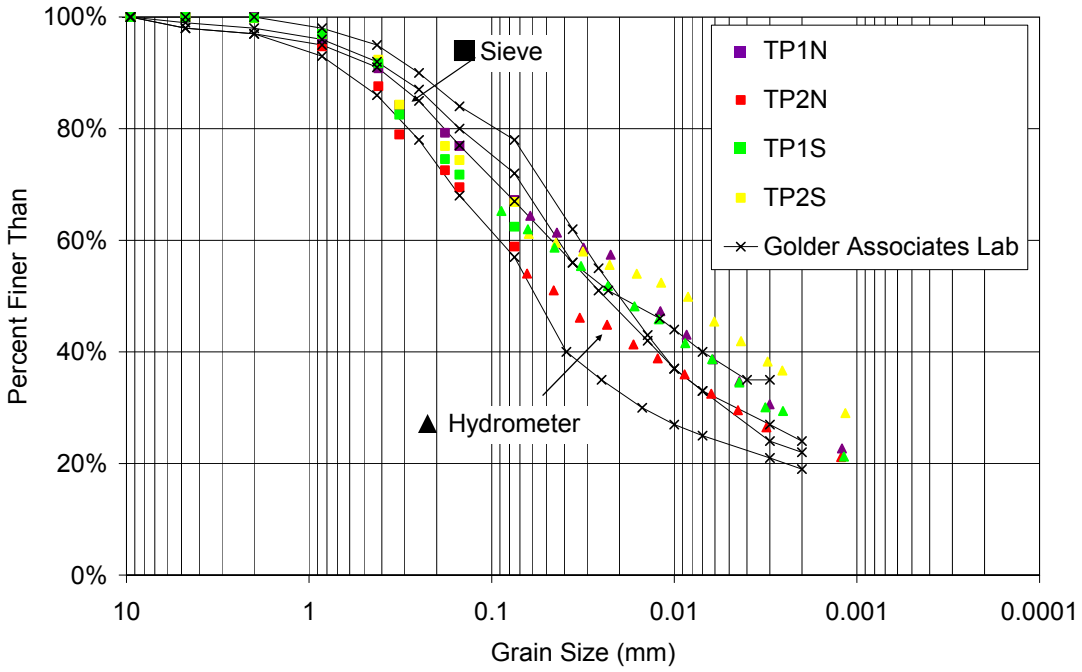

Figure 4-1 Grain size distribution for till from Fleet Street landfill test plots.

4.1.2. Atterberg Limits

The liquid and plastic limits for the till samples obtained from each plot are presented in Table 4-1 and indicate that the till had an average liquid limit of 33% and plastic limit of 15%. Table 4-1 also shows the results obtained by Golder Associates (GAL and OKC, 2005(b)) from samples of till gathered from the source pits. The results from Golder Associates Lab and the results measured in this study are similar.

4.1.3. Moisture Retention

Undisturbed samples of till were collected from each test plot with a Shelby tube. The depth of each sample was limited by the length of the Shelby tube and the accessibility from the surface of the test plot. Sample locations and depths are used to identify each sample. Samples were prepared and tested according to the procedures in ASTM D 6836-02. The resulting SWCC for each sample is presented in Figure 4-2. For comparison this figure also shows moisture retention curves measured by GAL which were from slurried and compacted samples. The GAL

curves were constructed using a combined Tempe Cell, large conventional pressure plate cell and desiccators with saturated salt solutions. Details of these tests can be found in GAL and OKC, (2005(b)).

Table 4-1 Atterberg limits for till

	Liquid Limit	**Plastic Index**
***In Situ* Samples Average**	33%	15%
St. Dev.	4.6%	1.7%
# of Samples	12	8
Golder Associates Lab	28.3%	13.8%

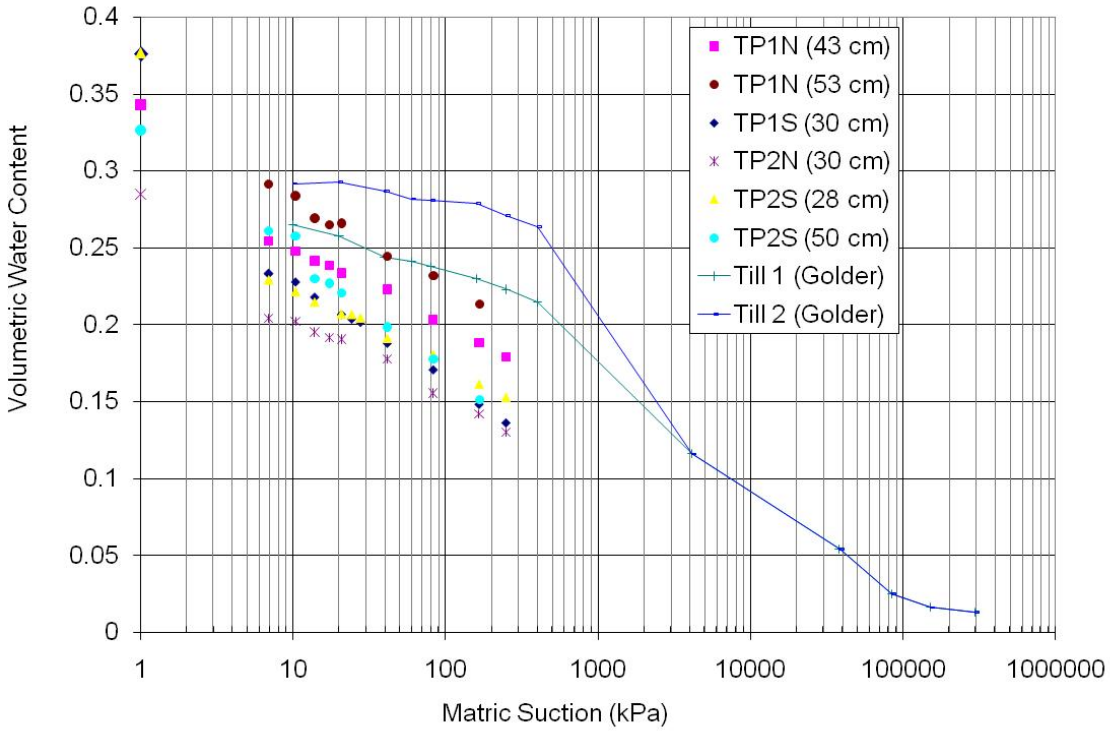

Figure 4-2 Soil water characteristic curve of till from Fleet Street landfill test plots with porosity indicated at 1 kPa.

The moisture retention curves for the undisturbed samples and those presented by GAL are quite similar; however, the GAL samples have higher water contents. This indicates that slurry preparation method used by GAL resulted in less macro-structure. The presence of this macro-structure results in lower air-entry values and increase drainage at lower suctions for the

undisturbed samples. The saturated volumetric water content of the undisturbed samples also appears lower, which is reasonable given that the density of these samples was higher than that of the slurried samples used by GAL.

4.2. *In Situ* Sampling and Measurements

This section describes the results of measurements or tests conducted in the field. Results of gas composition, vegetation sampling, density and hydraulic conductivity testing are presented in this section.

4.2.1. Gas Pressure and Composition

Gas pressure in the sampling tubes was measured periodically using a Dwyer Magnehelic Differential Pressure Gauge; however, no excess gas pressure was detected over the monitoring period.

Gas composition was measured at various locations on the test plots as described in Section 3.2.5. The samples were analyzed for the four main gases generally present in landfill gas: oxygen (O_2), nitrogen (N_2), methane (CH_4) and carbon dioxide (CO_2). The results for each test plot are shown in Figure 4-3 through Figure 4-6.

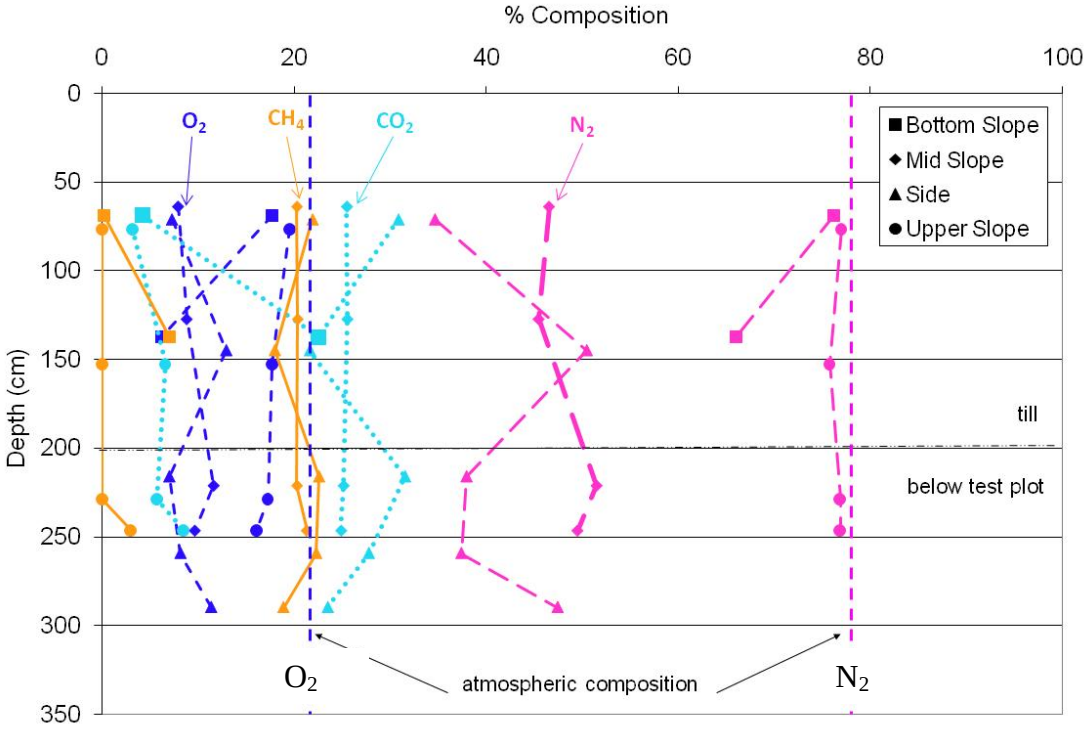

Figure 4-3 Gas composition for various locations on TP1N, samples obtained in summer 2005

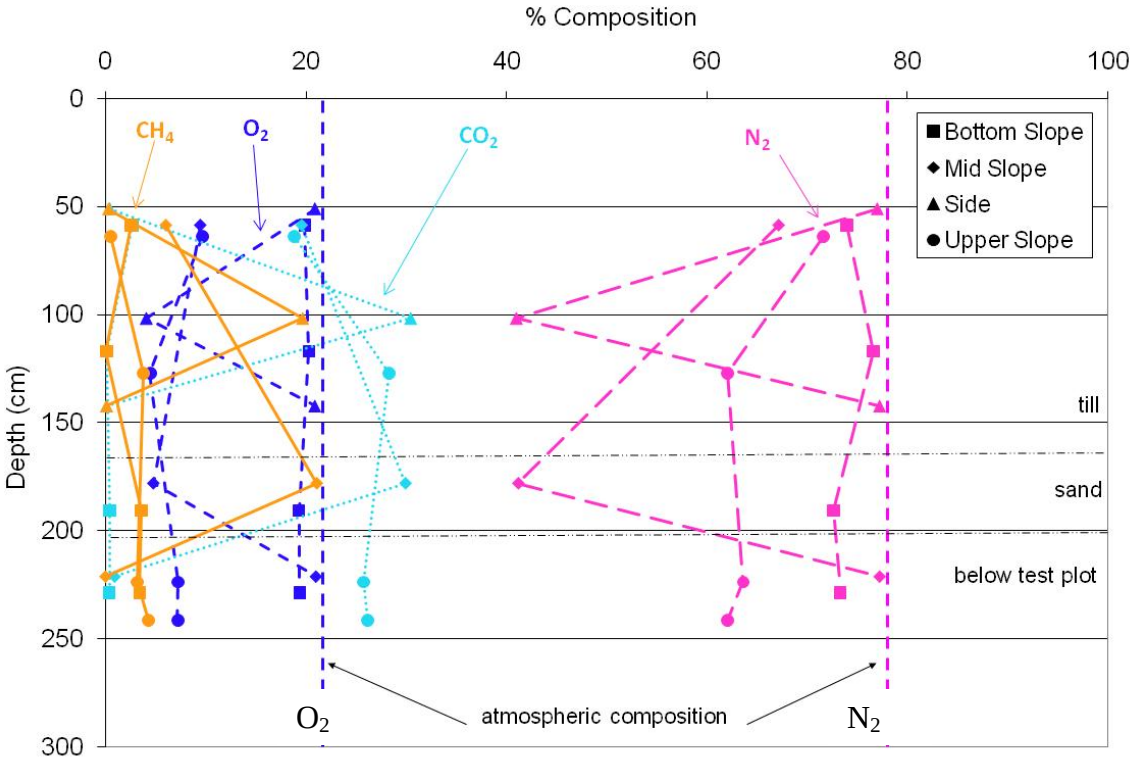

Figure 4-4 Gas composition at various locations on TP2N, samples obtained in summer 2005

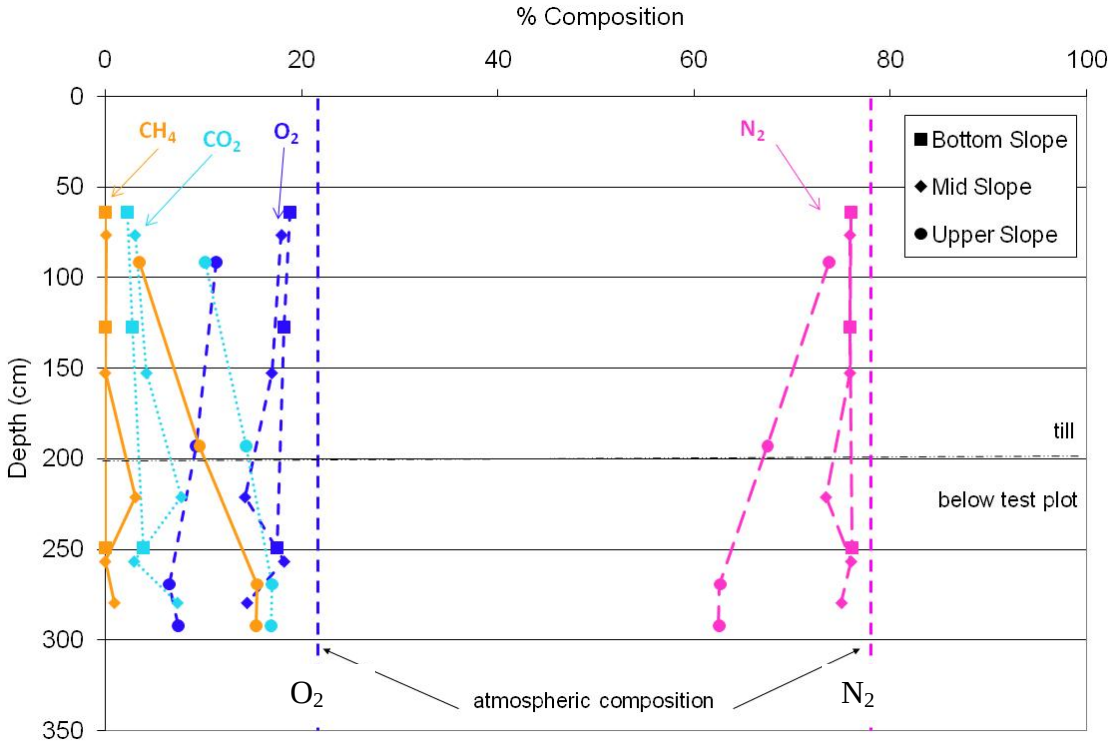

Figure 4-5 Gas composition at various locations on TP1S, samples obtained in summer 2005

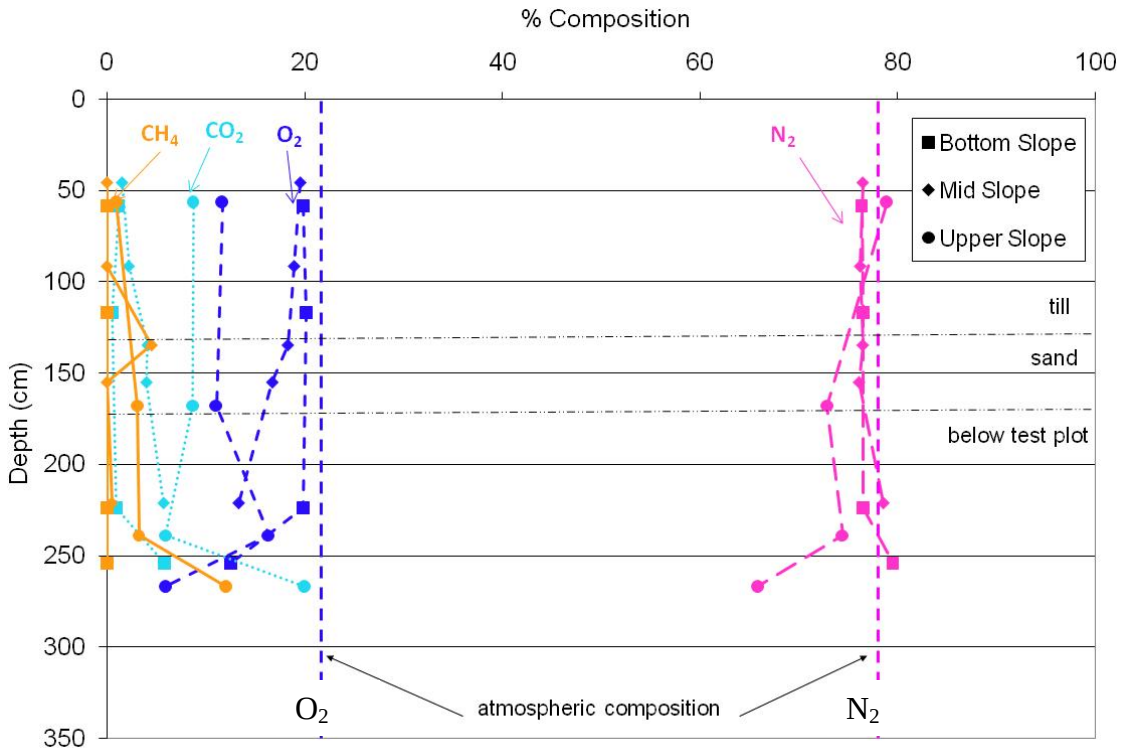

Figure 4-6 Gas composition at various locations on TP2S, samples obtained in summer 2005

Because of the small difference between sampled gas and the atmospheric composition, it is possible that the samples were contaminated with atmospheric air. However, the presence of methane and reduced carbon dioxide concentrations is evidence that landfill gas is present within the cover.

4.2.2. Vegetation Observations and Sampling

Observations of vegetation were made throughout the monitoring period. Photos were taken from the same location during each site visit in order to help monitor the changes. Some of these photos are shown below in Figure 4-7 through Figure 4-15.

Vegetation was categorized as being of three main types: poor, average and good based on above ground characteristics such as relative height and plant density. Vegetation was harvested from a one-meter square section and the plants dried and weighed to calculate a dried biomass value for each type of vegetation. The results are shown in Table 4-2. "Poor" vegetation had a biomass of 200 g/m^2, while "average" vegetation and "good' vegetation had biomass values of 400 g/m^2 and 600 g/m^2, respectively. Beeri et al. (2007) report an average biomass of approximately 500 g/m^2 for natural grasses in North Dakota.

The test plots were seeded with a native grass mixture in 2004. However, due to a large rainstorm shortly after seeding, a large amount of the seeds and topsoil were washed away before they could become established. Therefore, in the fall of 2004, the test plots were harrowed and reseeded (GAL and OKC, 2005(b)).

Table 4-2 Biomass per square meter for various vegetation characteristics

Location	Type	Biomass (g/m^2)
TP1N mid	average	400
TP1N bottom	poor	200
TP2N bottom	poor	200
TP2S mid	good	600

In the spring of 2005 the vegetation was beginning to grow. Figure 4-7 through Figure 4-10 shows each test plot on May 17, 2005 when vegetation was just beginning to grow.

As the vegetation became established differences in species composition were noted with time and within the various covers. The predominant species in 2005 was mustard. No mustard was in the seed mixture applied so it is likely that the source of the mustard seed was compost that was spread over the slopes in the fall 2004. Numerous species of grasses and various prairie weeds were also present.

Figure 4-7 TP1N May 17, 2005 showing vegetation beginning to grow.

Figure 4-8 TP2N May 17, 2005 showing vegetation beginning to grow.

Figure 4-9 TP1S May 17, 2005 showing vegetation beginning to grow.

Figure 4-10 TP2S May 17, 2005 showing vegetation beginning to grow.

There was a sharp difference between the vegetation down a centre strip of the test plot and the rest of the test plot. The center shows taller vegetation and different species than the rest of the test plot. This was likely due to the care taken not to disturb the instrumentation located along the centre of the test plots when the test plots were harrowed and reseeded. In general, the centre had a greater biomass than the sides. This is particularly evident in Figure 4-11.

After discussions between GAL and the City of Regina regarding the abundance of agronomic species and the lack of planted grasses, the City had some of the vegetation cut. The anticipated result was that the agronomic vegetation would die and allow the planted grasses to grow. The cutting took place between July 15th and August 10th 2005. Again, care was taken to avoid the instrumentation and thus vegetation was cut mostly along the area that had been replanted the previous fall. Some of the vegetation around the instrumentation was left tall. The contrast can be seen in Figure 4-12.

Figure 4-11 June 2005, showing contrast between the centre and outer vegetation on TP2S.

Figure 4-12 TP1N August 2005, showing vegetation left standing in a centre strip, on TP1N.

There was some regrowth of the vegetation after the cutting in 2005, although it was late in the season. The vegetation reestablished itself during the 2006 season, and once again comprised a large amount of mustard, although based on observations the amount of grasses increased over that of 2005.

The south slope received more net radiation than that received by the north slope. This allowed the vegetation on the south slope to start growing earlier in the year. The additional net radiation also allowed the vegetation to thrive, resulting in taller denser plants on the south than on the north side. However, at the top of TP1S and TP2S there was far less biomass than at the mid and lower slopes. Above Diviner 2000® access tube 31 on TP1S and above tube 40 on TP2S, the vegetation density decreased toward the crest. The vegetation on TP2S in June 2005 can be seen in Figure 4-11, while Figure 4-13 shows the vegetation on TP1S at the same time. All the vegetation species information is based on observations by the author and photographs taken of the test plots.

Figure 4-13 Vegetation developed on TP1S, June 2005

The north slope vegetation was not as abundant as the south slope vegetation but was still well established. The plants were again tall and dense, if just slightly less so than those on the south plots. The mid and upper slope on TP1N had more abundant vegetation, once again, along the centre strip, with less vegetation at the bottom. The bottom slopes had more grasses and fewer non-grass crop species from approximately 15 m from the base and lower on TP1N, resulting in less biomass, particularly in 2005 (Figure 4-14).

TP2N had a slightly different pattern of vegetation. The bottom slope was quite dense and mid slope had less biomass from the DAS and down approximately 15 m. The reseeded vegetation on both test plots on the north slope was quite uniform and well established however the vegetation along the centre of the test plots was still generally much more abundant. Figure 4-15 shows the vegetation on TP2N.

Figure 4-14 Poor vegetation at lower slope near centre or TP1N, June 2005

Figure 4-15 Vegetation on TP2N, June 2005

4.2.3. Root Samples

Root samples were collected from auger cuttings in late summer 2005 in order to establish a relationship between root density and depth. It should be noted that the sorting of roots from soil was a difficult process as the roots were very small and were also cut up from the auguring process. The key objective of these measurements was to determine the relative distribution of the roots with depth as opposed to the actual root mass. Samples were taken of good and poor vegetation as well as from areas where the vegetation had been cut on the south side. However, at the time of sample collection there was no good vegetation growing on the north slope so only root samples of poor and cut vegetation were obtained. The Good vegetation that was sampled was representative of that on all test plots at all locations as was the case with the Poor vegetation.

Table 4-3 summarizes the findings of the 2005 root investigation, broken down by vegetation type and location. The samples were collected after the vegetation had been cut; therefore, some of the vegetation that was good may have been affected and is thus labelled 'good but cut'.

Table 4-3 Root mass at various locations and depths sampled in summer 2005

Approx. depth (cm)	Root Mass (g)											
	TP1N mid (good but cut)		TP2N bottom (poor)		TP2S mid (good)		TP1S top (poor)		TP1S mid (good)		TP1S bottom (good but cut)	
	Incr†	Cum.‡	Incr.	Cum.	Incr.	Cum.	Incr.	Cum.	Incr.	Cum.	Incr.	Cum.
10-22	0.15	0.15	0.34	0.34	0.03	0.03	0.45	0.45	0.41	0.41	0.21	0.21
25-37	0.2	0.35	0.2	0.54	0	0.03	0.07	0.52	0.05	0.46	0.07	0.28
39-52	0.22	0.57	0.27	0.81	0.09	0.12	0.06	0.58	0.07	0.53	0.06	0.34
55-67	0.07	0.64	0.11	0.92	0.26	0.38	0.05	0.63	0.05	0.58	0.07	0.41
70-82	0.06	0.7	0.19	1.11	0.05	0.43	0.07	0.7	0.41	0.99	0.18	0.59
85-97	0.12	0.82	0.07	1.18	0.13	0.56	0.05	0.75	0.06	1.05	0.09	0.68
97-110	ns	0.82	Ns	1.18	ns	0.56	ns	0.75	0.17	1.22	Ns	0.68
107-119	0.01	0.83	Ns	1.18	ns	0.56	ns	0.75	ns	1.22	Ns	0.68
114-126	ns	0.83	Ns	1.18	ns	0.56	ns	0.75	ns	1.22	0.03	0.71
150-160	ns	0.83	Ns	1.18	0.08	0.64	ns	0.75	ns	1.22	Ns	0.71

* ns = no sample collected at this depth

† Incr. = Incremental mass

‡ Cum. = Cumulative mass

Figure 4-16 highlights that, in general, the roots of good vegetation tapered off at a depth of approximately 100 cm, although there is some evidence of roots as deep as 160 cm. The roots of good vegetation had a higher density at approximately 70 cm compared to other samples.

In contrast to the good vegetation, roots of the poor vegetation tended to be concentrated near the surface as shown in Figure 4-17. These differences could be linked to plant species. The poor vegetation was primarily shorter, less dense grasses while the good vegetation was mostly non-grass crop species such as mustard. Non-grass species tend to have tap roots that are characterized by a long primary root with some smaller roots branching off. Grasses tend to have fibrous roots, that is, have roots that are just several thin branching roots extending from the plant's stem (Raven et al., 1999).

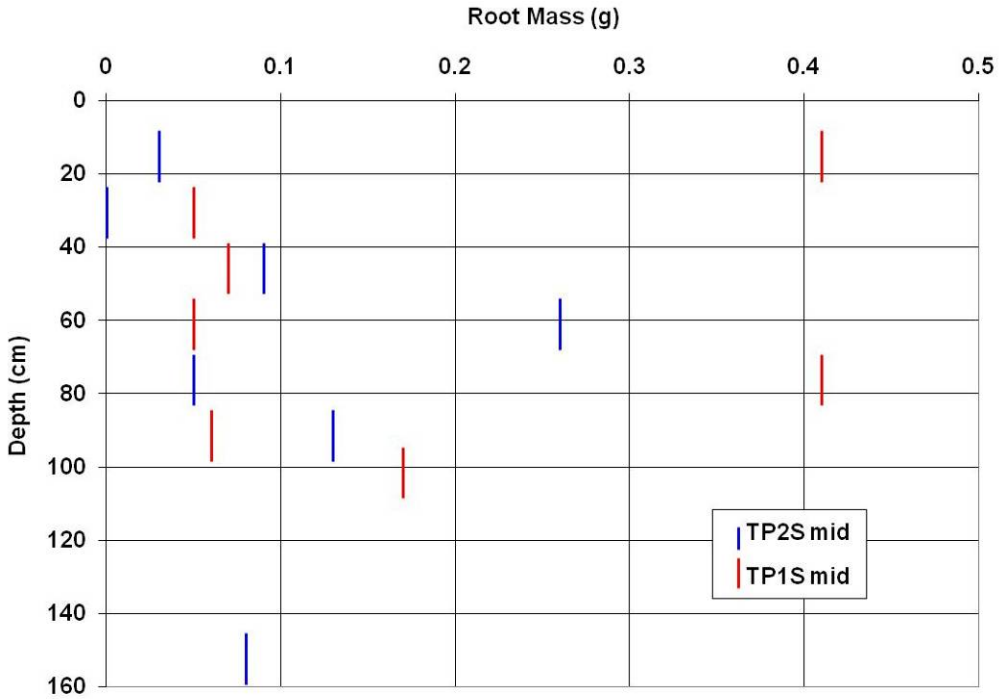

Figure 4-16 Root mass distribution for good vegetation

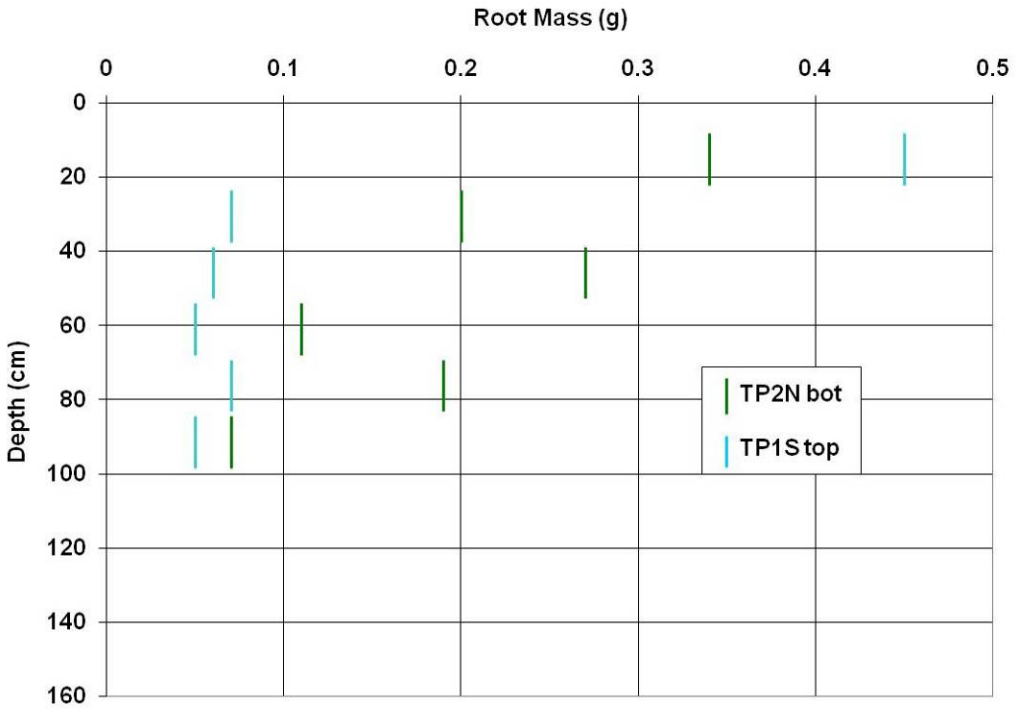

Figure 4-17 Root mass distribution of poorer vegetion

4.2.4. Density

Soil density was measured two different ways: directly from trimmed and weighed undisturbed samples; and, from *in situ* neutron probe measurements. Both results are presented here.

Undisturbed samples were obtained from each test plot at various depths using Shelby tubes. The undisturbed samples were trimmed to a known size and weighed, after which they were dried and weighed again. The *in situ* dry density values were then calculated from these measurements. Table 4-4 shows the density values obtained from the undisturbed samples.

Table 4-4 Field sampled densities

Location	Depth (cm)	Wet Bulk Density (g/cm^3)	Dry Density (g/cm^3)	Porosity
TP1N	43	1.91	1.78	0.34
TP2N	30	2.03	1.94	0.28
TP1S	30	1.78	1.69	0.38
TP2S	28	1.79	1.69	0.38
TP2S	50	1.94	1.83	0.33
Average		1.89	1.78	0.34

The CPN 501DR Depthprobe was lowered into the Diviner 2000® access tubes to measure a density distribution with depth. It should be noted that the neutron probe was not calibrated for this site or for use with the Diviner 2000® access tubes. Consequently, the results may only provide a qualitative pattern of density variation although they may not be quantitative. The results of the density testing are shown in Figure 4-18 through Figure 4-21. These figures also display the dry density as measured from the undisturbed samples. It can be seen that there was more variability on the north test plots than on the south with respect to depth as well as with respect to various slope locations. It is also evident there were no clear dense layers throughout the length of any test plot, although there were certainly areas showing higher density than others. The north slope had a greater average density than that on the south.

Based on compaction tests conducted by Golder Associates before construction, the maximum dry density from test pit material is 1.82 Mg/m^3 (GAL and OKC, 2005(b)) The average laboratory tested dry density based on field samples from the test plots was 1.78 Mg/m^3. The field sampled dry density is 98% of the maximum density as defined by compaction tests; therefore, the soil can be considered as heavily compacted. It is possible that during sampling the field samples were slightly compacted the samples, however the difficulty shoveling during instrument installation support a high density. The increased density affects the hydraulic conductivity and the porosity and thus, the water storage. For clay till, density greater than approximately 1.45 g/cm^3 will begin to limit root development (Agriculture Canada, 1992, and Barbour et al., 2007). Densities such as these that are evident on the test plots can reduce root development by up to 90% (Agriculture Canada, 1992).

4.2.5. Hydraulic Conductivity Testing

In situ hydraulic conductivity was measured using a Guelph permeameter. The hydraulic conductivity was calculated in two ways (dual height and single height method) as described by Meiers (2002). The dual height equation can overestimate hydraulic conductivity compared to the single height equation for fine-grained material (Elrick and Reynolds, 1992; and Meiers 2002). The results of the tests are shown below in Table 4-5.

The hydraulic conductivity of the topsoil varied by over three orders of magnitude depending on the individual test. Some variation may be attributed to large variations in the thickness of the

topsoil. If a test was conducted in an area with thinner topsoil, the resulting hydraulic conductivity would be a combination of that of the topsoil and the till.

The hydraulic conductivity of the till ranged over two orders of magnitude for different tests. Apart from spatial variability in cover material, this could also be affected by macro-pores providing a preferential flow path and leading to a higher hydraulic conductivity. Based on the average hydraulic conductivity for the topsoil, only approximately 0.4 mm of precipitation can infiltrate per hour. This is slightly less than the conductivity measured by Meiers et al. (2006) for a similar till on a soil cover near Fort McMurray, Alberta, perhaps due to an increased density at this landfill, or because of the lack of freeze/thaw effects and wet/dry effects on the relatively young cover.

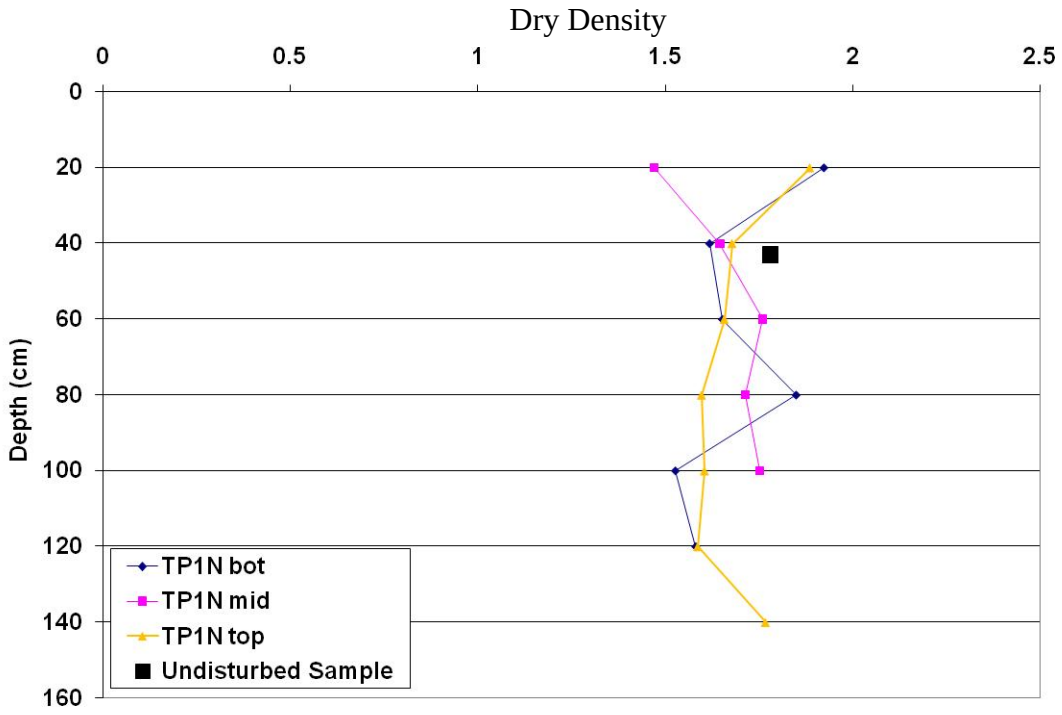

Figure 4-18 Dry Density as measured with Depthprobe and from an undisturbed sample at locations on TP1N

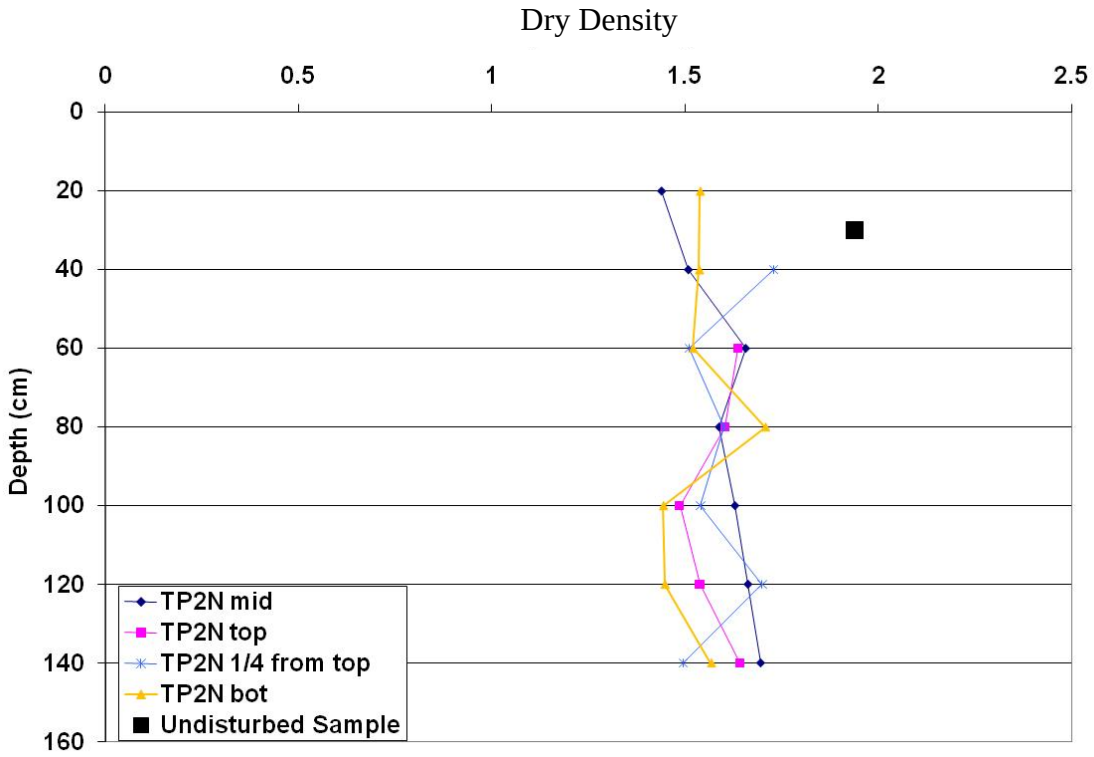

Figure 4-19 Dry Bulk Density as measured with Depthprobe and from an undisturbed sample at locations on TP2N

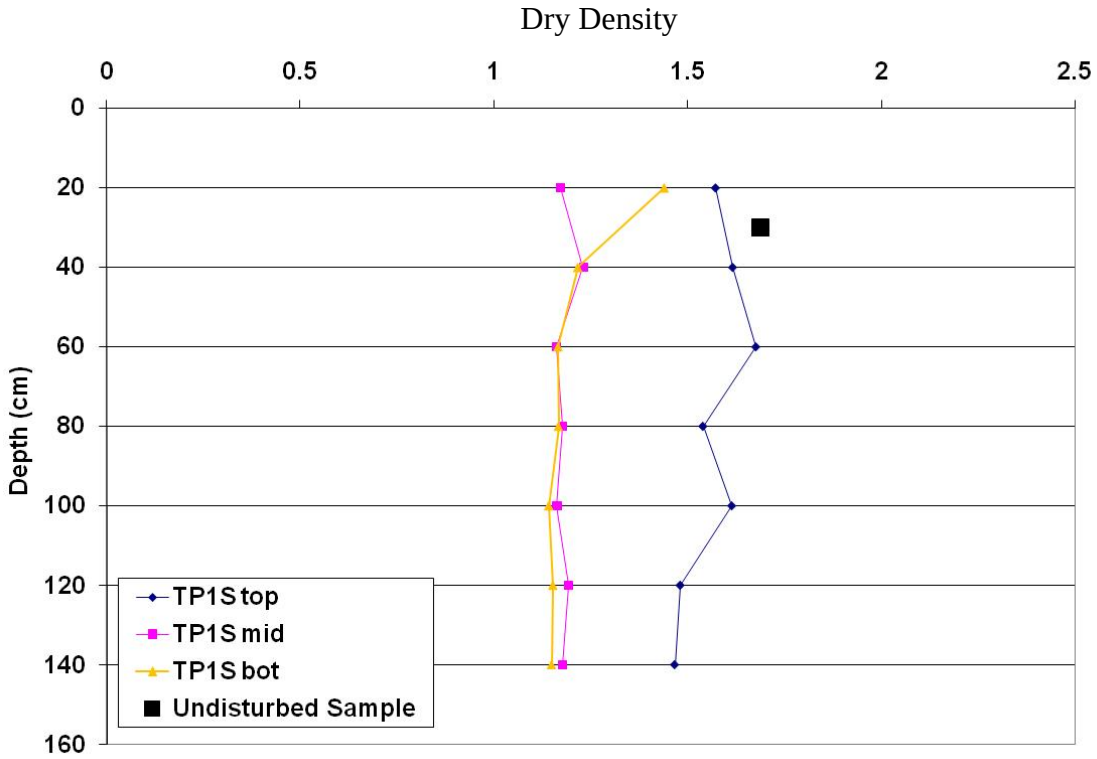

Figure 4-20 Dry Bulk Density as measured with Depthprobe and from an undisturbed sample at locations on TP1S

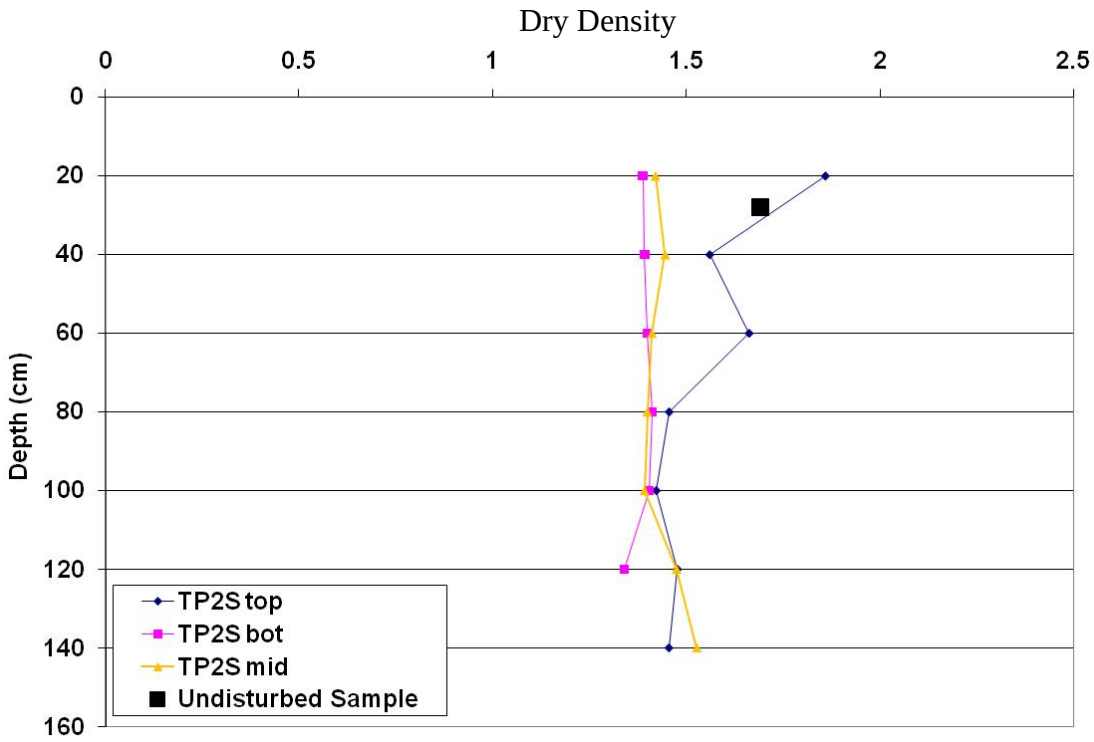

Figure 4-21 Dry Bulk Density as measured with Depthprobe and from an undisturbed sample at locations on TP2S

Table 4-5 Hydraulic conductivity from Guelph permeameter

	Hydraulic Conductivity (cm/s)	
	dual height	**single height**
Topsoil	7.1E-06	1.9E-04
	1.6E-04	3.8E-04
	4.4E-05	8.7E-06
	1.1E-03	4.2E-05
		8.5E-05
Geometric Mean	**8.61E-05**	**7.42E-05**
Till	2.2E-05	2.3E-06
	2.0E-04	3.6E-05
	1.7E-04	3.1E-06
	1.2E-05	5.8E-05
		1.5E-05
		1.7E-05
		1.7E-06
		2.3E-05
Geometric Mean	**5.47E-05**	**1.05E-05**

4.3. Field Instrumentation Program

This section presents and discusses the results from the field instrumentation. This section contains data from the following monitoring: climate, soil temperature, matric suction, soil moisture content, runoff and interflow.

4.3.1. Climate Data

Climate data was measured at a meteorologic station at the top of TP1N with net radiation also being measured on TP2S. This data includes precipitation, air temperature, net radiation, relative humidity, wind speed and wind direction as well as the results of snow surveys conducted in late winter 2005 and 2006.

Precipitation

A rainfall tipping bucket was installed on the top of TP1N. There were problems with sediment and debris reducing the amount of precipitation recorded by the tipping bucket. Also, the snowfall adaptor that was installed on the tipping bucket repeatedly blew over resulting in a loss of data. Due to several discrepancies, the precipitation data was considered suspect. The largest discrepancy was noticed during a large storm event in August 2005 when the soil moisture increased by approximately 30 mm, but the on site tipping bucket only recorded a precipitation of 14 mm. The Environment Canada weather station at the Regina Airport showed a precipitation of 35 mm for the same event. It is likely that daily measurements may differ between these two different locations due to the large distance between them (approximately 8 km); however, it was felt that the magnitude of differences would be less than the errors experienced on site. Therefore instead of using untrustworthy data from site, the data from the airport, will be used.

The difference between the City of Regina Airport and the on-site tipping bucket can be seen in Figure 4-22. The cumulative precipitation recorded by the on-site tipping bucket was 649.2 mm, from June 29, 2004 to October 31, 2006. The cumulative precipitation recorded at the airport was 821.6 mm for the same time period, a difference of 172.4 mm, or approximately 21%.

Monthly precipitation totals for both the tipping bucket and the Environment Canada COR Airport data are shown in Figure 4-23. June tends to be the month with greatest precipitation, averaging 83 mm from the Environment Canada site. This is slightly higher than the historical average from Environment Canada for that month, which is 75 mm. April 2006 (98.5 mm) can be seen to be much higher than April 2005 (8 mm). The historical average for the Regina Airport from Environment Canada for April is 23.5 mm, indicating that April 2006 was especially high, and April 2005 was very low.

For the rest of this thesis, when precipitation is referred to, it is referring to that from Environment Canada at the COR airport.

The precipitation was 190.2 mm during the 2004 monitoring period (June 29 to December 31), 332.4 mm in 2005 (January 1 to December 31) and 335 mm in 2006 (January 1 to October 31). The long-term average precipitation as recorded at the Regina Airport by Environment Canada is 388 mm, while the average precipitation during the monitoring period was 352 mm, a difference of only 9%.

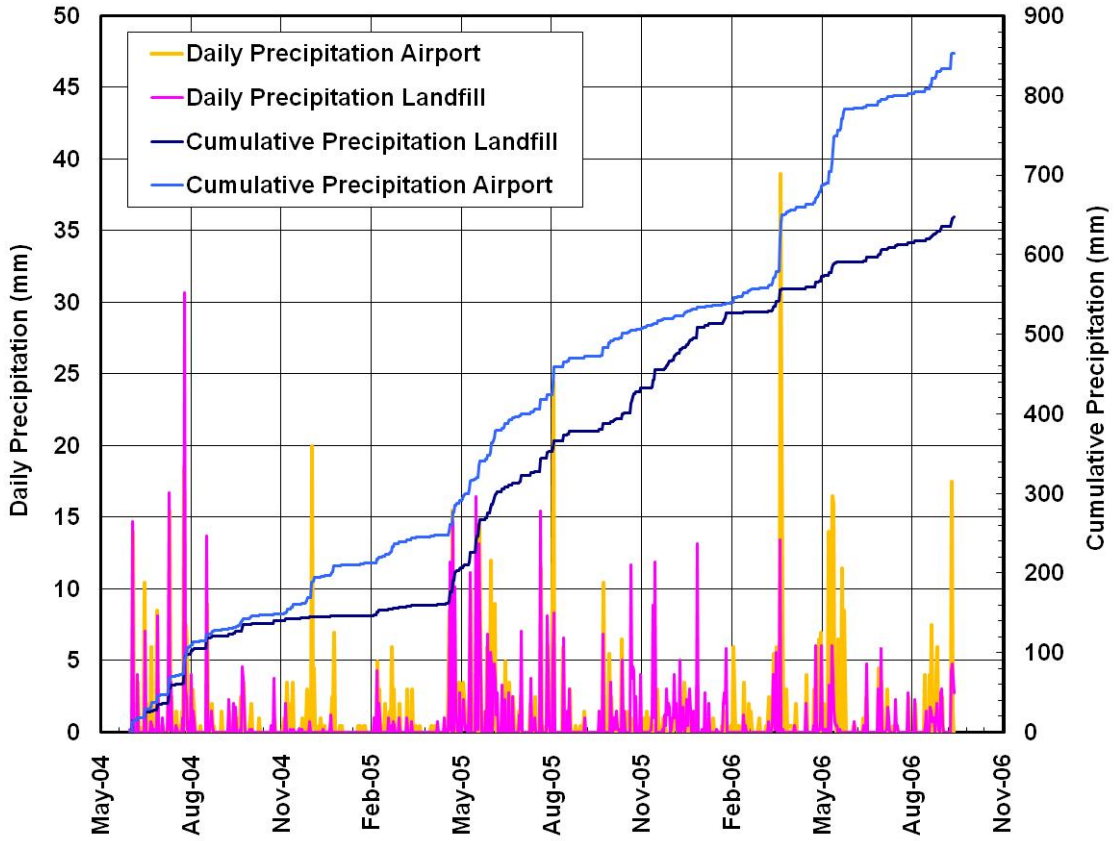

Figure 4-22 Precipitation from on site tipping bucket and from City of Regina Airport

There were 10 precipitation events greater than 15 mm recorded during the monitoring period. The largest single precipitation event (39 mm; recorded at the Regina Airport) occurred on April 17, 2006.

A snowfall adaptor was installed for the winter months, but due to the need for regular maintenance of antifreeze levels, as well as the possibility of snow either building up on top of the adaptor or blowing off before it has time to be measured, the precipitation measured from the tipping bucket during the winter months may not be accurate. For these reasons, along with concerns that the tipping bucket was malfunctioning, the winter precipitation data is not used in subsequent interpretations of the water balance.

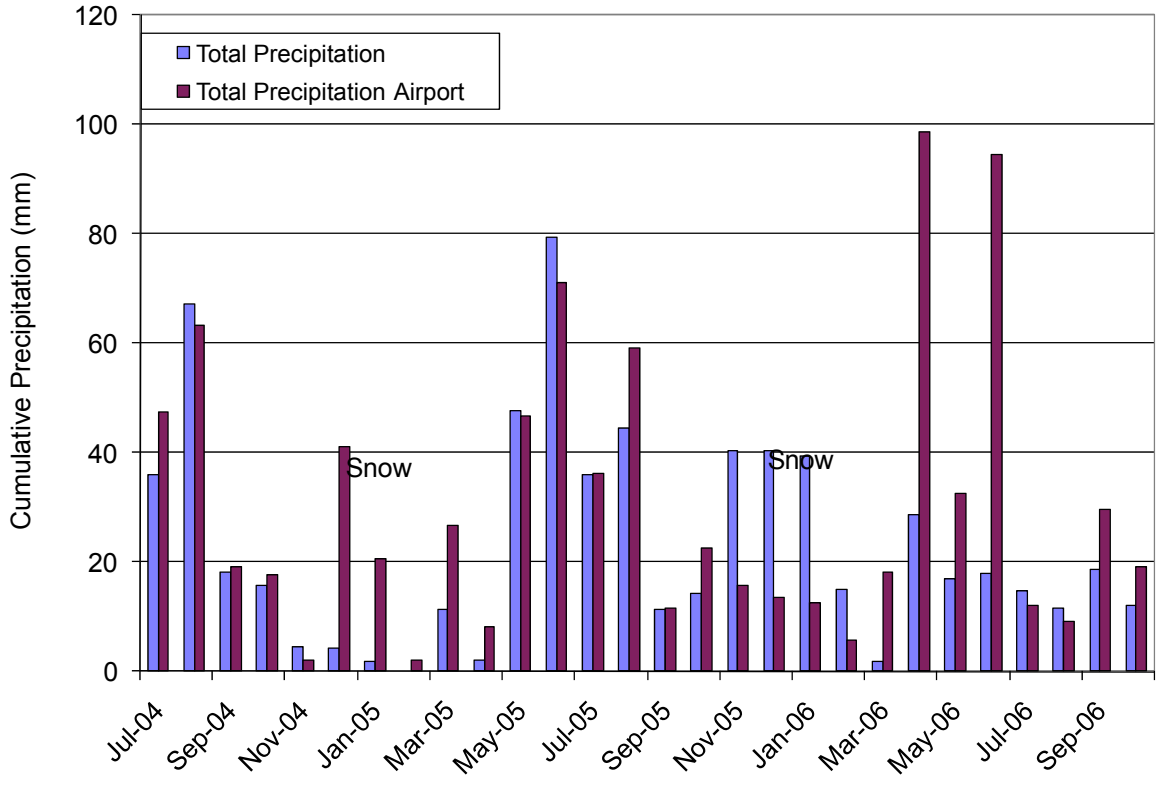

Figure 4-23 Distribution of Cumulative Precipitation at the Landfill and at Regina Airport

The primary interest in precipitation is to understand how it interacts with the soil. Because of little water movement with the soil occurs in the winter months, the amount of snowfall on a site is of little interest. However, the amount of snow that melts on the test plots does interact with the soil and play a role in the water balance. The amount of snow that melts can best be estimated as the snow water equivalent (SWE) measured from the snowpack just prior to melt.

Therefore, for subsequent calculations and analysis, the rainfall plus SWE from snow surveys conducted prior to melt are used instead of the total precipitation.

The results from the snow surveys conducted at the site are summarized in Table 4-6. The year 2005 had much greater (SWE) than 2006, 2.5 times greater on the south, 3.1 times greater on the north. Looking at the precipitation totals (Figure 4-23) it can be seen that the airport measured much more precipitation in the winter months in 2005 than in 2006, particularly close to spring melt. This timing is important because this snowfall would have less chance to sublimate or blow off the test plot.

Table 4-6 SWE from snow surveys in 2005 and 2006

	SWE (mm)	
	North	**South**
2005	42	22
2006	14	9

The distribution of SWE for 2006 is shown in Figure 4-24 through Figure 4-27. The zero of the axis is at the lowest slope position and on the left when looking at the slope at base of the test plots and the measurements are in mm. The north test plots showed greater SWE on the right (west) side of each test plot. This was likely due to wind redistribution, which was primarily from the northeast or southwest (discussed subsequently). The distribution of snow on the south slope was much more variable and this is attributed to wind redistribution. On all test plots, the redistribution was affected by vegetation as the accumulated snow pack was generally deeper in taller vegetation and shallower where the vegetation is shorter. Snow fences were also placed on the test plots by the COR and the locations are approximated on each figure as the white dashed line. Snow generally was deeper around the snow fences, particularly on the south slope.

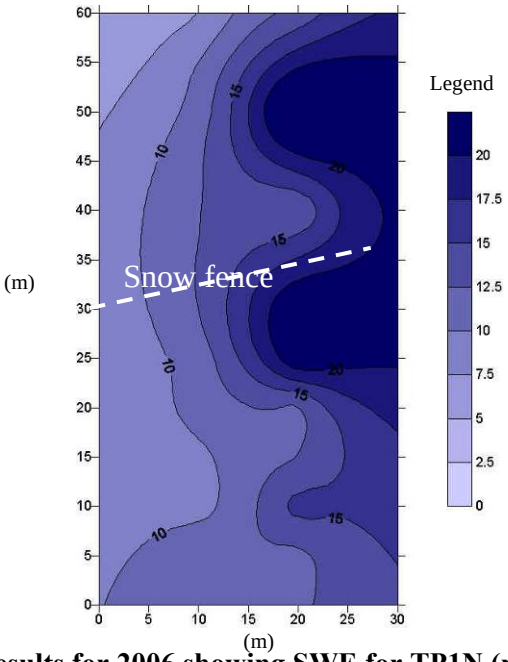

Figure 4-24 Snow survey results for 2006 showing SWE for TP1N (mm)

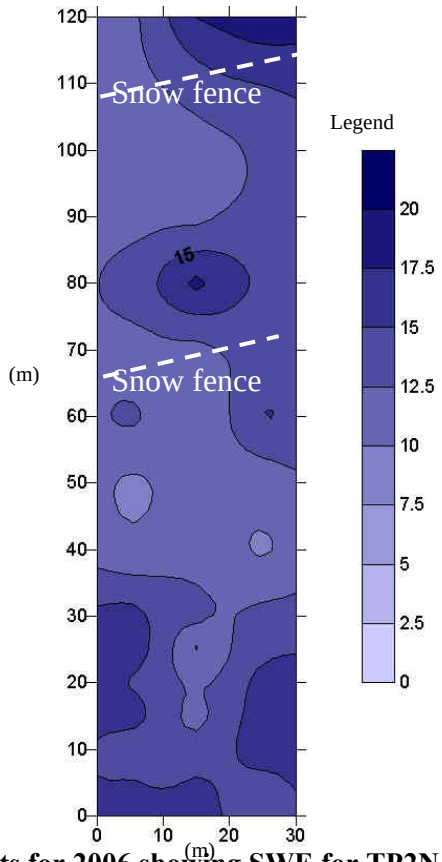

Figure 4-25 Snow survey results for 2006 showing SWE for TP2N (mm)

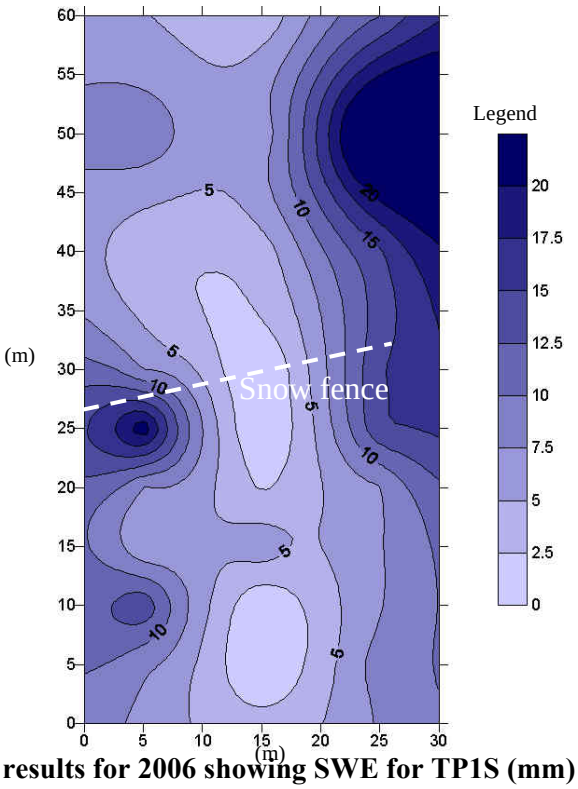

Figure 4-26 Snow survey results for 2006 showing SWE for TP1S (mm)

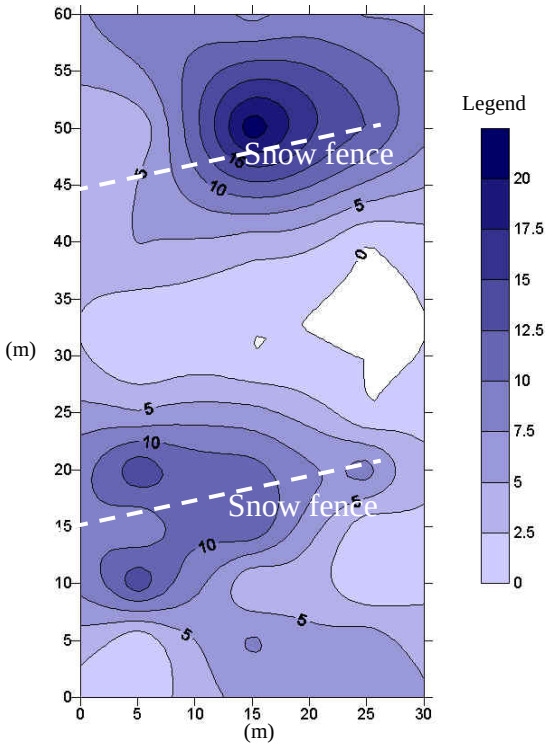

Figure 4-27 Snow survey results for 2006 showing SWE for TP1S (mm)

Air Temperature

Air temperature had been recorded at the test plots since June 24, 2004. Figure 4-28 shows the daily minimum, average and maximum air temperature recorded at the test plot. The only full year of data is 2005, which had an average air temperature of 3.7˚C, compared with the historical average temperature (Environment Canada, 2007) of 2.8˚C. The yearly daily temperature varied between -34.8˚C and 36.4˚C.

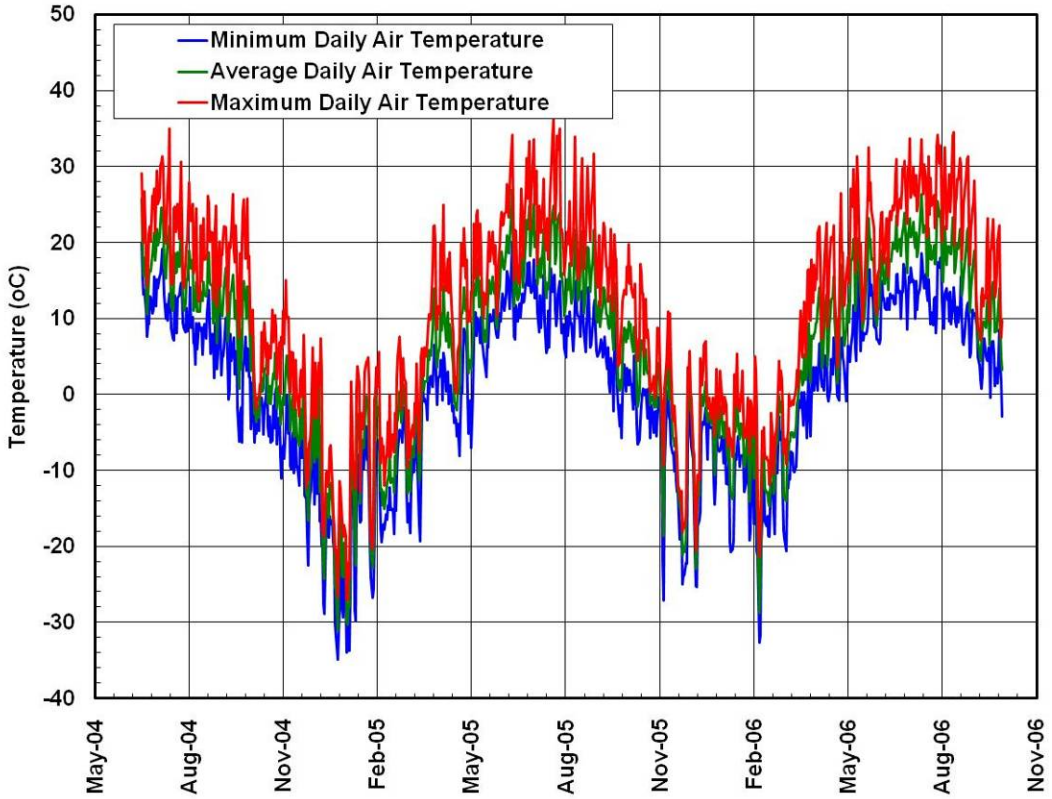

Figure 4-28 Daily minimum, average and maximum air temperature on the test plots

The average monthly temperature recorded on the site closely matched the historical average recorded at the Regina Airport by Environment Canada. This is shown in Figure 4-29. July was the warmest month and January was the coldest.

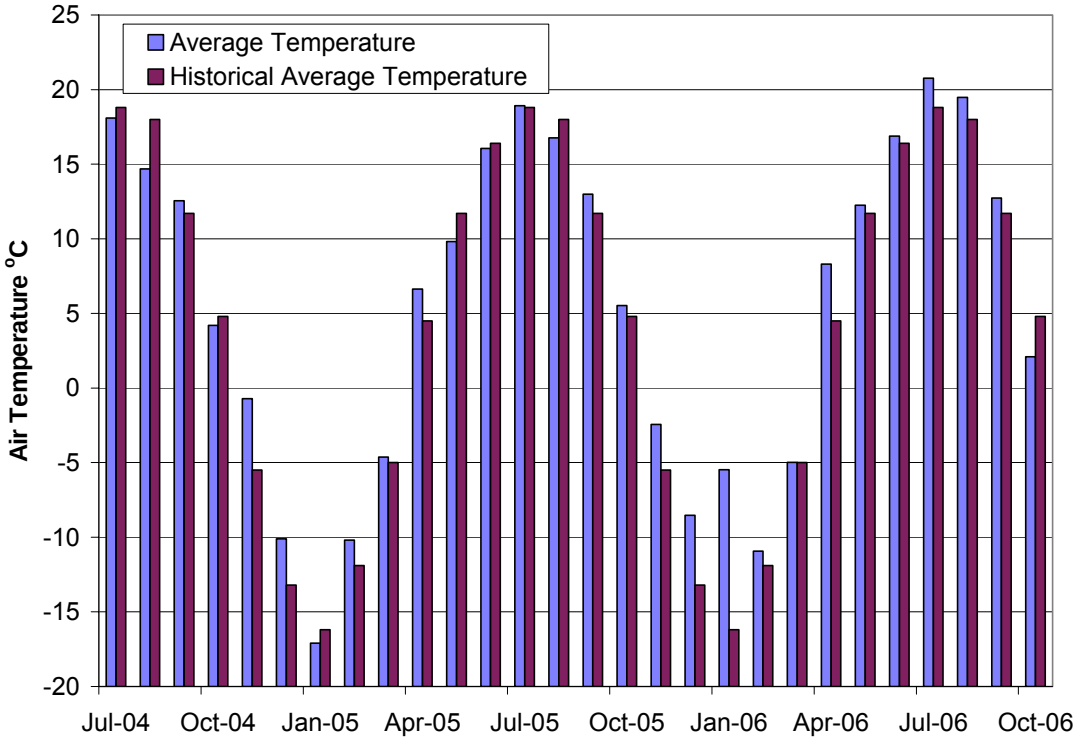

Figure 4-29 Average monthly temperature recorded on site and historically

Relatively Humidity

The relative humidity measured at the site varied between 12% and 100% for the monitoring period. The minimum, average and maximum values of daily relative humidity are shown in Figure 4-30. The average relative humidity was 72%, which matches closely to the historical average relative humidity of 69%.

The average relative humidity is higher in the winter months with a maximum monthly average being 90% in January 2006 and the minimum 54.2% in August 2006. The average monthly relative humidity is shown in Figure 4-31.

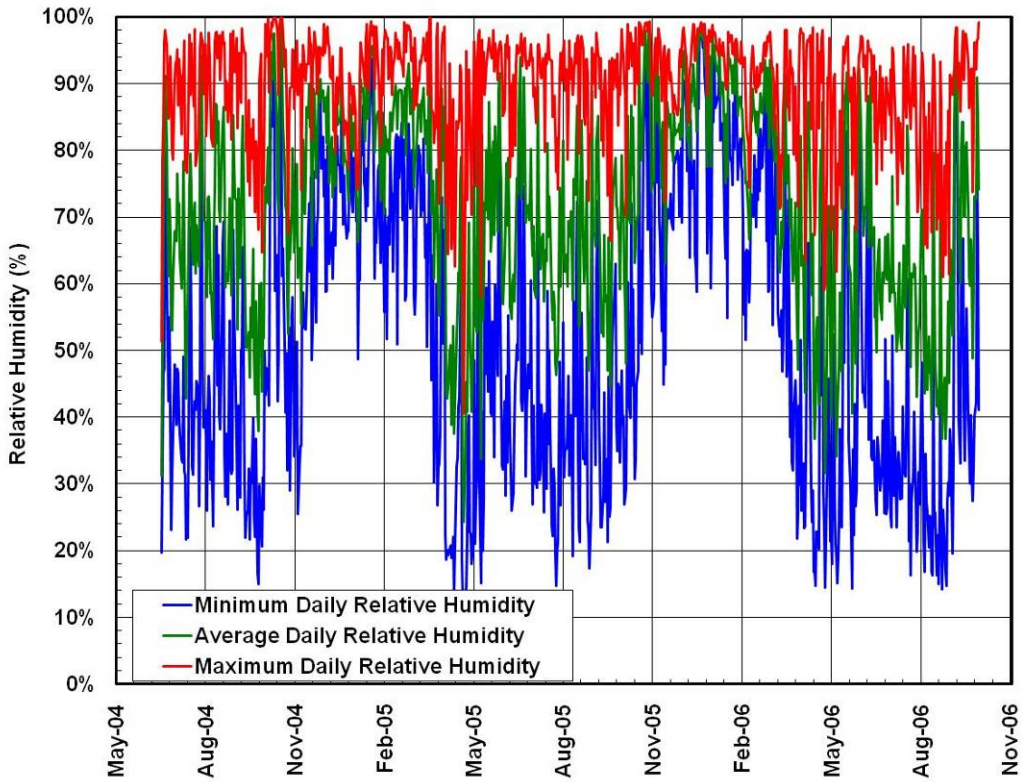

Figure 4-30 Minimum, average and maximum daily relative humidity

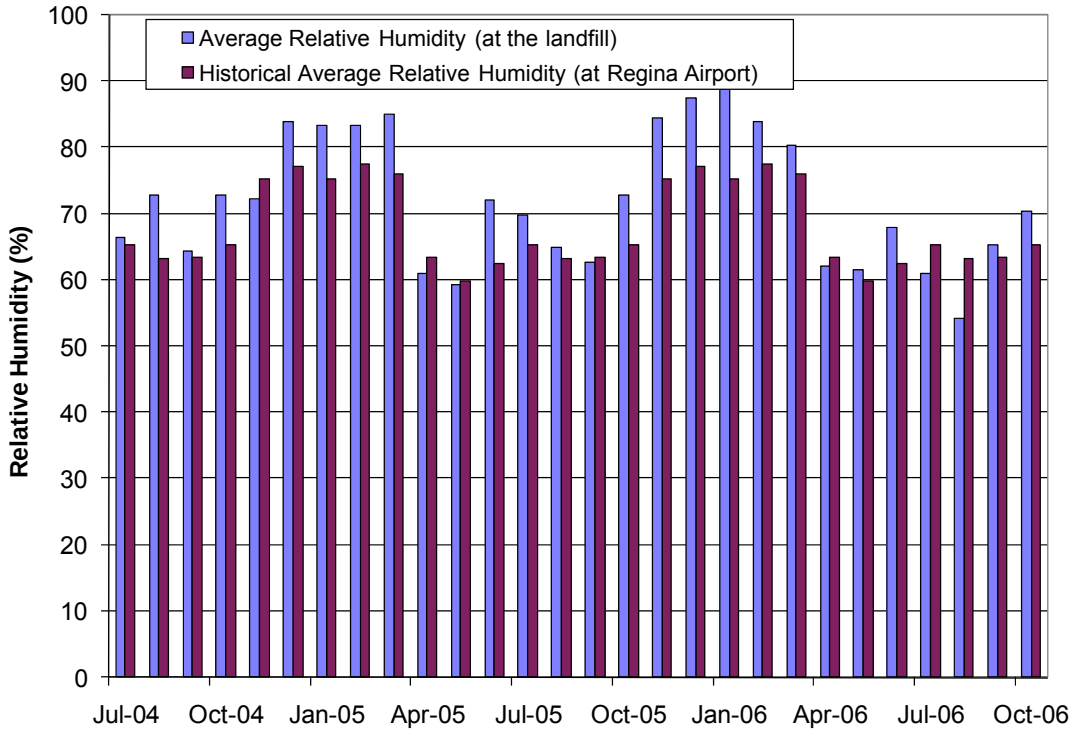

Figure 4-31 Monthly average and historical values of relative humidity

Wind Speed and Direction

Wind speeds of between 0 and 17.8 m/s were recorded during the monitoring period. The minimum, average and maximum values of daily wind speed are shown in Figure 4-32. The average wind speed was 4.0 m/s for the entire monitoring period. While the wind direction was quite variable, the wind was primarily from either the northeast or southwest. There was no clear seasonal difference in wind directions. Wind speed is important as stronger winds will cause more evapotranspiration.

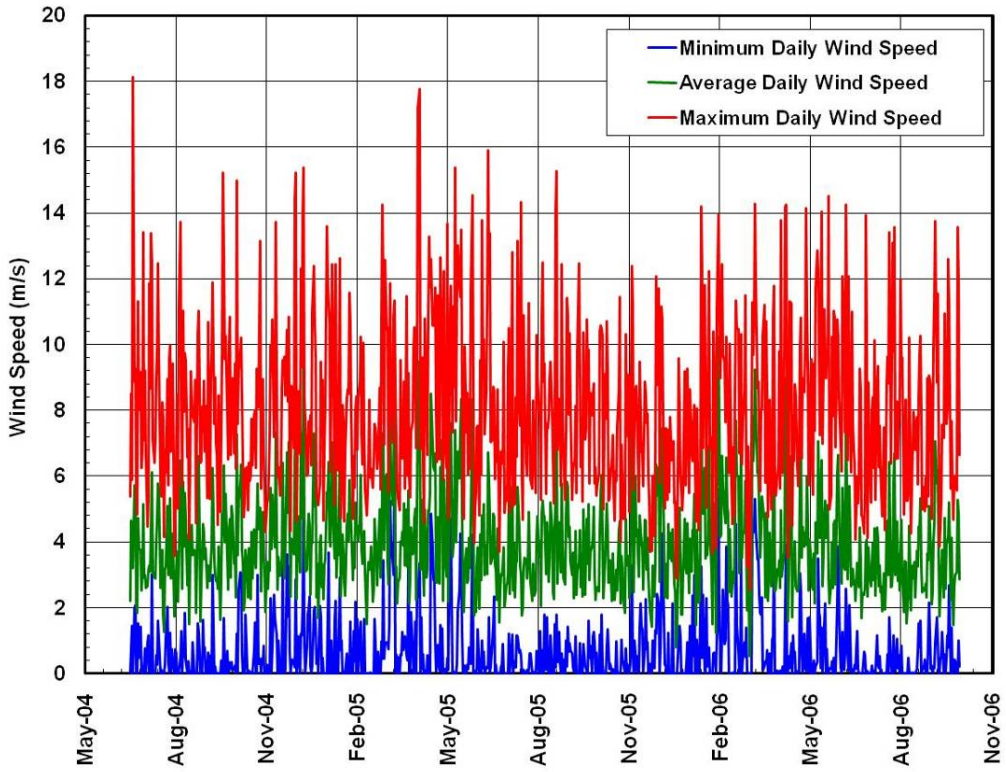

Figure 4-32 Minimum, average, and maximum daily wind speed

Net Radiation

Net radiation was measured on both the north and south slopes to assess the difference based on slope aspect. The daily net radiation for both slopes is shown in Figure 4-33. Net radiation was positive in the summer months, and negative in the winter months. Negative net radiation indicates that the radiation from the ground is greater than that coming from the sun. The net radiometer on the north slope was not functioning between November 2005 and April 2006, likely due to interference from snow or debris, and the net radiometer on the south slope was not

functioning from August 2006 to the end of monitoring due to damage from wildlife. To determine the cumulative radiation as shown in Figure 4-34, the net radiation from the previous year was used for periods during which the sensors were not functioning. The cumulative net radiation was greater on the south slope than the north with the greatest difference occurring in the fall as the south continued to experience large positive daily net radiation further into the fall. By filling in missing data with data from the same time period in different years, the estimated net radiation totals are 3,732 MJ/m^2 on the south and 2,657 MJ/m^2 on the north. Calculated net radiation for the south slope, based on Weeks and Wilson (2006), is approximately 3,040 MJ/m^2, and for the north is 1,733 MJ/m^2, an average of 27% less than that measured on site. During only the unfrozen dates the net radiation on the south is approximately 16.8% greater than that on the north. The Weeks and Wilson (2006) method requires daily estimates of albedo which may contribute to the difference between the estimated and measured values. Also, the exact slope angle and orientation of the test plots was not used in the calculation, only an exactly north and south facing and slope angle measured at construction. The Weeks and Wilson calculations are included in the CD accompanying this thesis. This has large implications for the water balance, as net radiation is the energy source for both evaporation and transpiration.

Runoff and Interflow

Each test plot had a runoff collection channel and each capillary break test cover had an interflow collection channel to collect and measure water diverted above the sand layer. There were several problems with the runoff channels causing the readings to be untrustworthy. Debris would interfere with the channel flow and sometimes block water from entering the channel, or from draining from the channel. Holes in the geomembrane lining the channel, perhaps caused by wildlife, allowed collected water to escape without being measured by the sonic depth probe. The entire channel shifted over time, perhaps from settlement and movement of the covers, causing some channels to become too shallow to contain all the runoff. As a result runoff water flowed off the test plot. Debris would also occasionally sit in the weir box causing a falsely high reading of water height. The sonic depth probe used to measure depth is temperature sensitive, and was corrected using a temperature sensor in the hut. The sensor in the north hut malfunctioned during the first year of monitoring. The data was manually adjusted in order to remove false readings due to debris or temperature errors. Therefore, the data presented are only estimates of what was experienced at the site.

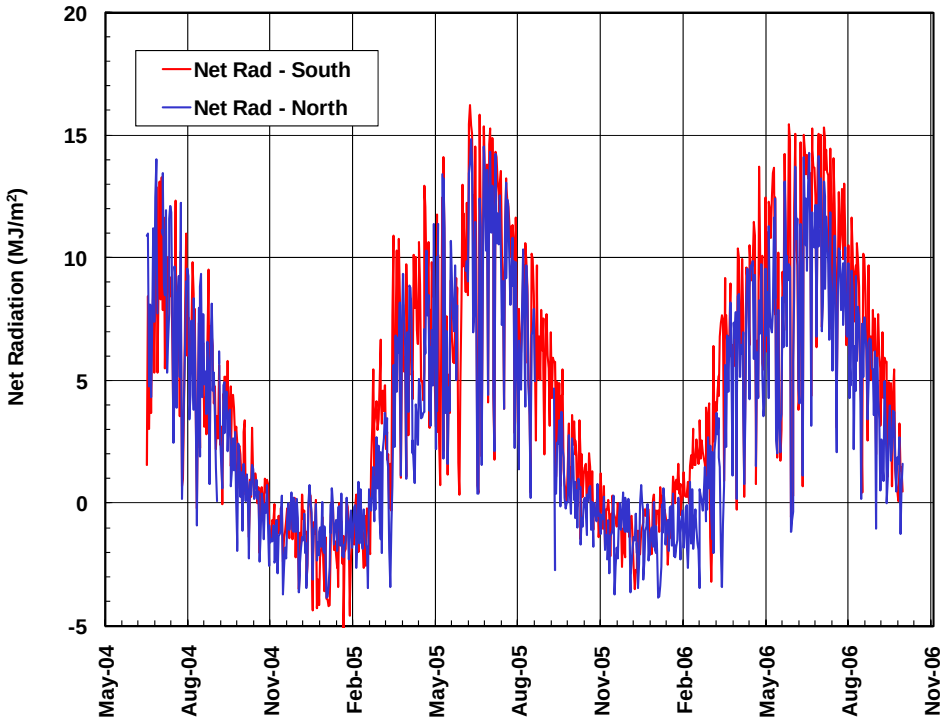

Figure 4-33 Daily net radiation measured during the monitoring period.

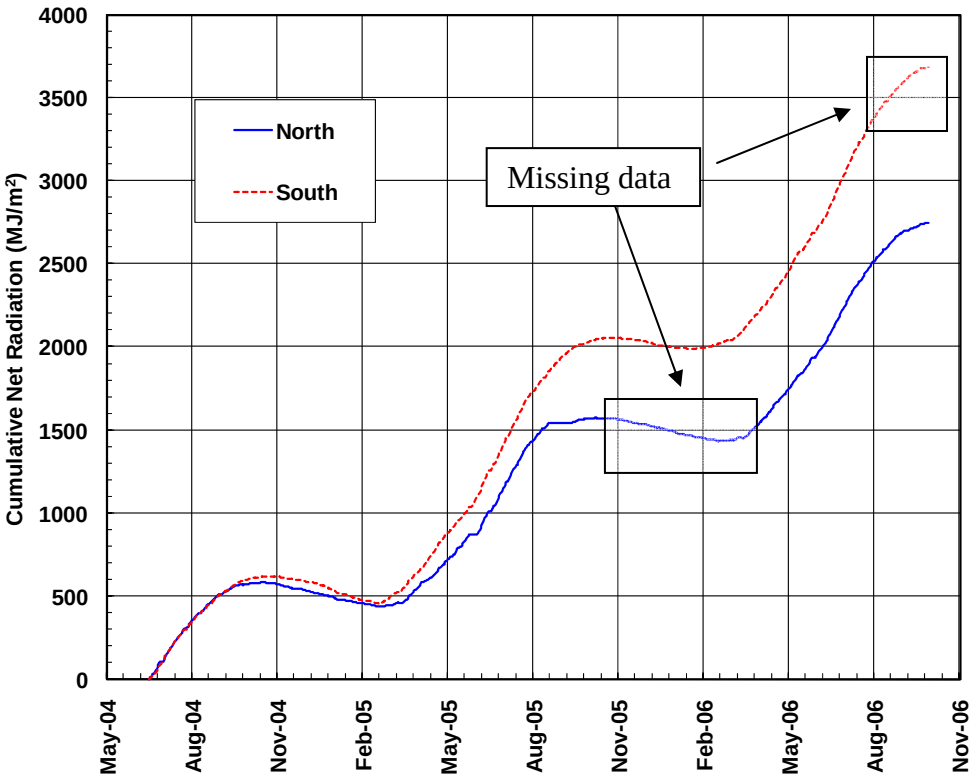

Figure 4-34 Cumulative net radiation in the monitoring period with assumed missing data.

Cumulative runoff for the four test plots is shown in Figure 4-35 as a depth, (total volume divided by the area of the test plot). The shaded area indicates when the average air temperature was less than 0ºC. It can be seen that the majority of the runoff occurred from snowmelt in the spring, with very little attributed to summer rain events. The north slope experienced much more runoff than the south slope. This was largely due to the greater snowpack on the north slope.

The cumulative runoff for each test plot is estimated at 42 mm, 38 mm, 14 mm and 16 mm for TP1N, TP2N, TP1S and TP2S respectively. Approximately 28% and 100% of the SWE on the north slope appeared as runoff in the spring of 2005, and 2006, respectively. The south showed runoff as 19% in 2005 and 37% in 2006 of SWE. The wide variation was likely a result of uncertainty in the estimation of runoff from the poor field data.

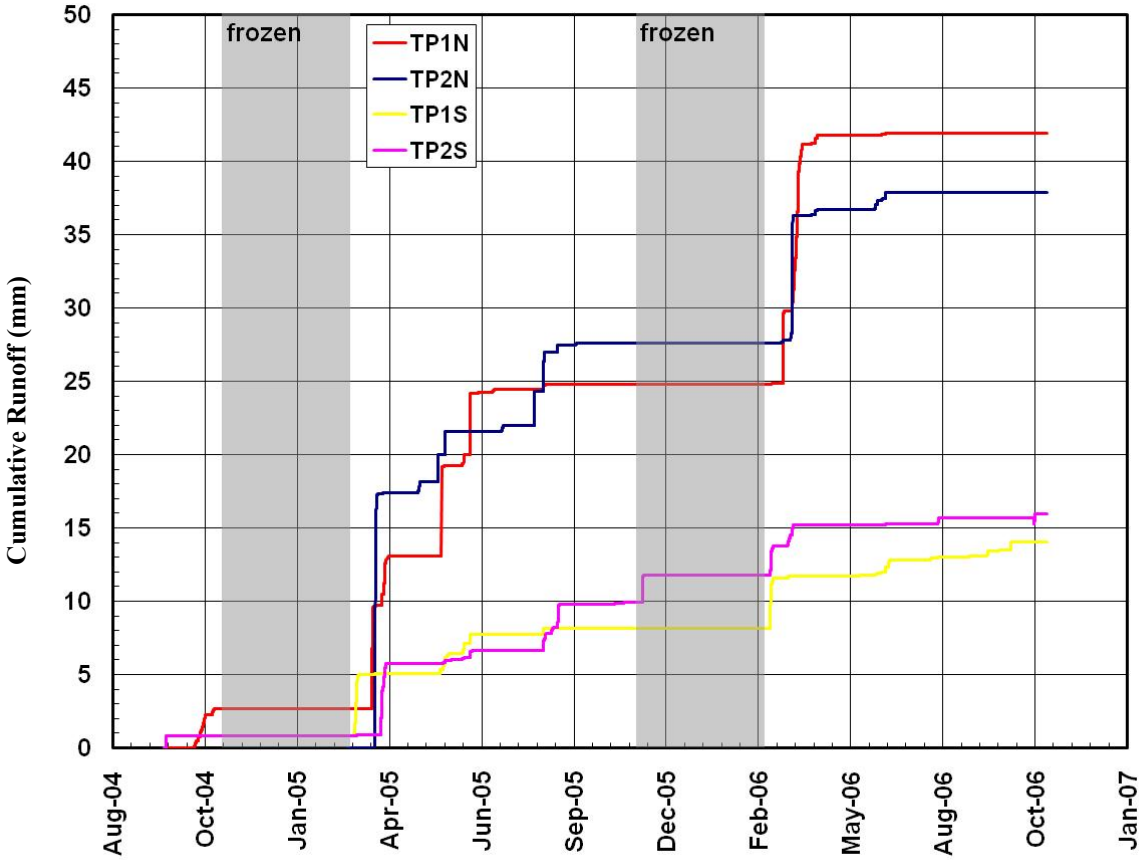

Figure 4-35 Cumulative Runoff from each test plot

Interflow measured on the capillary break test plots over the monitoring period was negligible. The design of the interflow collection system was such that it would collect water moving laterally through the till above the sand. However, if the suction in the till above the sand

decreased sufficiently, the interflow water would break through into the sand. Therefore, if substantial interflow had occurred, it would have been in the sand layer and would not have been collected by the interflow collection system.

4.3.2. Soil Temperature Data

Automated Measurements

The temperature recorded at midslope on each test plot was plotted in the contour map in Figure 4-36. Blank areas in the plot are due to either sensor errors or errors due to estimating temperature between discreet data points. The minimum temperature recorded was -19.9˚C on TP2N, and the maximum temperature was 43.3˚C on TP2S. The greatest extremes occurred at the surface and the range of temperatures decreased with increasing depth.

The covers tended to cool down from the top but warm up from both the top and the bottom. This was evident when looking at the slope of the contour lines in the figure above. When the cover was cooling, the contours changed from warm to cool with the slope of the contour lines from upper left to lower right, indicating that cooling was occurring at shallower depths first. When the cover was warming up and the contours were changing from blue to red, the contour lines were nearly vertical, sloping slightly to the right, particularly toward the bottom of the cover. This indicated that the entire profile reached the same temperature on the same day at the top and bottom of the cover but not at the middle of the cover. This might suggest that the landfill was heating the base of the cover. Based on the work of Bendz and Bengtsson (1996) it can be assumed that the upward heat flow from the waste is approximated with a steady state equation during the winter months. Using the method outlined in Bendz and Bengtsson (1996), with an assumed thermal conductivity of 0.75 W/m/K (based on Abu-Hamdeh and Reeder, 2000), the heat flux from the waste varies from approximately 1.0 to 8.5 W/m^2.

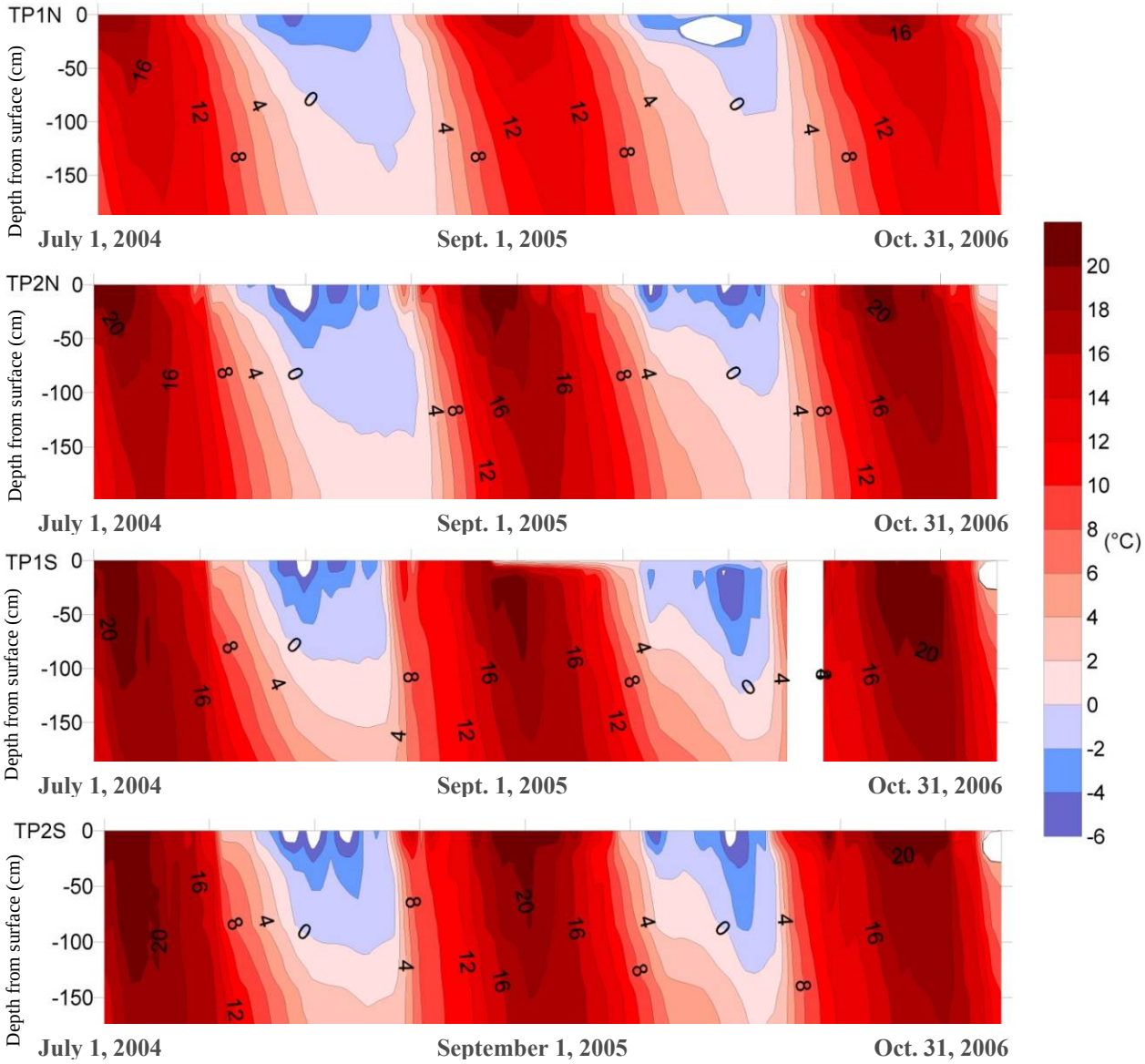

Figure 4-36 Spatial and temporal distribution of temperature in covers..

The depth of freezing during the monitoring period was estimated based on the *in situ* temperature data and is presented in Table 4-7. The depth of freezing is important as freeze-thaw cycles can cause changes in the hydraulic conductivity (GAL and OKC, 2005(b)). In 2004/2005 the north slope displayed a greater depth of freezing than that displayed by the south; however, in 2005/2006 the south slope showed a greater zone of freezing than that shown by the north.

Table 4-7 Depth of freezing through cover profiles

	2004/2005	2005/2006
TP1N	155 cm	100 cm
TP2N	140 cm	75 cm
TP1S	100 cm	125 cm
TP2S	110 cm	140 cm

Manual Temperature Readings

Temperature was also measured manually at the top and bottom of each test plot and the results of this are shown in Figure 4-37 through Figure 4-40. The dashed line shows the downslope location and the solid line shows the upslope location. The upslope nest of temperature sensors on TP1S was destroyed, presumably by wildlife. A repair was attempted in the summer of 2005; however, it became dislodged again shortly after and was therefore unavailable for periods of time.

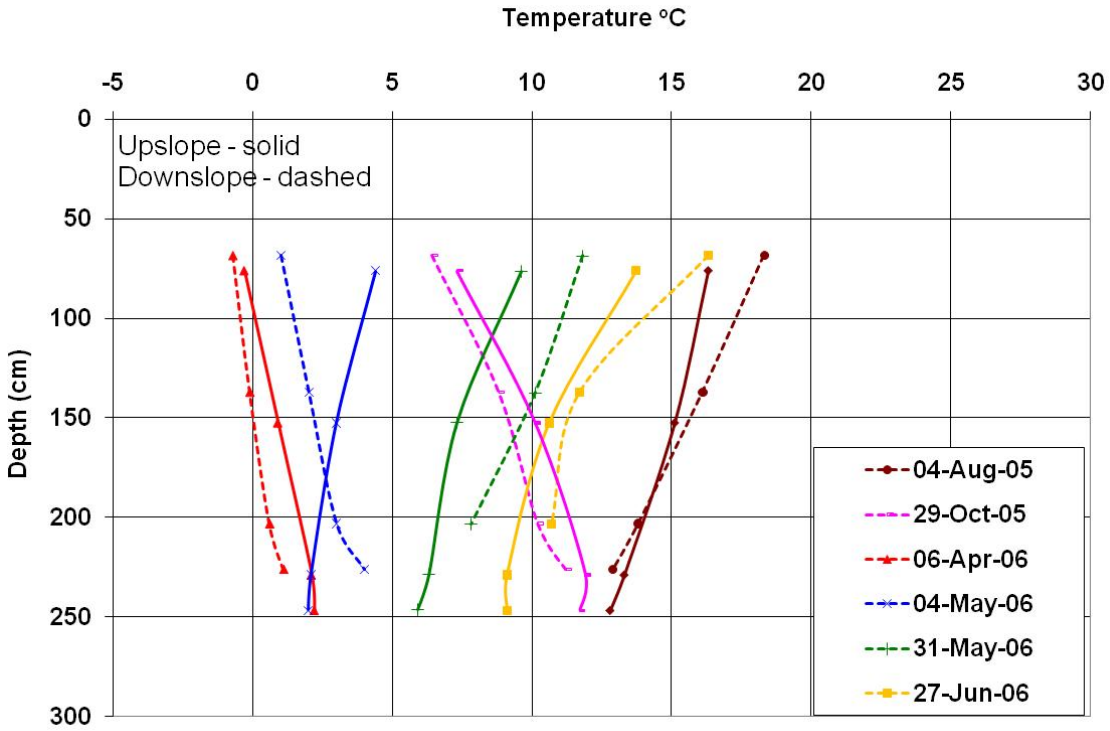

Figure 4-37 Manual temperature readings TP1N

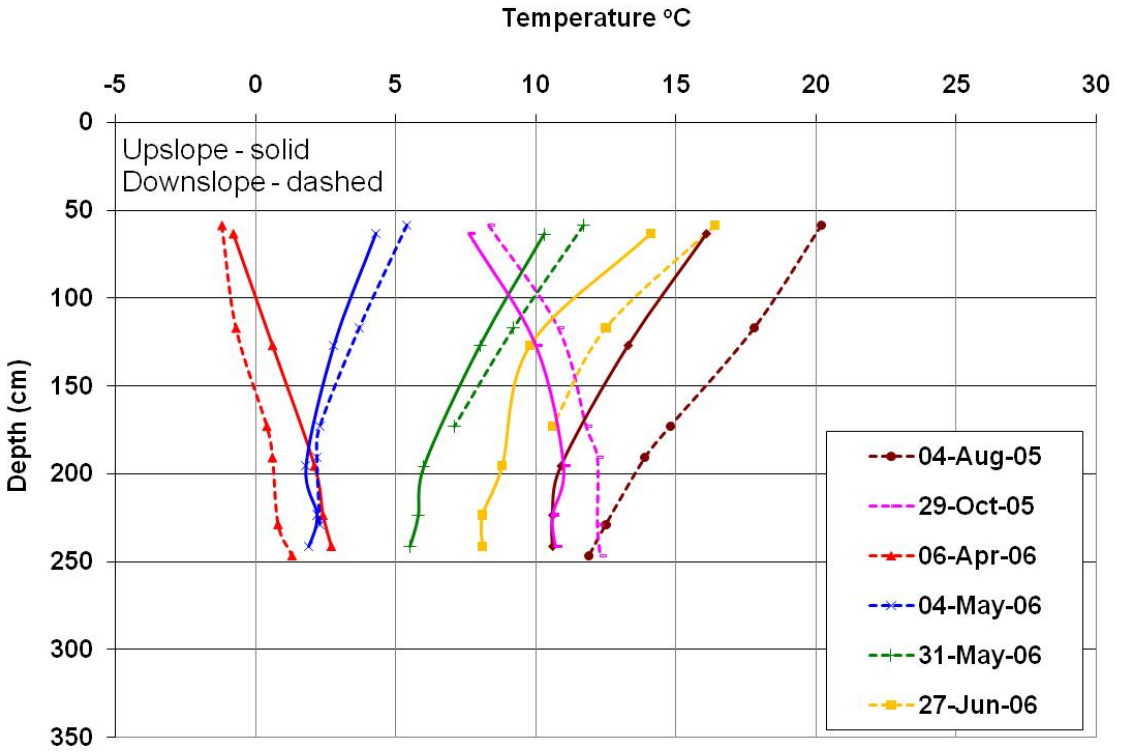

Figure 4-38 Manual temperature readings TP2N

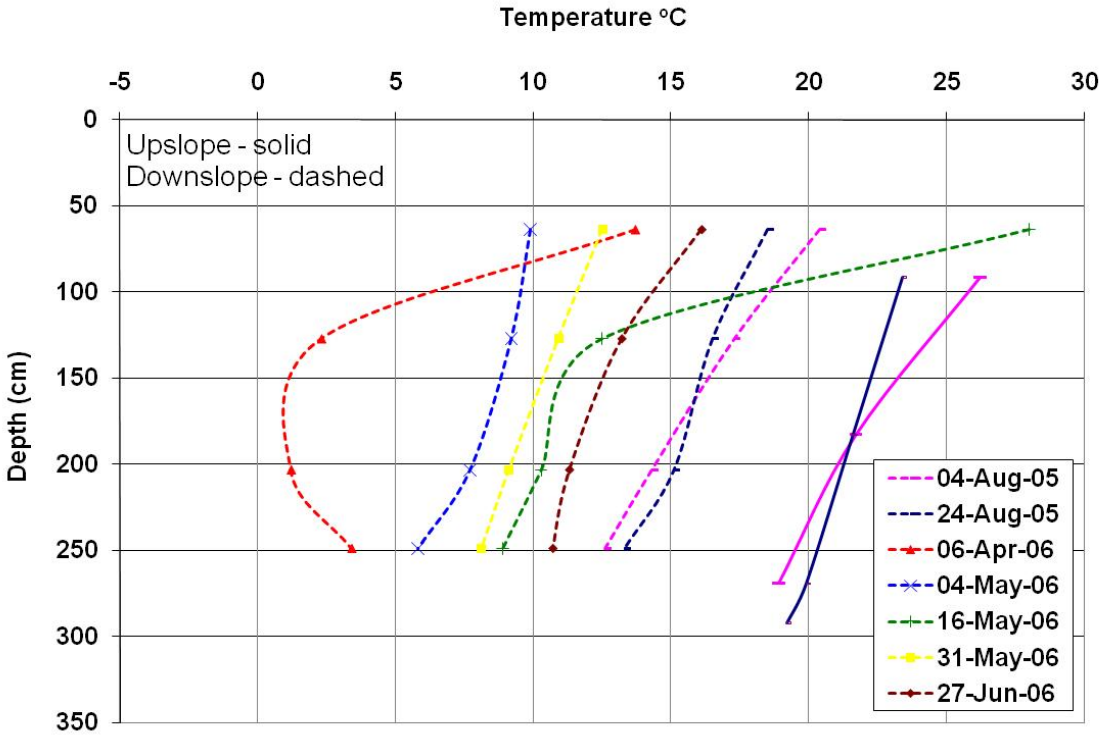

Figure 4-39 Manual temperature readings TP1S

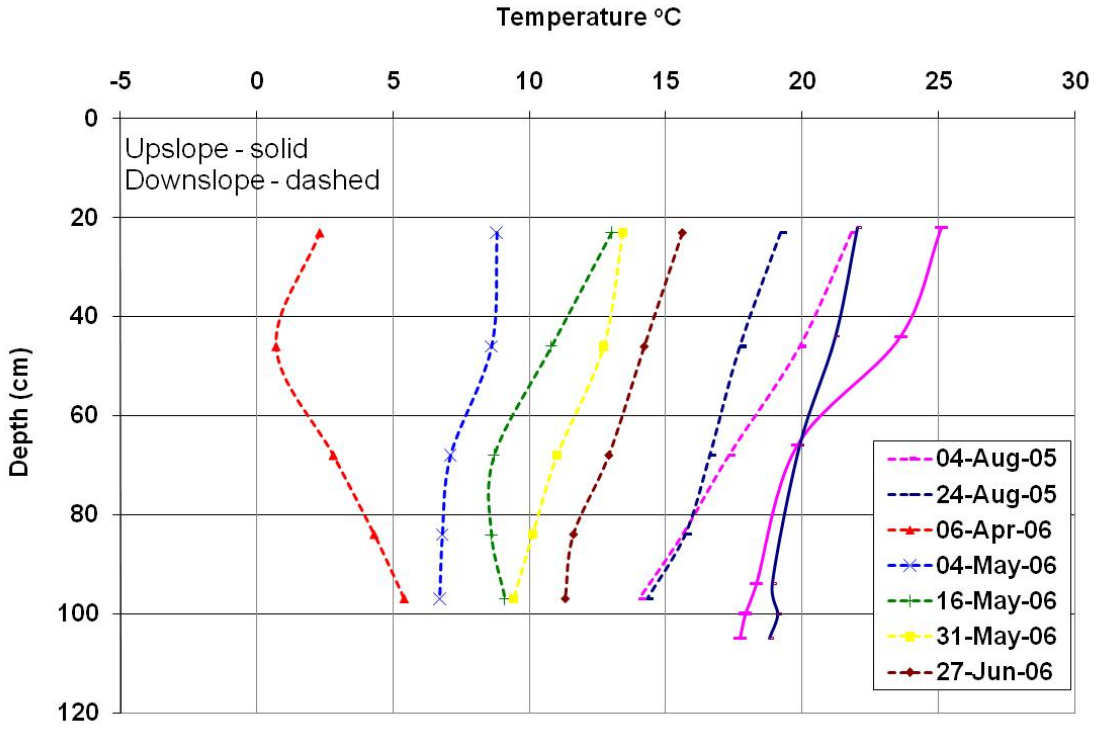

Figure 4-40 Manual temperature readings TP2S

The difference in temperature with respect to slope location can be seen for each test plot. Differences between temperatures at different slope locations were minimal on TP1N; however, it can be seen that the cover began warming up earlier at the upper slope than at the lower (particularly on May 4). The lower slope temperature on TP2N in the hotter summer months was 2 to 4˚C higher than that at upslope. The upslope temperatures in TP2S were lower than the downslope temperatures in the spring and early summer; however, in August the upslope location was warmer than the downslope location. Temperature at TP1S was higher at the upslope than at the downslope by up to 6˚C when readings were available at both locations.

As discussed above, the soil appeared to heat from both the top and the bottom of the cover in the spring. The top heating was due to temperature increasing in the spring and summer. However, the warming from the bottom indicated a heat source below the cover in the waste. The waste decomposition process releases heat (Bendz and Bengtsson, 1996), which is the source of the base heating. The heat conducted upwards from the waste may also contribute to the differences in soil temperature between the north and south slope if the base heating varied with location, as well as spatial differences on each test plot.

The depth of freezing was different between the north and south slope for each of the monitoring years. In the winter of 2004/2005, the north test plots froze to a greater depth than the south plots. In the winter of 2005/2006, the south test plots froze deeper than the north. The depth of freezing was controlled by two factors: the ambient temperatures from both above and below; and, how readily the temperature is conducted through the cover. There was believed to be little difference in air temperature between the north and south slope; however, the heat flux from the base appeared greater on the south plots in 2004/2005 than the north, and greater on the north plots than the south in 2005/2006 based on estimations using the temperature gradient on each slope. Also, the snow depth above the test plots differed with a greater snowpack depth on the north test plots. The snow cover acted as an insulator, reducing the effect of the cold air on the cover temperature. Also, since the south test plots were much steeper than the north, and since the depth to each sensor was measured vertically, not perpendicularly from the surface, the actual distance from each sensor to the atmosphere was slightly shorter (by approximately 5 cm) on the south test plot than on the north plot, thereby increasing the influence of the ambient air temperature.

Some of the variable temperature differences on each test plot can also be accounted for by water content and net radiation. TP1N began warming earlier at the upslope location. This was likely due to net radiation being greater here than that at the downslope location earlier in the spring. TP2N was warmer at the lower slope during the summer months than the upper slope, perhaps due to the reduced vegetation around the sensors, which would block and absorb much of the incoming net radiation allowing much more energy to penetrate the soil. The same thing occurred at upslope on TP1S and TP2S as there is little vegetation in these locations to block the incoming net radiation.

4.3.3. Suction Data

Suction measured at the midslope of each test plot has been plotted in Figure 4-41. Blank areas in the plot are due to either sensor errors or errors in estimating suction between discreet data points. All suction values are in kPa. It should be noted that suctions recorded when the soil was frozen can be misleading as the sensor calibration is based on the thermal conductivity of liquid water rather than that of ice. All suctions during freezing (when the soil temperature is less than zero) have been blacked out in the figures below. It should also be noted that this type

of sensor really only provides reliable data between 5 and 500 kPa (Fredlund and Rahardjo, 1993); therefore, values outside this range may not be accurate.

It can be seen in these figures that the test plots on the south experienced much higher values of suction than those on the north. There also appears to be little correlation between suction values and cover design (capillary break or store-and-release design). The magnitude of suction varied over five orders of magnitude. The contours of particular interest are those for 1500 kPa and greater. At suctions of 1500 kPa and greater, plants are no longer able to draw water from the soil. Figure 4-41 demonstrates that this plant limiting suction only occurred within the top 50 cm on the north slope but occurred right to the base of the cover on the south. The suction sensors in the sand layer of the south capillary break test plot showed readings greater than 3000 kPa. Based on the assumed moisture retention curve for the sand used in the predictive modelling by OKC-GAL, 2005(b), the sand should be at a residual water content by suctions of approximately 100 kPa. Therefore, recordings of suction as high as 3000 kPa suggests sensor errors.

Overall, it appears that the south covers became drier regularly, with much higher suctions and therefore lower water contents, possibly to the point where vegetation would become stressed. On the north slope, the capillary break cover experienced higher suctions at a lower depth than the store-and-release cover. Based on this it appears that the store-and-release cover had a greater moisture storage than the capillary break.

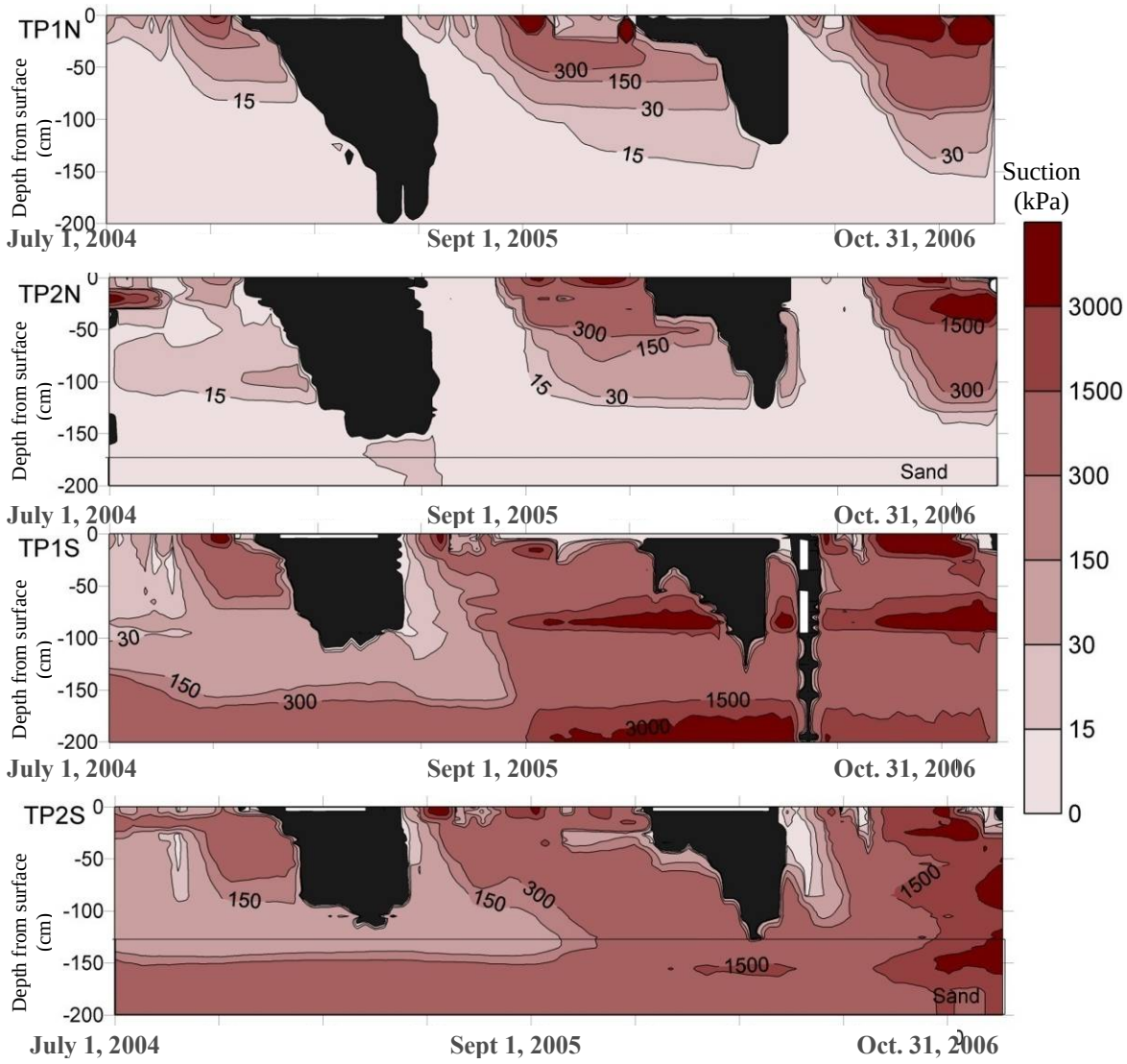

Figure 4-41 Suction values in kPa for each test plot during the monitoring period (midpoint of each slope)

4.3.4. Water Content Data

Automated Measurements

Automated water content measurements were made at lower, mid and upslope locations on each test plot with EnviroSCAN sensors and are shown in Figure 4-42, Figure 4-43, Figure 4-44 and Figure 4-45. Blank areas in the plot due either sensor errors or errors in estimating water content between discrete data points. As the water content sensors do not record accurate water

contents when the soil is frozen, the data is blacked out in the graphs below when the soil temperature is below 0˚C.

The top few centimeters of all the test plots were very dry (water content less than 0.05 m^3/m^3). This may be due to actual drying near the surface but also may be due to erosion around the access tube leaving the top sensor exposed to air.

Generally, water content increased after the soil thawed, presumably as a result of snowmelt infiltration and spring rainfalls. Then throughout the summer and into the fall, the water content decreased from the surface. Generally, the variability in water content decreased with depth from the surface.

The TP1N cover was the wettest at the deepest locations and the water content increased from the upslope of the cover to the downslope. The cover dried throughout the summer reaching its driest conditions just before freezing. Upper locations in TP1N displayed a dry layer at approximately 100 cm from the surface. This does not appear to be related to density, as there is no noticeable difference in density around this location (Figure 4-18). It may be related to the maximum rooting depth being approximately 100 cm (Figure 4-16) and therefore water was being drawn from this area, yet not below. The water content ranged from 0.00 to 0.42 m^3/m^3 on TP1N with the maximum values occurring at the lower slope location.

TP2N also showed an increase in water content with depth at the mid and lower location; however, this extended only to the sand layer of the capillary break (~120 cm), the sand being much drier. This “perched” higher water content above the sand might indicate that the capillary break was working at this location. The maximum water content occurred at the midslope location on TP2N with a value of 0.39 m^3/m^3.

Water content sensors on TP1S experienced multiple problems during the monitoring period. The water content sensor at the upslope location on TP1S was not functioning properly between December 28, 2005 and April 20, 2006. The problem was believed to be due to condensation on the SDI-12 interface board connected to these sensors. The board was replaced and the problem was resolved. The same problem occurred between January 27, 2005 and September 21, 2005 at the midslope location. Again, the SDI-12 board was replaced and the problem was corrected.

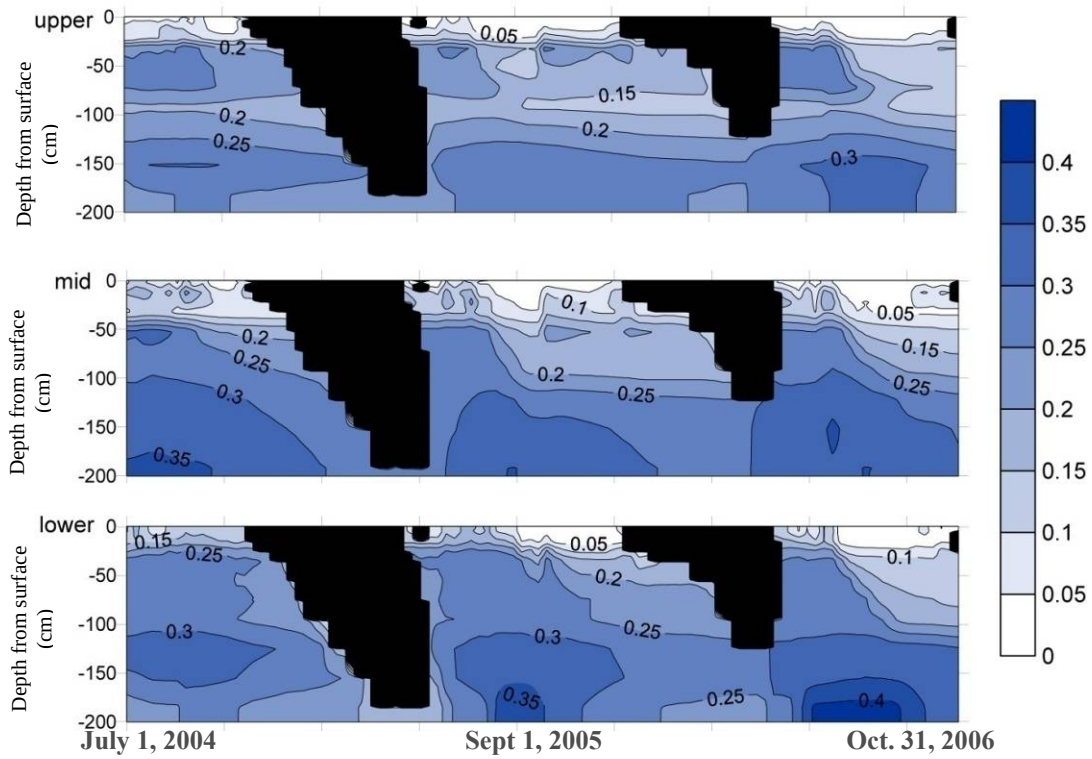

Figure 4-42 TP1N automated water content

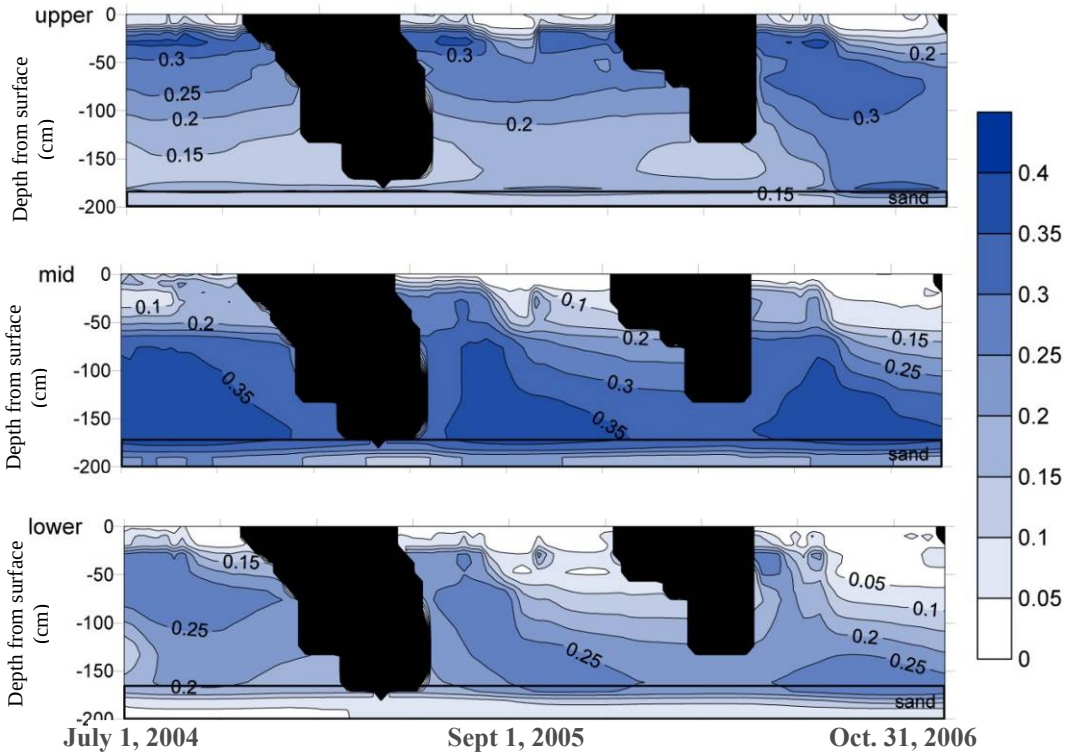

Figure 4-43 TP2N automated water content

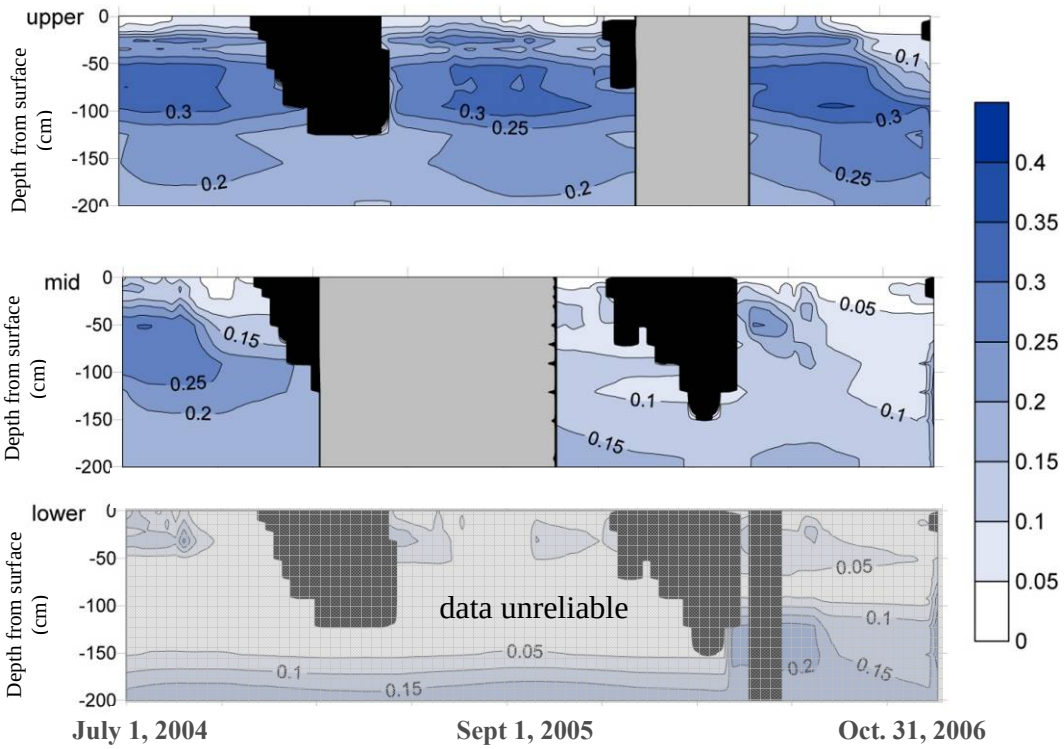

Figure 4-44 TP1S automated water content

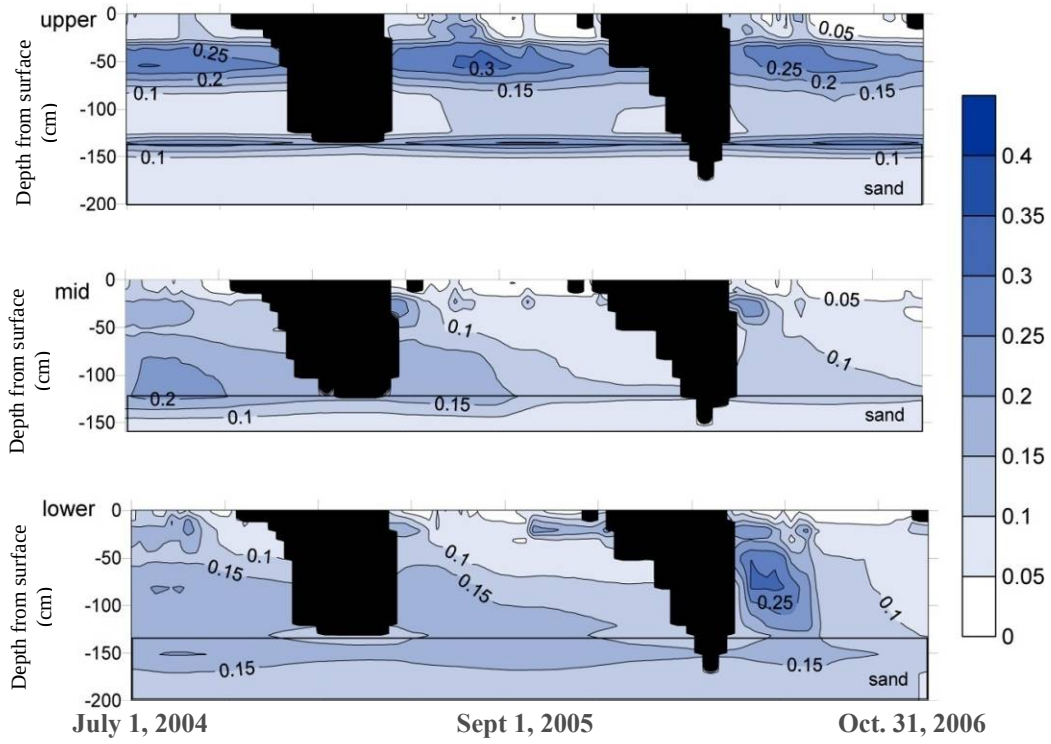

Figure 4-45 TP2S automated water content

The TP1S downslope water content sensors installed between 55 cm and 155 cm showed little sensor response to the atmospheric variables. This was attributed to poor contact between the PVC access tube and the surrounding soil between these depths since the time of installation. This is confirmed with comparisons to Diviner 2000® manual water content measurements at adjacent locations, which do not match those obtained using the EnviroSCAN®. The readings at this location changed drastically on March 23, 2006, likely from sediment shifting or perhaps from settlement filling the gap between the sensor tube and the soil. However, the readings were still not comparable with those measured at adjacent locations and are not used in analysis.

On TP1S, although the near surface was extremely dry (partially due to the top sensors being exposed to air) the bottom 50 cm of the cover was drier than the top 50 cm. As the summer progressed, the cover dried from the surface, indicating evapotranspiration. The maximum water content on TP1S was 0.37 m^3/m^3 at the upper slope location.

TP2S was also much drier overall than the north test plots. The lower area was slightly wetter than the midslope location, although it appeared drier than the upslope. The water content of the till just above the till/sand interface (120 cm) was very similar to that of the sand just below the interface at a value of 0.15 m^3/m^3. This indicates the cover was too dry for the sand to cause a capillary break effect here. The highest water content experienced on TP2S was 0.33 m^3/m^3, which occurred on the upper slope location.

It is interesting to see elevated water contents at depth on TP1N similar to those seen above the sand on TP2N. This may indicate that a capillary break effect was being achieved due to the presence of either the temporary cover placed over the waste (below the till) or perhaps due to the waste itself. This did not occur on the south slope as there was not enough water in the covers.

The general trend for all covers is that evapotranspiration dried the covers throughout the summer and fall and that the depth and extent of transpiration increased each successive year. This presumably reflects the vegetation becoming more established and making increased demands on stored water.

Manual Diviner 2000® Measurements

Water contents were measured manually approximately every month during non-frozen conditions with the Diviner 2000®. Diviner 2000® access tubes that were installed on the edge of each test plot did not respond appropriately to atmospheric conditions and this was believed to be due to a poor contact between the soil and tube as a result of non-ideal installation. Because of the unreliability of the data from those tubes the data will not be used for analysis.

The readings from all tubes on each test plot at a depth of 95 cm for selected days are shown in Figure 4-46 through Figure 4-49. The profile numbers were lowest at the toe of the slope and become highest at the top. The porosity used in the figures is the average porosity calculated from field samples.

It should be noted that the value of volumetric water content cannot actually exceed the porosity. Where this appears to be the case in the graphs (e.g. 95 cm TP1N profile 7 and 5) it may be that the porosity at that location is actually greater than the average measured porosity (section 4.2.4) as shown, or just a result of precision of the instrument coupled with the natural heterogeneity of the soil.

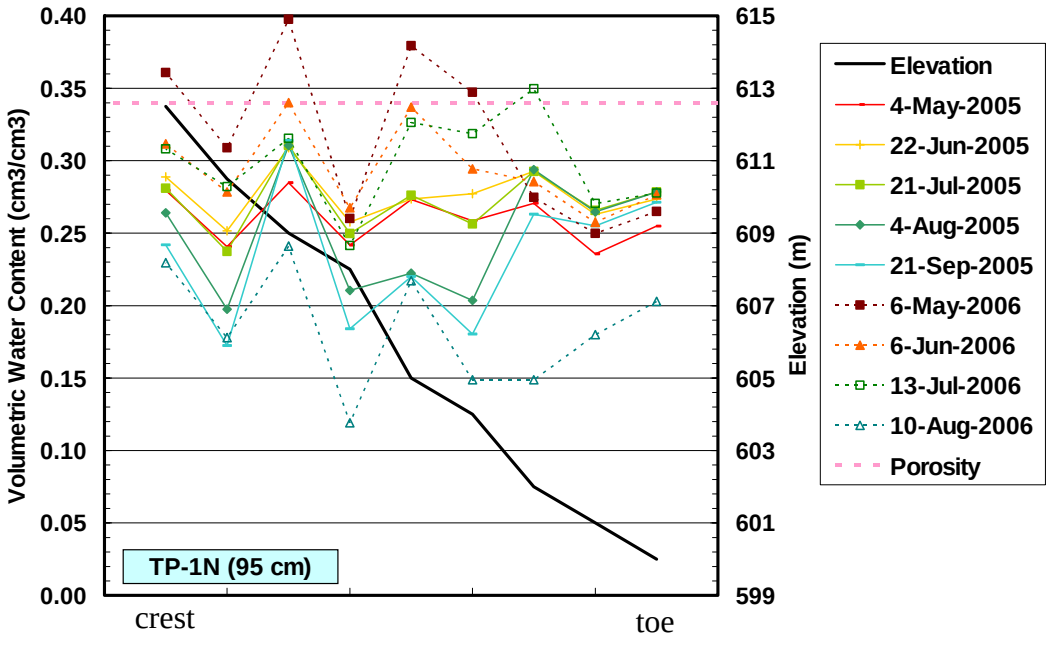

Figure 4-46 Diviner 2000® water contents for TP1N at 95 cm depth

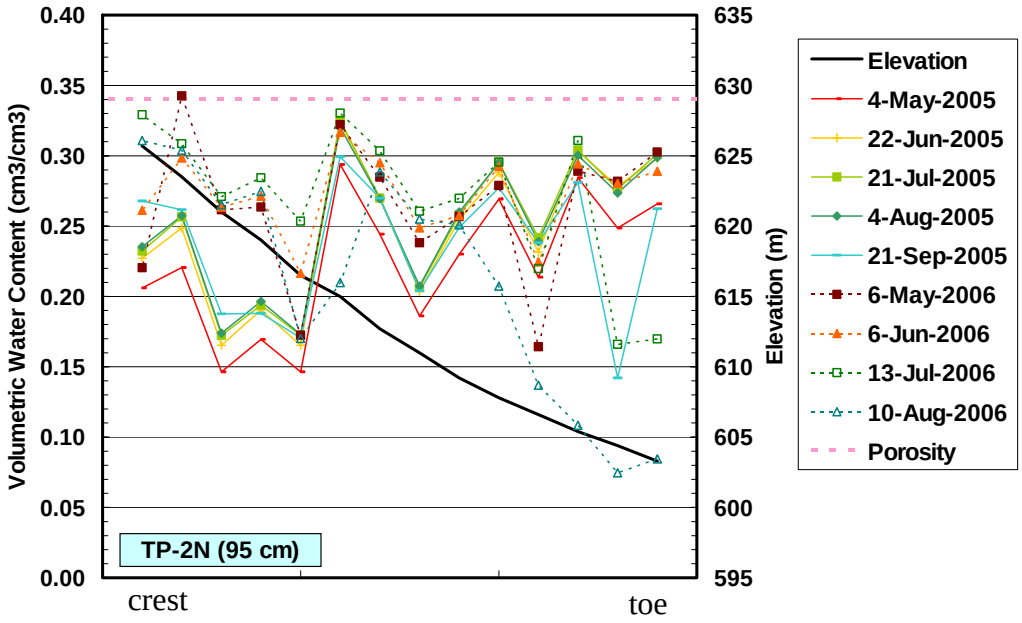

Figure 4-47 Diviner 2000® water contents for TP2N at 95 cm

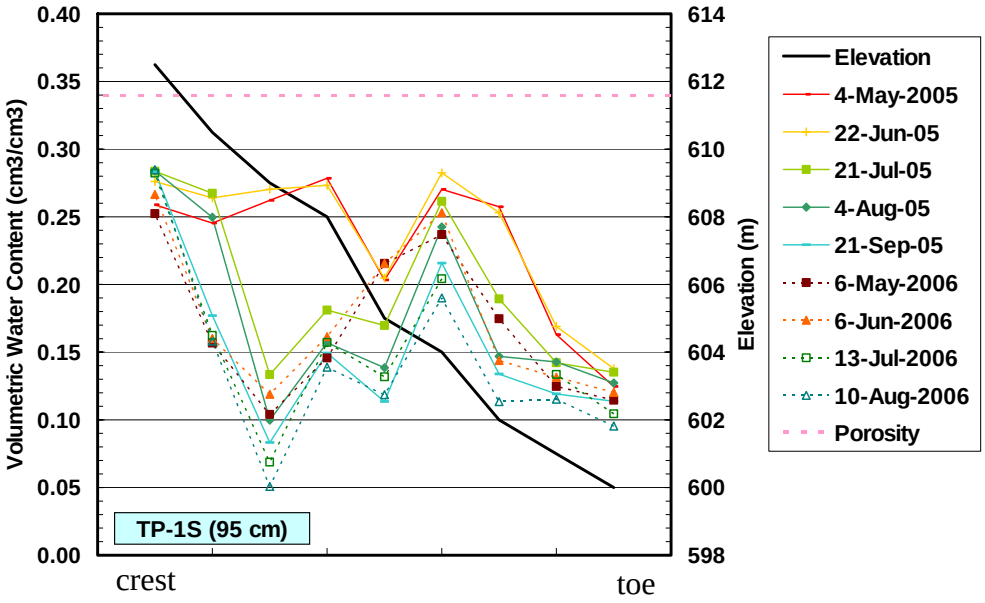

Figure 4-48 Diviner 2000® water contents for TP1S at 95 cm

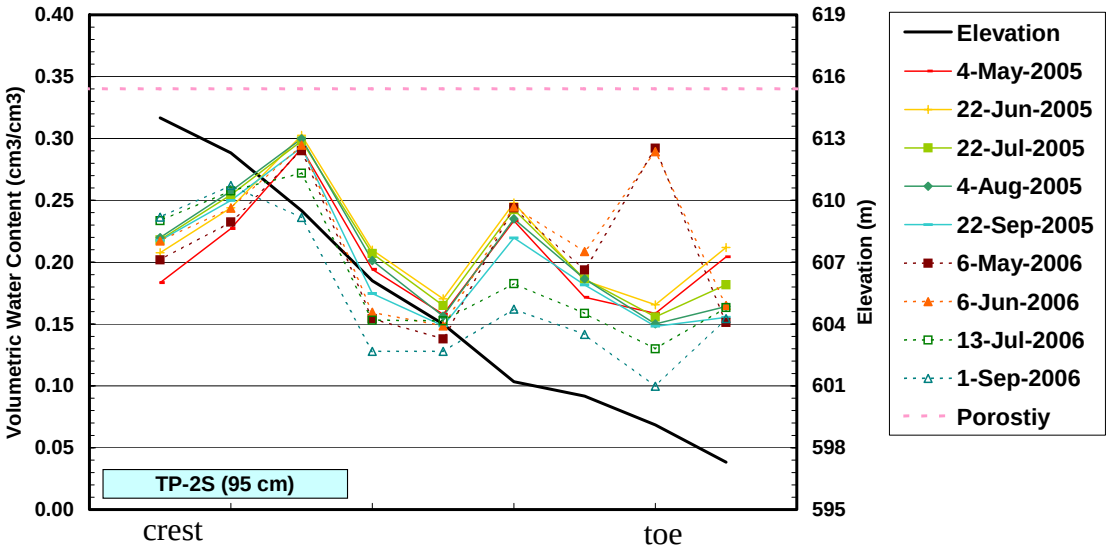

Figure 4-49 Diviner 2000® water contents for TP2S at 95 cm

The distribution of water content does not clearly show any location to be particularly wetter or drier than another on the north slope. The north test plots showed a general trend in which the test plots were wettest in the spring and dried continuously throughout the summer, reaching the driest water content in the fall. TP1N displayed the most variation out of all test plots. Early 2006 water content values for the north test plots approached saturation.

The south test plots were drier than the north slope and showed lower variability throughout the monitoring period. The increase in water content in the spring was far less on the south test plots though there was still a gradual drying throughout the year. Both test plots on the south slope showed a slight decrease in water content moving downslope.

The variation of water content with slope location is most likely related to vegetation differences along the slope. The water balance within the covers appeared to be primarily vertical with little evidence of lateral water movement within the cover.

CHAPTER 5
DATA INTERPRETATION AND ANALYSIS

The purpose of this chapter is to establish a preliminary estimate of the relative performance of the various covers based on a development of a water balance. The components of the water balance for this analysis are:

$$\Delta S = PPT - R - DP - AET \qquad \text{Equation 5.1}$$

where, ΔS represents change in soil moisture storage (S), PPT is precipitation, R is combined runoff and downslope moisture translocation, DP is deep percolation, and AET is actual evapotranspiration, each expressed as a depth of water (mm). Each of these elements involves various assumptions and interpretations that will be explored further in this chapter.

5.1. Key Processes

5.1.1. Meteorology

The precipitation data used in this analysis are the Environment Canada readings at the COR airport as discussed in Chapter 4. Precipitation was assumed to be the same on all four test plots. While there was likely some spatial variability, the amount cannot be quantified. Precipitation over the winter was not used in the water balance; rather snow depths as measured in the snow surveys were applied during the spring. Winter was defined as the period where the maximum daily air temperature remained below 0°C. Precipitation events that contribute directly to storage rather than snowpack during this period are ignored.

Potential evapotranspiration was calculated using the modified Penman equation, which requires wind speed, air temperature, relative humidity, and net radiation. Bendz and Bengtsson (1996) noted that in a landfill, heating from the base can increase the energy available for evaporation. However, from an uncovered landfill surface, they estimated that actual evaporation was increased by only 10% due to ground heating. Therefore, even though the estimations of PET do not consider energy from within the cover, the amount is likely very low through the daily cover on top of the waste. Also, by estimating the actual evapotranspiration

(AET) as a ratio of PET, the actual value of AET (including that caused by ground heating) can be estimated through use of a greater ratio than from a surface without ground heating. AET is discussed further below.

Calculations for all test plots used the wind speed, temperature and relative humidity measured at the top of TP1N. Net radiation measured at the top of TP1N was used to calculate PET for test plots on the north slope and net radiation measured on TP2S was used to calculate PET for test plots on the south slope. The net radiation used was that described in Section 4.3.1 with missing data filled in from previous years. As net radiation was greater on the south slope than the north slope, the PET calculated for the south slope was greater than that on the north slope. The cumulative PET for each slope is shown in Figure 5-1. Over the entire monitoring period, the south PET was approximately 16% greater than the north PET.

The increased PET on the south slope contributed to the good vegetation generally found on the south test plots as well as drier overall conditions.

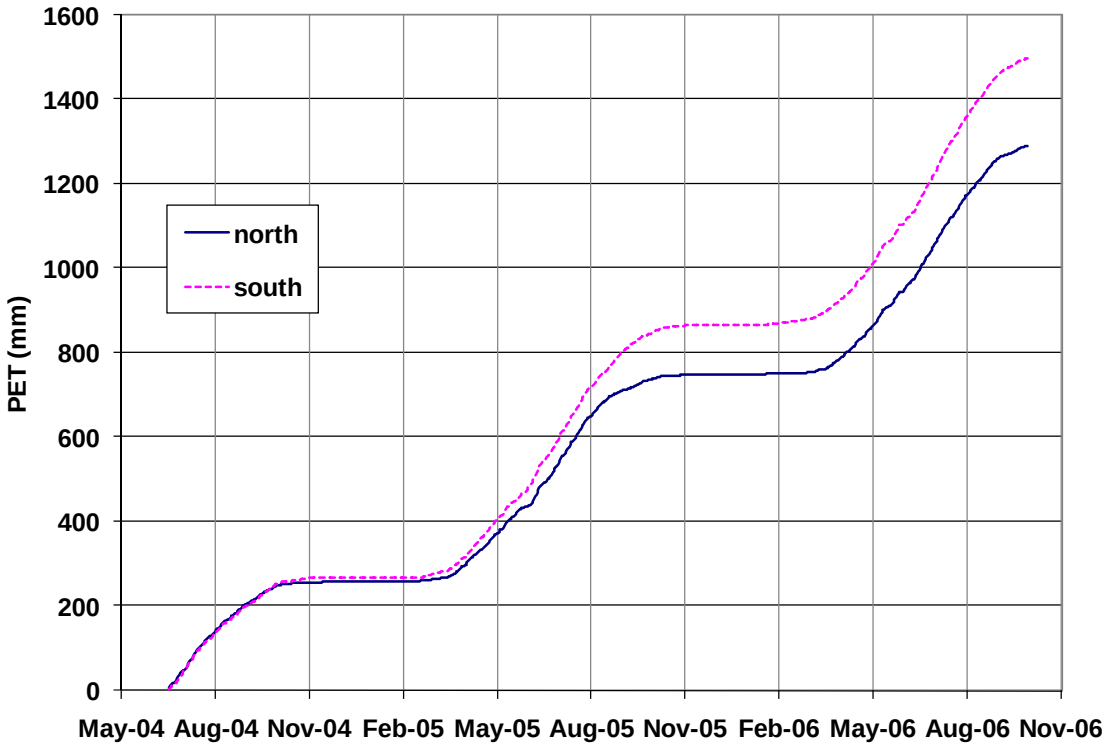

Figure 5-1 PET for north and south slopes

5.1.2. Actual Evapotranspiration (AET)

Actual evapotranspiration will generally be less than PET due to moisture limitations and vegetation response. As discussed in 4.2.2, the vegetation varied over all of the test plots from good to poor with ranging rooting depths. The distribution of good vegetation and poor vegetation were also related to differences in plant species at each location as well as water availability, since species type, plant growth and water availability are likely related. For example, at the top of the south test plots, there were significantly more grasses and less agronomic species, in spite of the fact that all locations were seeded uniformly. Either the planted vegetation washed away before they could establish themselves leaving only the grass seeds, or the conditions at the top of the south slope were more suitable for grasses than for mustard and other species found at the other locations.

The daily water balance assumes AET as a percentage of PET. This factor varied primarily based on quality of vegetation and is discussed later in this chapter. The PET calculations do not include heating from the waste, but because AET is simply an assumed portion of PET, the ratio will simply be higher since the effect of surface heating is to increase PET.

The depth of soil from which water can be drawn for transpiration is controlled by the root distribution. The root distribution will be a function of the type of vegetation and the topsoil and planting management on the covers to date. Some consideration must be given to soil density, since the cover appears to be highly compacted (Section 4.2.4) and is likely to impede root development (Agriculture Canada, 1992).

The vegetation in the center strip of each test plot is noticeably different from the rest of the plot area, as discussed in Section 4.2.2. Given that all the soil data to be used in the water balance will come from the center strip, it stands to reason that this may not be representative of the entire test plot. For example, the amount of AET in the center strip may not be the same as that averaged over the entire width of the test plot.

Plant available water is most commonly present at water contents ranging from field capacity to the permanent wilting point. Field capacity represents the water content following cessation of gravity drainage. The wilting point is the water content at which plants can no longer extract water from the soil. Values of field capacity and wilting point were selected based on a review of the measured moisture retention curves and on literature values for similar soil types. The

values selected for the till used in the covers were 0.22 m^3/m^3 for field capacity and 0.11 m^3/m^3 for wilting point corresponding to the approximate water content, at 33 kPa, and 1500 kPa respectively (Barbour et al., 2007).

The vegetation was generally stronger on the south facing test plots. This is likely due to the increased net radiation, warmer temperatures, and slightly longer growing season brought on by the differences in net radiation. The AET on the south slope therefore is expected to be greater than that on the north slope.

5.1.3. Deep Percolation

Deep percolation (DP) is defined for the purposes of the water balance as water that drains through the base of the covers into the waste. DP was estimated based on several factors. In order for net percolation to be considered in the water balance, the bottom of the cover had to be near or at saturation, unfrozen with a hydraulic gradient at the base of the cover that represented downward flow.

Hydraulic gradients were calculated using the suction data and sensor locations near the base of each test plot. Hydraulic head gradients define the direction and magnitude of water flowing through the covers and were used here to determine if net percolation through the cover was occurring. Positive gradients indicate a downward flux, negative an upward flux. Hydraulic gradients at the base of the covers are presented in Figure 5-2 through Figure 5-5 for data collected during the monitoring period. The depth of freezing never extended to the depth of these sensors; therefore, no data are removed.

As seen in the figures below, the hydraulic gradient varied widely. The gradient on the north test plots were low and relatively stable compared to those on the south, which showed large and rapid fluctuations. Hydraulic gradients on the north test plots were approximately +1 for a large part of the monitoring period. This suggests a ‘perched’ saturated system in which the net percolation is controlled by the saturated hydraulic conductivity. The north test plots showed downward flow from June through October 2005. The downward flux in 2006 was between March and September. The reason for this was likely an increase in vegetation biomass and root density which allows ET demand to influence moisture movement near the base of the cover.

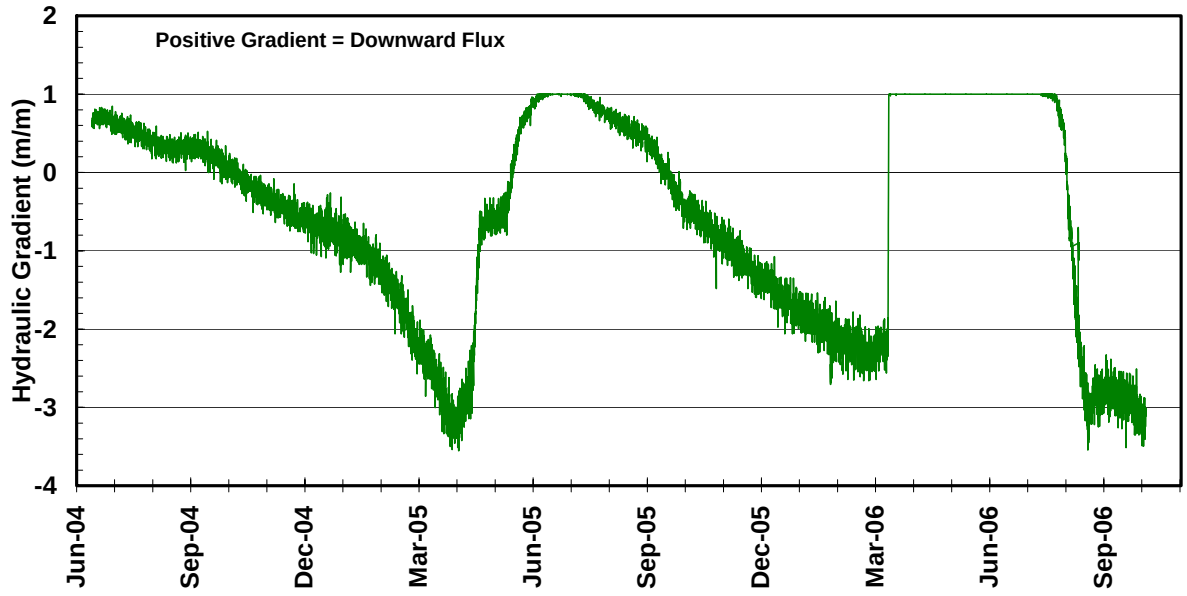

Figure 5-2 Hydraulic gradient for TP1N from 155 cm to 195 cm

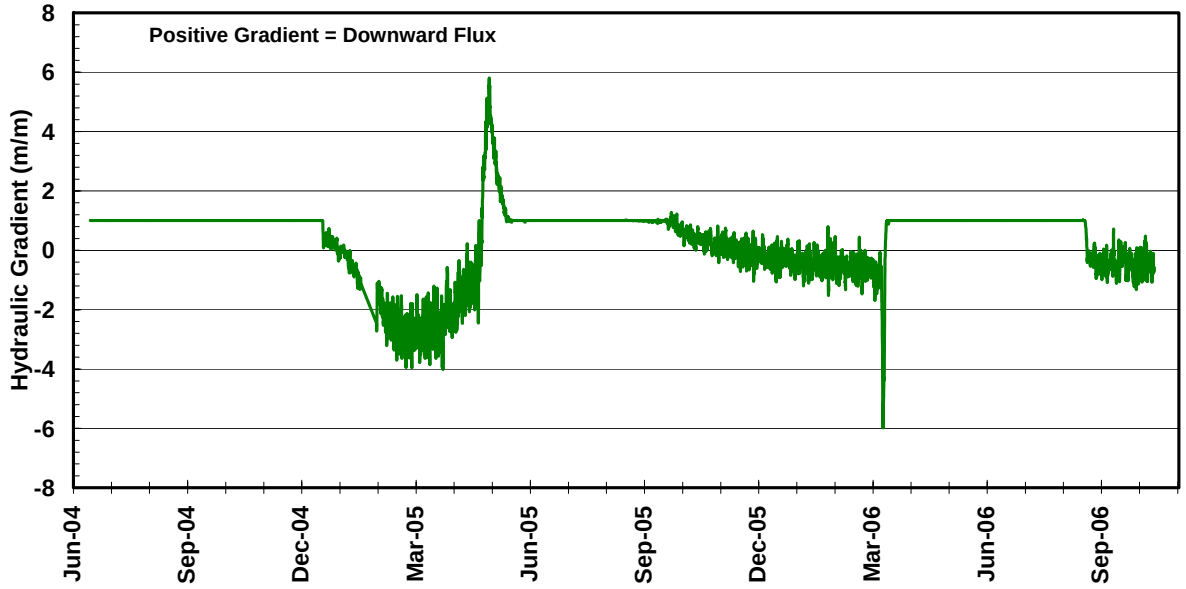

Figure 5-3 Hydraulic gradient for TP2N from 175 cm to 185 cm

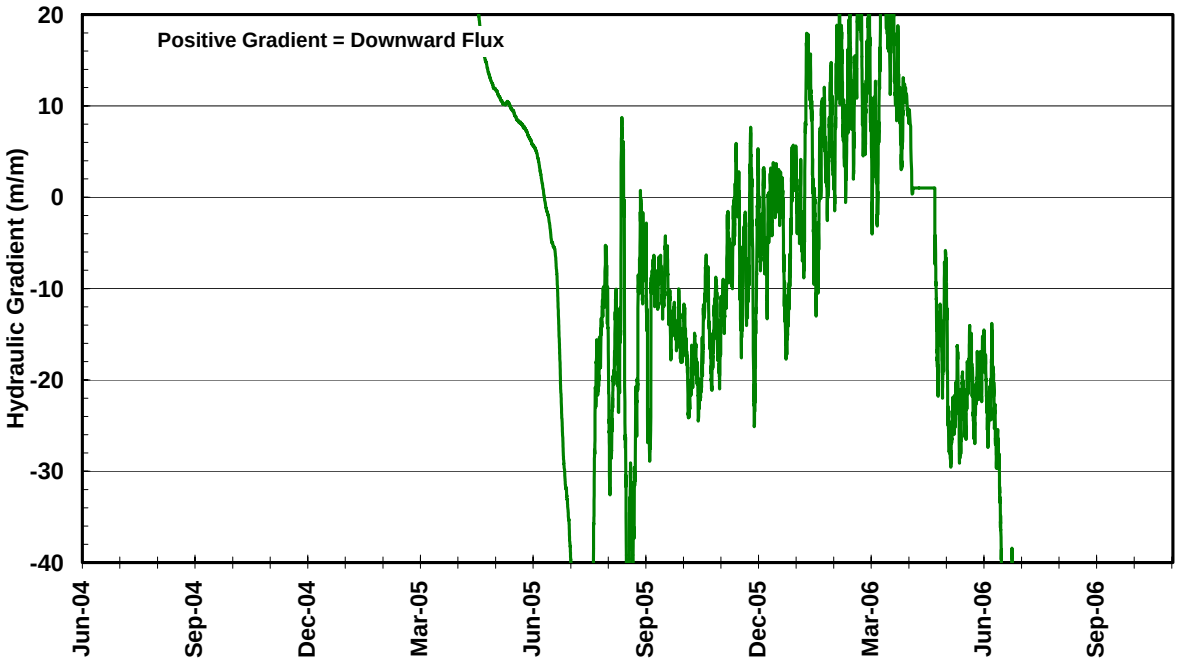

Figure 5-4 Hydraulic gradient for TP1S from 125 cm to 155 cm

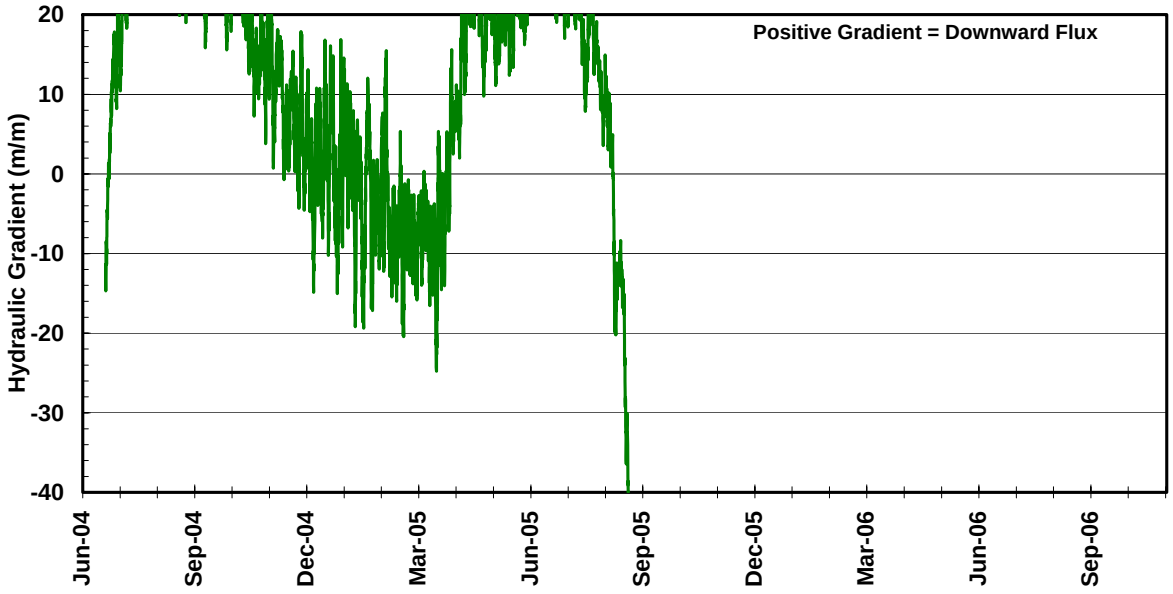

Figure 5-5 Hydraulic gradient for TP2S from 155 cm to 175 cm

The south test plots only show a downward flux during the first half of the monitoring period up to approximately July 2005. These gradients changed to upward flow as the vegetation

became established and ET demands increased. TP1S again experienced a positive gradient early in 2006 although not to the degree it was in 2005. TP2S does not show a downward flux again.

The atmospheric demand for moisture caused the gradient to be negative as water is drawn upwards in response to ET demand. This situation occurred at the base of both covers on the south slope and to some degree on the north slope by the end of 2006. The north test plots showed a downward gradient during the spring due to wet conditions and low PET demands. Therefore, net percolation was initiated shortly after spring melt and continued until late summer when ET demands reached the base.

In the development of the water balance, net percolation was applied if the gradient was positive and the water content at the base was near saturation. A rate of between 1 and 3 mm per day was found to best match the data on each cover. This is much less than the average hydraulic conductivity measured with the Guelph permeameter (between 16 and 85 mm/day) which would be the maximum net percolation assuming a unit hydraulic gradient at the base of the cover. It is likely that the hydraulic conductivity of the soil at the base was much lower than that near the soil surface where the Guelph testing was performed due to surface weathering and freeze thaw effects (Meiers et al., 2006). The work of Kim and Daniel (1992) shows that the hydraulic conductivity of a compacted clay can increase by 2 to 100 times that at placement over just 5 freeze-thaw cycles. Since the base of the cover was not exposed to freeze-thaw effects but the surface was, it is not surprising that the hydraulic conductivity is lower at greater depth.

An *in-situ* moisture retention curve was also created using the measured water contents and suctions at each site using the Instantaneous Profile Method. The measured *in situ* data points were obtained by plotting the suctions and volumetric water contents measured at the same time at a similar location in the soil profile from continuous drying periods. Figure 5-6 shows the *in situ* SWCC from measurements taken on TP1N at the midslope location. The data was separated into wetting and drying trends; however, there was very little difference in the two sets of data due to the large amount of scatter. The dotted black lines represent general curves which envelopes the measured data. The moisture retention curve for the uncompacted till used in preliminary modeling (GAL and OKC, 2005(b)) is shown in Figure 5-6 and generally fits within the envelope. The SWCC measured from undisturbed samples are shown in red in Figure 5-6 and generally fit the field data at low suctions; however, the curves for the lab tests change more gradually than the *in situ* results.

The procedure for calculating the unsaturated hydraulic conductivity can be found in Meerdink, et al., 1996, and Khire et al., 1995. Essentially, Darcy's law is employed in the following manner:

$$K(\psi) = \frac{\upsilon}{\frac{dh}{dz}} \qquad \text{Equation 5.2}$$

where $K(\psi)$ is the hydraulic conductivity at matric suction ψ, υ is the discharge velocity, *h* is hydraulic head, *z* is the vertical coordinate and *dh/dz* is the vertical gradient. Only periods with continuous drying were used since fluctuations due to wetting and drying would not be picked up simultaneously by both the suction sensors and the water content sensors.

The field estimated hydraulic conductivity function for the till is shown in Figure 5-7. This figure also shows the saturated hydraulic conductivity measured from *in situ* Guelph testing as well as the hydraulic conductivity function estimated using the Van Genuchten (1980) method based on the saturated hydraulic conductivity measured with Guelph testing and the author's laboratory measured moisture retention curve. Also included is the function used by GAL and OKC to do the preliminary modelling for the cover trials (GAL and OKC 2005(b)). There is a fairly good correlation between the function used in the model and the instantaneous profile method.

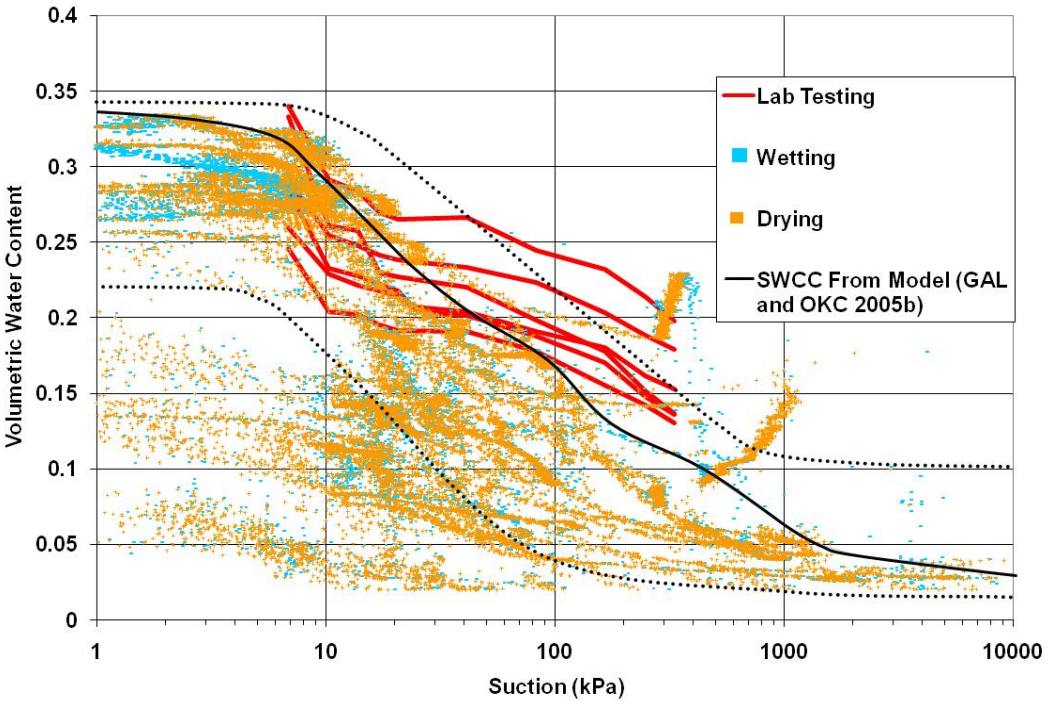

Figure 5-6 *In Situ* SWCC

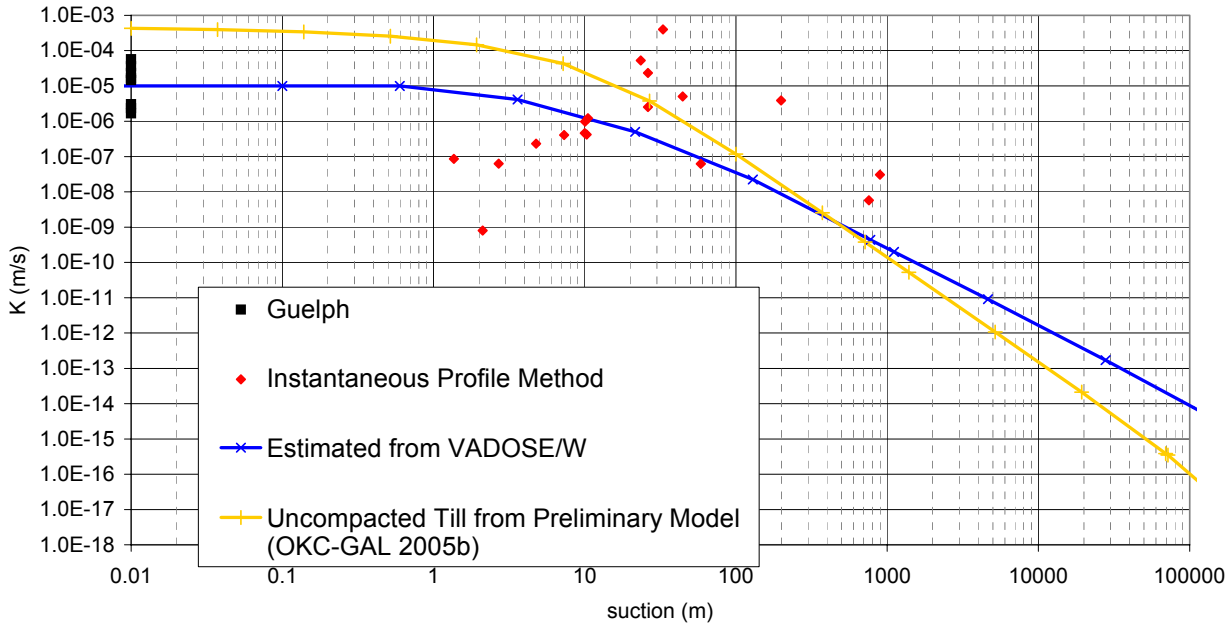

Figure 5-7 Hydraulic Conductivity Function from the Instantaneous Profile Method

5.1.4. Runoff

For the purposes of the water balance, runoff will be defined as any loss of precipitation due to runoff as well as any translocation of water to areas downslope.

As runoff measurements made on site were unreliable and so many assumptions were required to estimate relative values, values for runoff are difficult to quantify and are assumed to be zero for the water balance calculations. Runoff measurements during non-frozen conditions was very low in the estimated measurements; therefore the error that may be caused by assuming runoff to be zero will be negligible. However, evidence of runoff in the water balance will appear when precipitation water cannot be accounted for by changes in soil storage.

5.1.5. Interflow

Measuring interflow was attempted on the capillary break test plots; however, no water was measured. While this may indicate the absence of substantial interflow, it may also point out a possible flaw in the design of the collection system. Some of the water content data presented in Chapter 4 suggest that there may be some interflow occurring on the south slope. However, the interflow collection channel was keyed into the sand layer. Therefore, if water migrated downslope in the finer till layer, it would have to break through into the sand at the base of the slope in order to be measured. Collection of interflow water from the base of the clay till layer would have required that a cutoff apron of geomembrane be extended upslope at the base of the till in order to capture water in the till as it transitions from negative to positive pressures.

5.1.6. Change in Storage

The EnviroSCAN® water content monitoring data was used to calculate the volume of water stored in the entire depth of each cover. The soil profile at each sensor location was partitioned into representative soil units associated with each sensor (e.g. halfway between each sensor). Water volumes were calculated by multiplying the volumetric water content reading by the corresponding depth for that soil unit. Individual water volumes were summed to calculate the total water volume stored in the cover at that location. Water volumes are presented in Figure 5-8 through Figure 5-11 for the upper, mid and lower slope locations of each test plot. Water volumes calculated from the assumed values of wilting point and field capacity are also shown

for the entire depth of the profile at each location. The grey area indicates frozen soil conditions; therefore, the accuracy of these data is doubtful. It should also be noted that due to the accuracy of the sensors, water volumes may differ from those presented by approximately +/- 100 mm.

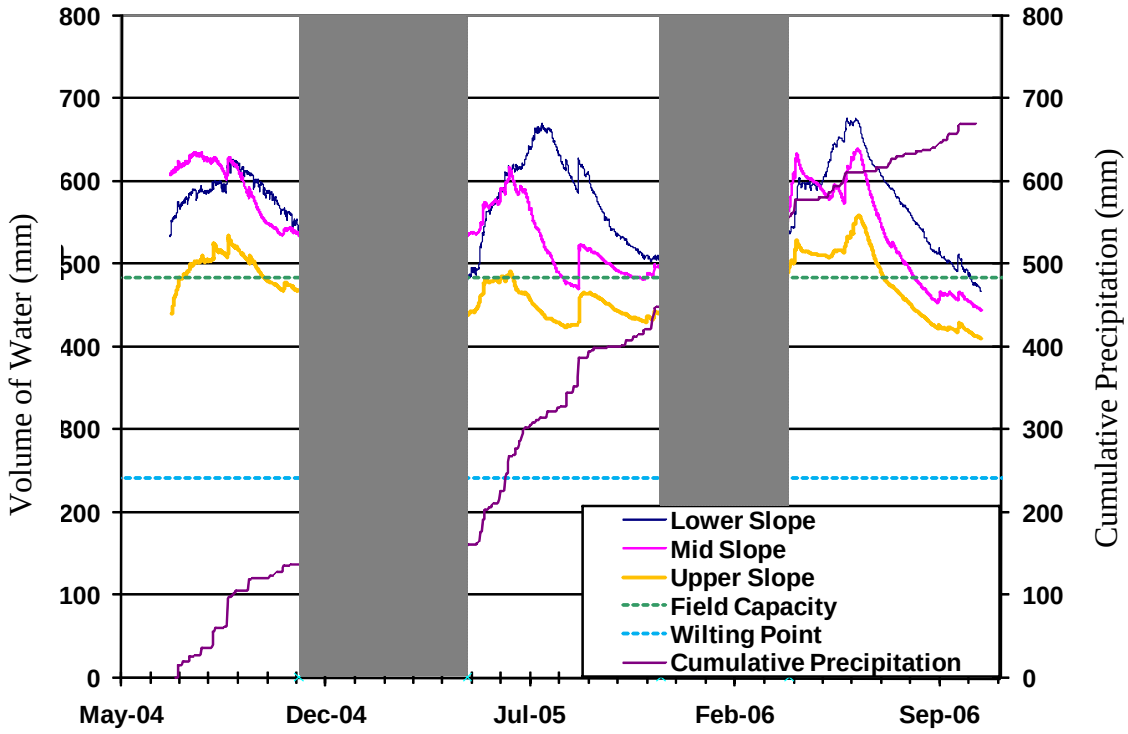

Figure 5-8 Water Volumes TP1N

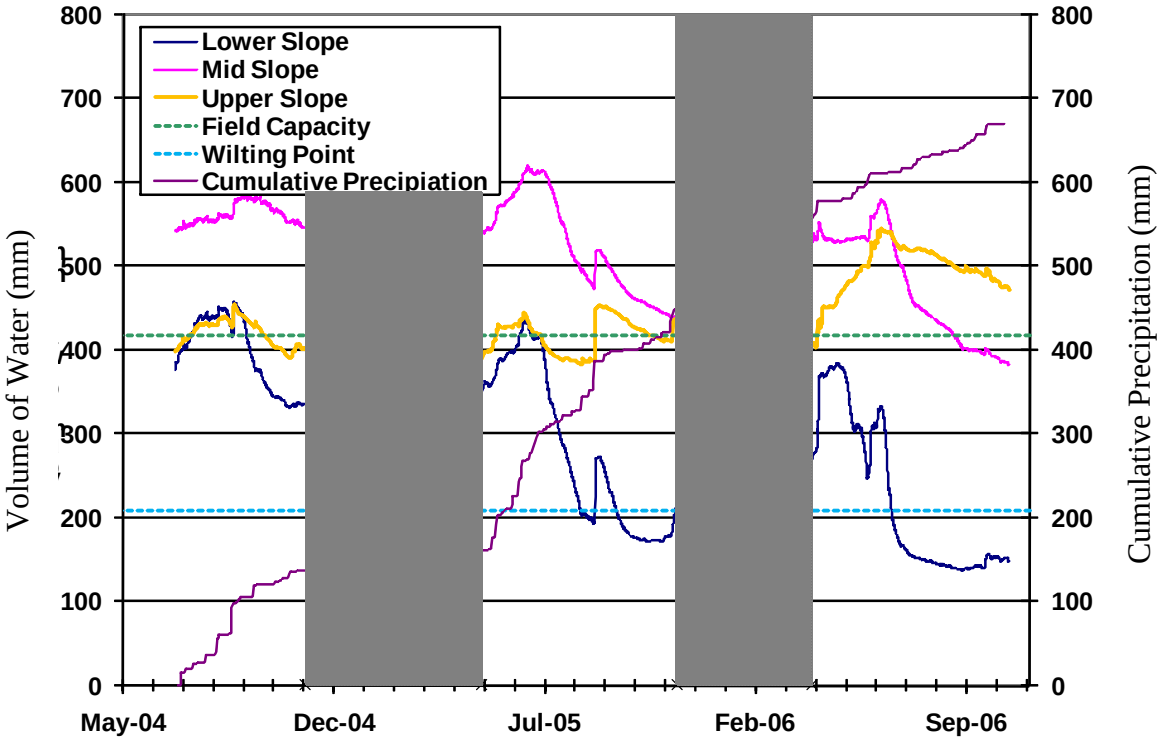

Figure 5-9 Water Volumes TP2N

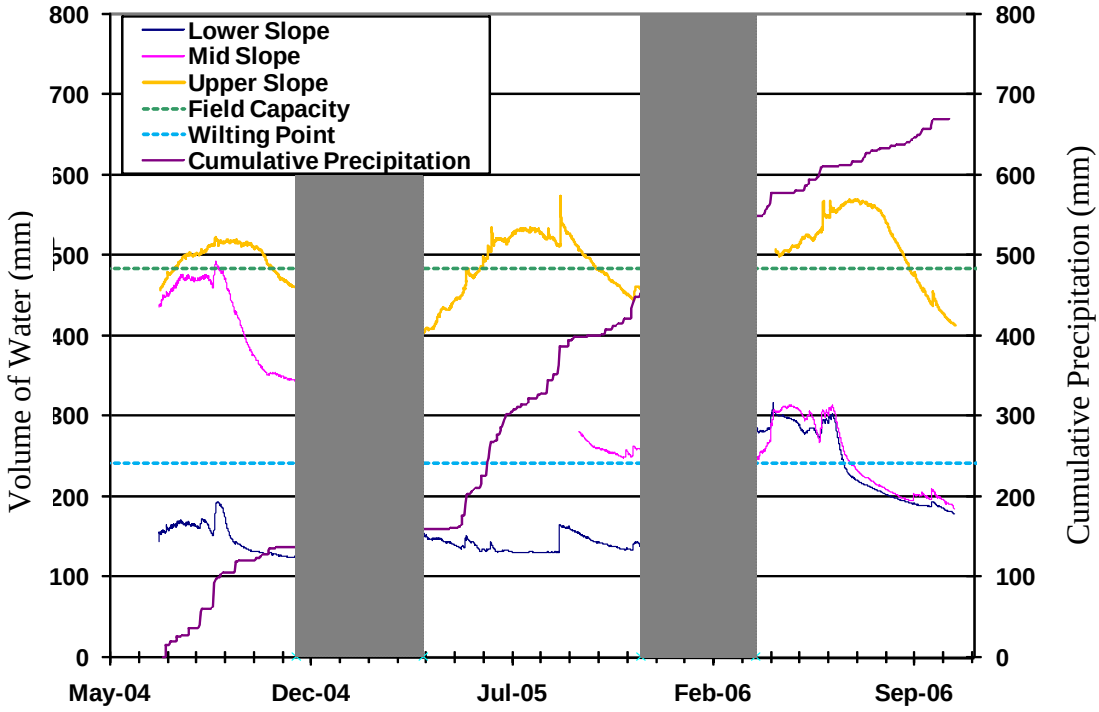

Figure 5-10 Water Volumes TP1S

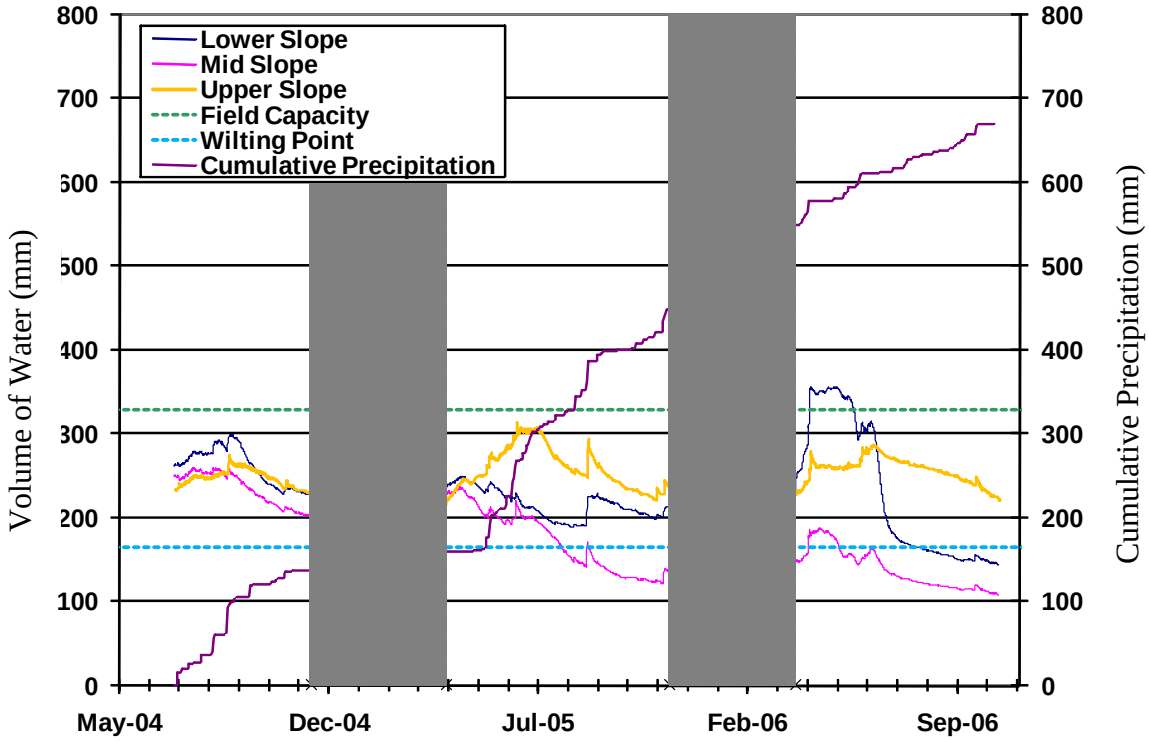

Figure 5-11 Water Volumes TP2S

Each of the covers show an increase in water volume as the snow melt water enters the cover followed by a gradual decrease in water volume over the growing season. The water volumes varied more on the north test plots than the south, which was likely due to the availability of more water for moisture redistribution and to differences in net radiation and vegetation development. For most locations, more water was stored and subsequently released at lower positions of the slope. This may be due to runoff occurring on the upper slope and subsequently infiltrating the cover further downslope. The changes in moisture for each cover at the midslope location are shown in Figure 5-12, while the data for all locations are shown in Table 5-1.

This data shows that an increase in water volume occurred each spring, at each location, except for the south slope in 2004. In the summer and fall, there was generally a loss of water. The seasonal fluctuations were most likely driven by vegetative demands and ET. Early in the spring the plants were not yet established and the large amount of water from spring melt and precipitation events entered the cover. Late in the year, the plants were full grown and could remove much greater amounts of water out of the cover.

With a few exceptions, the greatest increases in the volume of water in the spring generally occurred at the lower slope location (TP1S excluded for lack of data). This was probably caused by snowmelt water running off upslope and infiltrating further downslope rather than snow distribution as the snow survey results do not show greater snowpack at the lower slope. These locations also generally show the greatest subsequent decrease through the summer and fall. The midslope locations on each test plot have shown the greatest net loss over the monitoring period. This is likely due to the vegetation being generally classified as "good" at these locations resulting in a large amount of evapotranspiration, but with less water infiltrating during snow melt than at the lower slope locations.

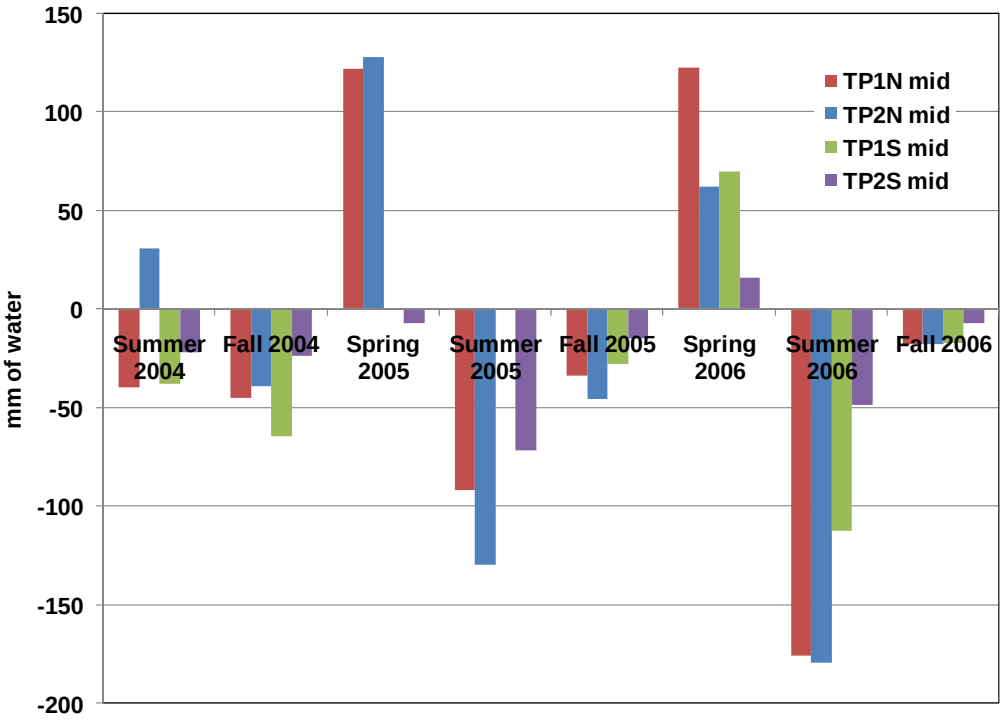

Figure 5-12 Change in water storage for each test plot at midslope by season

Table 5-1 Seasonal changes in moisture store at each slope location in mm based on volumetric water content measurements on each test plot (mm)

		TP1N				TP2N			
Season	**Dates**	**Up**	**Mid**	**Down**	**Average**	**Up**	**Mid**	**Down**	**Average**
Summer 2004[1]	July 1 to Sept 21	26	-40	40	9	15	31	-31	5
Fall 2004	Sept 22 to Nov 15	-40	-45	-59	-48	-29	-39	-42	-37
Total 2004		**-14**	**-85**	**-19**	**-39**	**-14**	**-8**	**-73**	**-32**
Spring 2005	April 1 to June 21	59	122	128	103	73	128	217	139
Summer 2005	June 22 to Sept 21	-24	-92	-42	-53	6	-130	-225	-116
Fall 2005	Sept 22 to Nov 15	-15	-34	-66	-38	-34	-46	-30	-37
Total 2005		**20**	**-4**	**20**	**12**	**45**	**-48**	**-38**	**-14**
Spring 2006	April 1 to June 21	119	123	162	135	140	62	139	114
Summer 2006	June 22 to Sept 21	-134	-176	-167	-159	-51	-180	-194	-142
Fall 2006[1]	Sept 22 to Oct 31	-12	-18	-41	-24	-24	-18	8	-11
Total 2006		**-27**	**-71**	**-46**	**-48**	**65**	**-135**	**-47**	**-39**
Total		**-21**	**-160**	**-45**	**-75**	**95**	**-192**	**-158**	**-85**
		TP1S				**TP2S**			
Season	**Dates**	**Up**	**Mid**	**Down**	**Average**	**Up**	**Mid**	**Down**	**Average**
Summer 2004[1]	July 1 to Sept 21	42	-38	-18	-4	20	-22	-7	-3
Fall 2004	Sept 22 to Nov 15	-51	-65	-14	-44	-24	-24	-28	-25
Total 2004		**-9**	**-103**	**-32**	**-48**	**-4**	**-46**	**-35**	**-28**
Spring 2005	April 1 to June 21	115	ND	-17	49	97	-7	6	32
Summer 2005	June 22 to Sept 21	-13	ND	19	3	-55	-72	-1	-43
Fall 2005	Sept 22 to Nov 15	-58	-28	-20	-35	-22	-15	-19	-19
Total 2005		**45**	**-28**	**-17**	**0**	**20**	**-94**	**-14**	**-29**
Spring 2006	April 1 to June 21	ND	70	18	44	50	16	102	56
Summer 2006	June 22 to Sept 21	-93	-113	-113	-106	-40	-49	-166	-85
Fall 2006[1]	Sept 22 to Oct 31	-52	-17	-11	-27	-25	-7	-6	-12
Total 2006		**-145**	**-60**	**-106**	**-104**	**-15**	**-40**	**-70**	**-42**
Total		**-109**	**-190**	**-156**	**-152**	**1**	**-180**	**-119**	**-99**

[1] this period is not the same period of time as others

[2] the readings are unreliable

ND sensors were not functioning properly during the entire season

Looking specifically at each test plot (Figure 5-12) other trends can be explained. TP1N shows evidence of snowmelt runoff and infiltration with small increases in water volume at the upslope and midslope locations, and a larger increase in water volumes at the downslope location. The larger volume of infiltrated snowmelt water at the lower slope location allowed more water to evapotranspirate from this location during the growing season than from the upslope. However, despite the greater volume of water available at the downslope location on TP1N, this area also had generally poor vegetation; therefore, the amount lost in the summer and fall was not as great as that at the midslope. The upslope location also had good vegetation;

however, as there was less water available at this location, not as much water can be lost through AET. Water volumes on TP1N appear above the field capacity for most of the monitoring period at the lower and midslope locations and just below field capacity at the upper location, though these values are within the +/- 100 mm sensor accuracy.

TP2N shows a trend that is similar to that for TP1N in 2005, with the greatest amount of water gained at the downslope location and the least at the upslope in the spring prior to the start of the growing season. This indicates that snow melt runoff and subsequent infiltration is occurring downslope. The spring infiltration at the mid-slope location in 2006 does not follow the pattern shown in 2005 since the increase in water volumes is much less than at the other locations, which are quite similar to each other. This may be in part due to distribution of the snowpack or perhaps accounted for with the instrument accuracy. Water volumes at the lower and midslope location were greater than the field capacity for much of the monitoring period, indicating that the soil was not free draining. The lower slope location shows water volumes fluctuating between field capacity and wilting point, indicating that at times, water volumes would be limiting to plant growth.

It is difficult to interpret the data for TP1S as both the upslope and midslope locations were offline at times and the downslope location provides unreliable data. The increase in water volume at the upslope location was nearly equal to precipitation indicating that all precipitation enters the cover at this location. The water volumes at the midslope location vary from field capacity to wilting point, indicating that there was sufficient water volume early in the monitoring period for plant growth, but that these water volumes drop below wilting point in 2006.

The behaviour of TP2S is also difficult to interpret. The total water volume on this test plot was very low, approximately 1/3 of that on the north slope. There is less increase in water volumes in the spring on this test plot than others. The relatively sharp increase and decrease in water volumes in 2006 at the downslope location indicates possible preferential flow around the instrumentation due to possible gaps between the instrument and soil. The lower slope water volume approached the wilting point by the end of the monitoring period, indicating limitations on plant growth while the midslope water volume was at or below wilting point for approximately half of the monitoring period.

The remarkably low volume of water at most locations on the south slope may be due to a combination of factors such as higher PE, higher vegetative growth, lower snow packs and a steeper slope, which may have produced more runoff during spring snow melt as well as in summer storm events. This would also be enhanced by more rapid snow melt events as a result of the higher net radiation on this slope.

A review of water volumes in each cover with respect to the estimated water volumes at field capacity and wilting point highlights some interesting trends. The water volume at each location was broken into depth ranges corresponding to topsoil, rooting depth, below rooting depth, and sand when present. A few examples of these plots are provided in Figure 5-13 through 5-16 with the remaining locations presented in Appendix B. Note that the water volume scale is different on TP2S (Figure 5-16) as the volumes are lower.

Looking at the water volume in the various depth intervals for TP1N upslope (Figure 5-13) it is evident that although the overall profile may be below the field capacity, the zone below the rooting depth appears to be above field capacity for the entire monitoring period. Due to the sensitivity of the water content sensors (~+/- 0.05 m^3/m^3), the water volume on each cover is approximately +/- 100 mm. Because of this large degree of uncertainty, the water volume may not be above field capacity; however, it is clear that water volumes were elevated here. This suggests that there was some mechanism holding water within the test plot at a higher saturation than gravity drainage would allow. The mechanism responsible for elevating water contents above the field capacity was likely linked to compaction and a lower hydraulic conductivity within the base of the cover. The density profiles for the TP1N do not extend to the full depth of the cover; therefore, it is unknown whether the density was greater at the base of the cover, however this would help to explain how the water was being held up and not draining freely. The average porosity of the till, based on density measurements is 0.34 m^3/m^3. This corresponds to a water volume of 272 mm for the below rooting depths. Based on this estimate, the base of the cover was not yet saturated, but it was moving towards that condition over time.

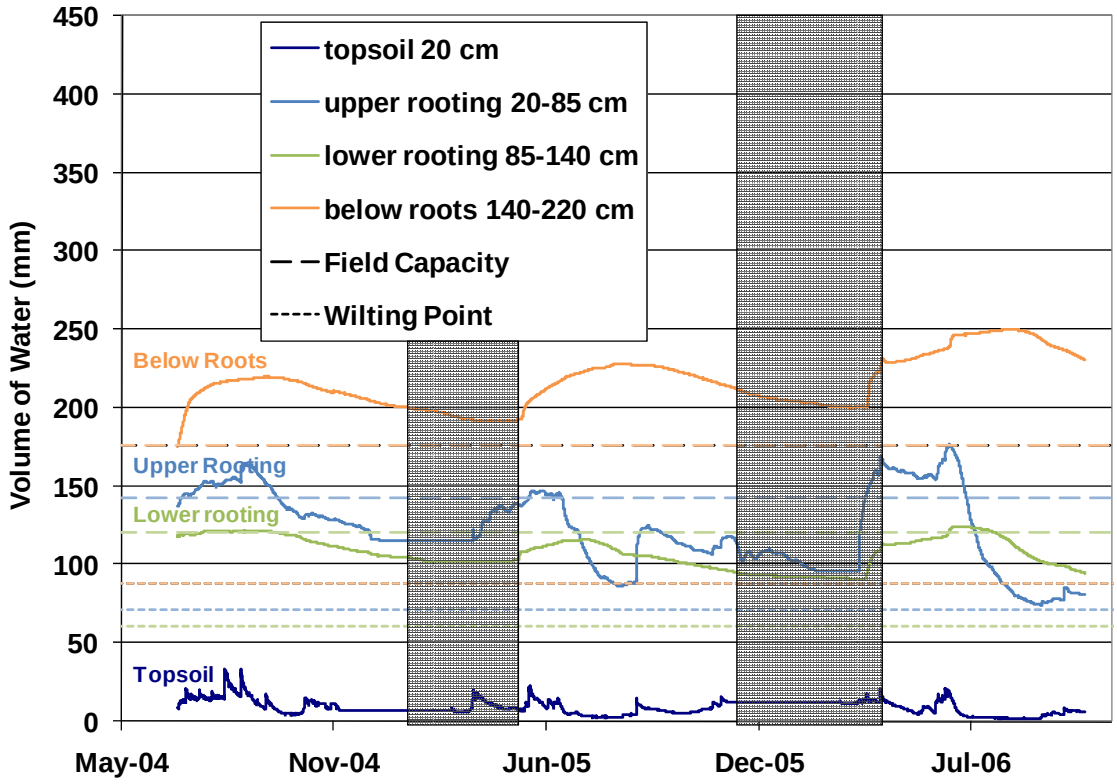

Figure 5-13 TP1N upper slope water volumes

In TP2N, the water volume at the midslope location was greater than field capacity for much of the monitoring period. Although this may be explained in a similar manner as for TP1N in terms of more compacted layers at depth, the presence the capillary break may also be responsible for elevating water volumes above field capacity. Looking at the distribution of water volumes with depths (Figure 5-14) the volume of water in the below rooting area was much higher than field capacity over the entire monitoring period. Based on the average porosity (0.34) the below rooting area was saturated for the majority of the monitoring period. As the upper rooting area approached wilting point and could no longer supply water to the vegetation, the roots began to draw more water from the lower rooting area. This explains why the lower rooting volume decreased below the field capacity when the upper rooting dips below wilting point.

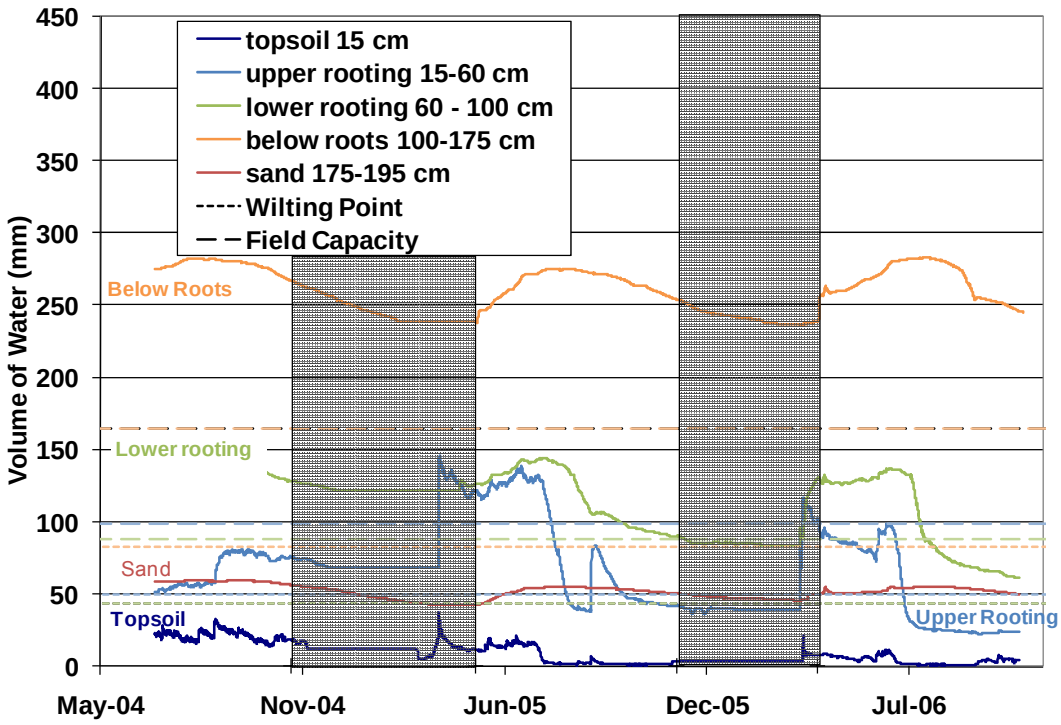

Figure 5-14 TP2N mid slope water volumes

The trends at TP1S are again difficult to interpret. The upper slope location had water volumes greater than field capacity for periods in the summer and then dropped below field capacity for the rest of the monitoring period. The short periods of higher water volume were likely due to increased water from snowmelt and summer precipitation before evapotranspiration began. When the water volumes are viewed in terms of depth increments (Figure 5-15), it is apparent that the upper and lower rooting depths were above field capacity, which supports this interpretation. The midslope location, though offline for a period, showed a gradual reduction in water volumes from field capacity to below wilting point. The vegetation, which was very good at this location, was likely using up all available precipitation as well as any available stored water. Assuming this was the case, the vegetation was requiring more water than that provided by precipitation at this location. If this trend continued the vegetation would begin to be affected as the volume of water moves below the wilting point. This was not the case at the upslope location as the vegetation was poor.

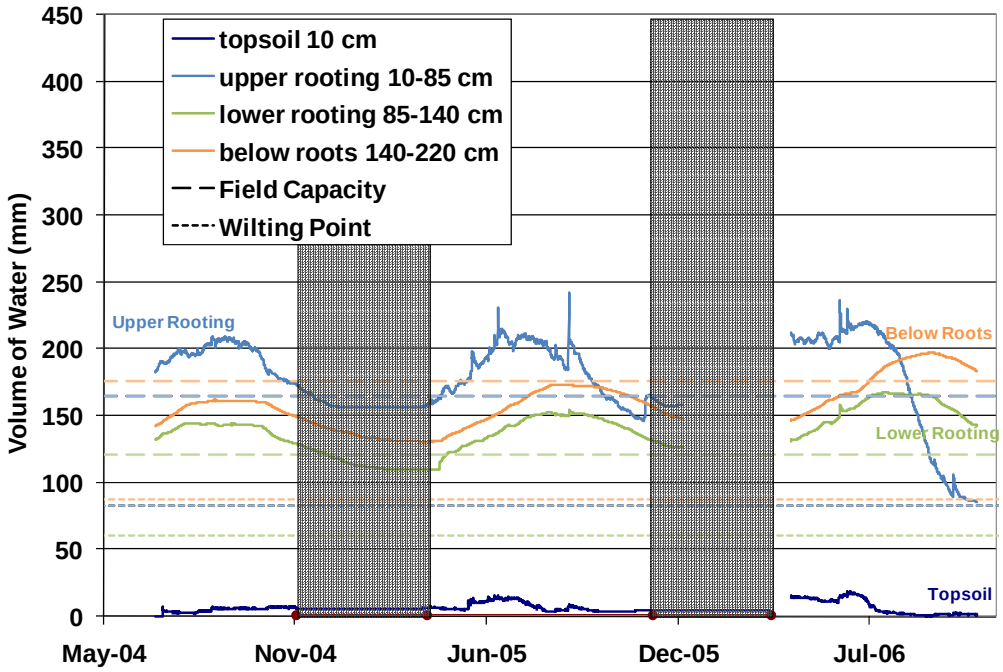

Figure 5-15 TP1S upper slope water volumes

The distribution of water on TP2S was quite different from the other test plots. At all slope locations the water volumes were below field capacity. The lower and upper slope locations approached wilting point and the midslope location had been below wilting point since approximately July 2005. The water volume at the upslope location, although it fluctuated seasonally, did not appear to be either wetting or drying with time. The downslope and midslope locations were gradually becoming drier. These locations had very good vegetation, which was utilizing all precipitation water and depleting any available stored water as well. This will become a problem as the water volume is below the wilting point and vegetation will no longer be able to draw from the stored water.

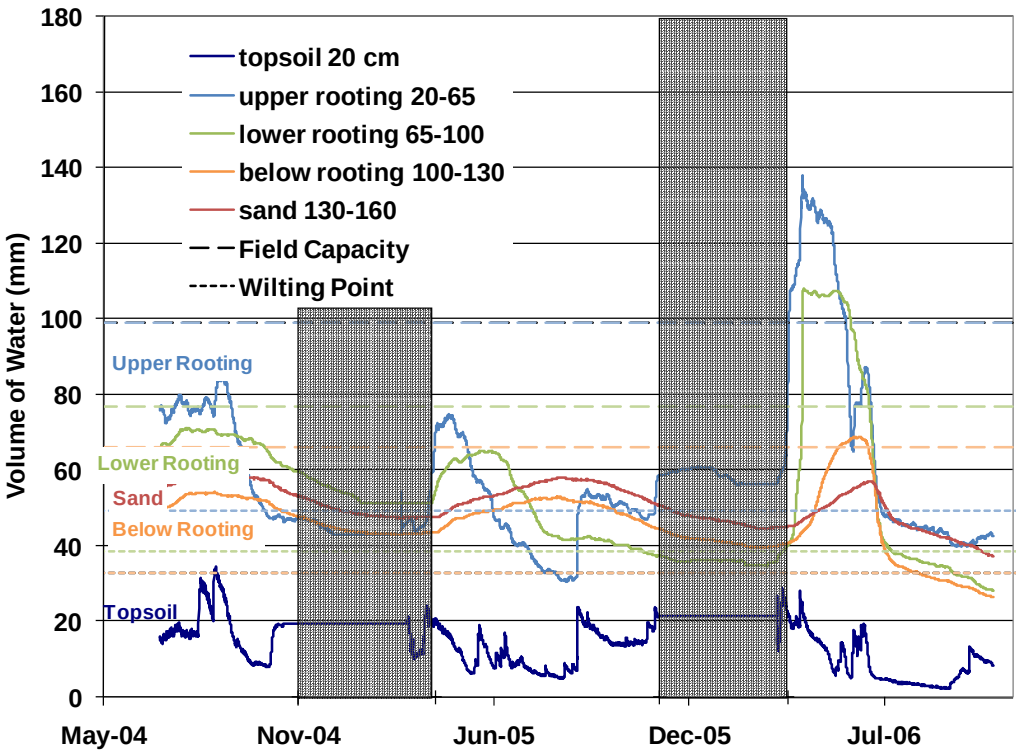

Figure 5-16 TP2S lower slope water volumes

The greatest decrease in water volume on all test plots occurred in the rooting zones. This is because the rooting zone is where plants draw water from for transpiration. The decrease of water volume in the rooting zone was occasionally more rapid than PET. This indicates that water was being lost to downward percolation as well as transpiration. This can be seen especially well in Figure 5-13 in 2006, and Figure 5-14 in 2005 and 2006.

Specific locations and times can demonstrate some of the processes that were evident and provide insights into where the water was going after it entered the test plots. Figure 5-17, and Figure 5-18 show select periods of interest, with rooting divided into an upper and lower rooting zone.

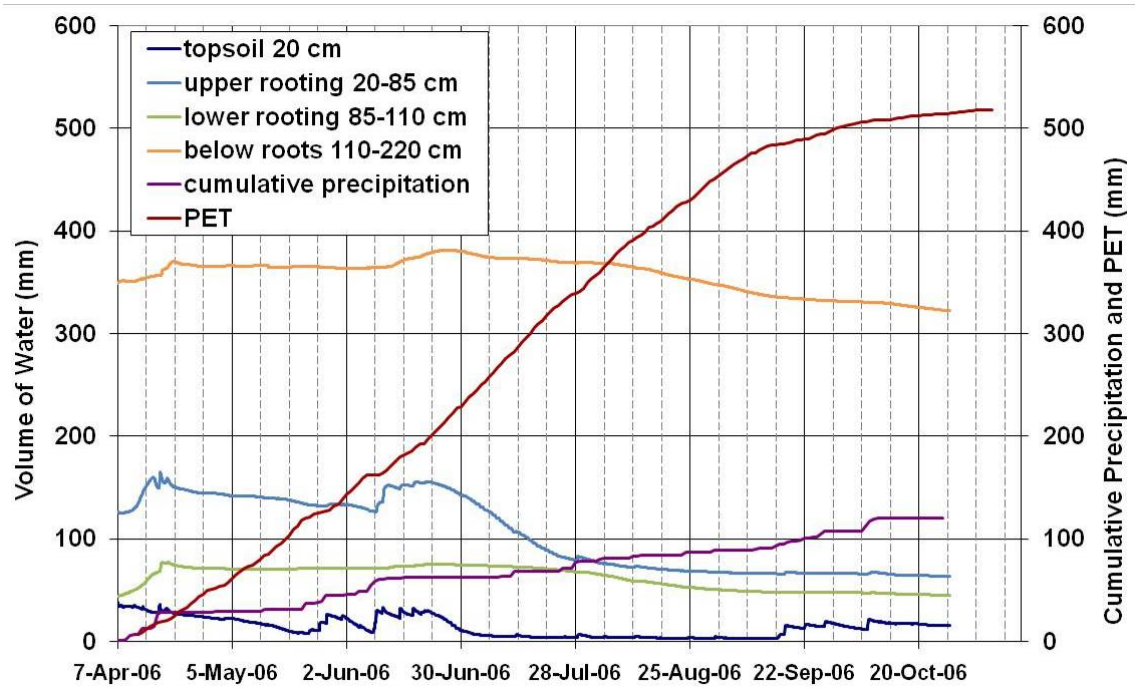

Figure 5-17 TP1N midslope water volumes 2006

Looking closely at TP1N midslope in 2006 (Figure 5-17) the sharpest decrease in water volume occurred in the topsoil and upper rooting zones beginning in the third week of June 2006. The drop continued in the topsoil for only approximately 1.5 weeks. At this point, the water content in the topsoil was so low and the suction was so high (approximately 1200 kPa from suction sensors) that it was unavailable for plant use. Water then began to be drawn from the upper rooting layer, shown by the water volume decreasing more sharply in upper rooting and leveling out in the topsoil after approximately June 30, 2006. The total decrease in water volume between June 23 and July 14, 2006 was 82 mm. The PET over this same time period was 86 mm. This indicates that either the ratio of AET to PET was nearly 100% or some water was lost was due to runoff, net percolation or interflow as well as PET. After July 14, 2006, the available water in the upper rooting zone began to decrease and water was drawn from the lower rooting zone as well as the upper rooting zone. After July 28 the volume of water in the upper rooting zone began to level out and the water volume in the lower rooting began to decrease. From July 28 to August 25, most of the water lost is in the lower rooting and the below rooting zones. After August 25, there was very little decrease in water volume in the upper rooting, however, the lower rooting and the below rooting areas had a continuous gradual decrease. The

hydraulic gradient at the base after August 27 was upward, (Figure 5-2) therefore, the loss in the below rooting zone was not due to net percolation but upward migration of water for AET.

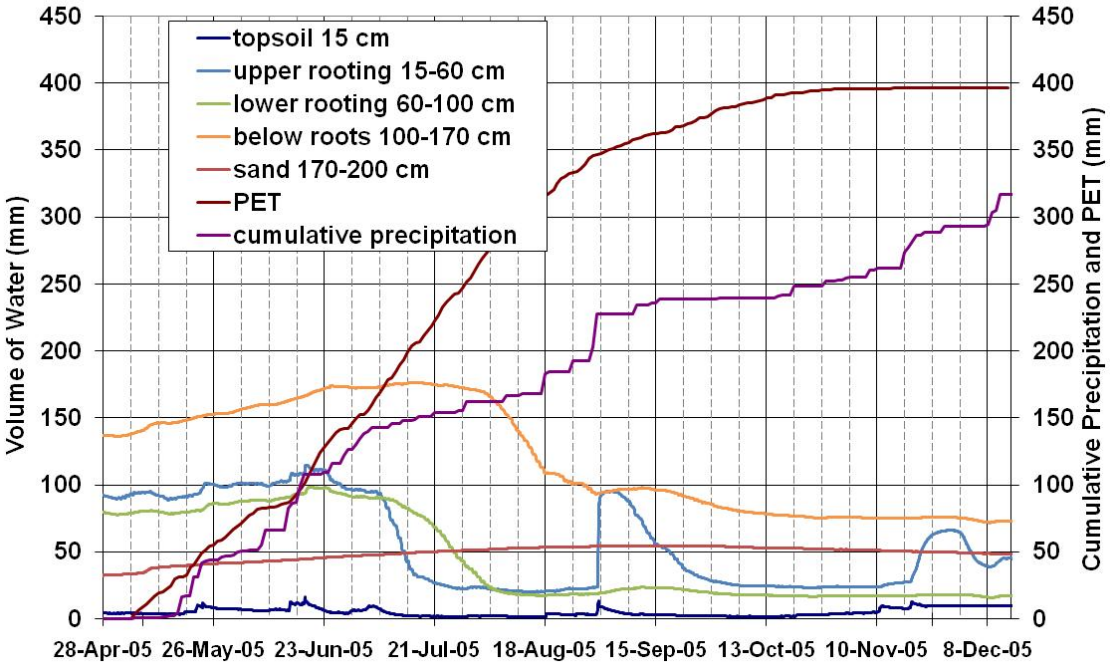

Figure 5-18 TP2N lower water volume 2005

On TP2N at the lower slope location in 2005 (Figure 5-18) drying began around July 7 in the topsoil and upper rooting zones. The rate of drying in these layers was approximately 7.7 mm per day. After approximately 1 week the decrease in water volumes in the upper rooting zone slowed down and the lower rooting began to decrease. The water content in the lower rooting zone was decreasing at approximately 2.8 mm per day for two weeks. After this the water volume in the lower rooting and the below rooting zones began to decrease (August 4). The below rooting zone decreased at approximately 4.1 mm per day for two weeks. The drying never reached the sand layer. Such high rates of decrease indicate losses from net percolation in addition to AET, as PET averages only 3.5 mm/day over this time period.

5.2. Water Balance

The interpretation of the various processes discussed previously along with the monitoring data to develop a daily water balance for each cover, based on Equation 5.1.

In the daily water balance, the assumption was made that the AET is a percentage of PET, and this factor was varied between covers and over the growing season. This factor was varied based on quality of vegetation and was then adjusted to fit the observed changes in storage within the water balance. For example, it stands to reason that the AET would be a greater percentage of PET in areas of stronger vegetation. AET/PET ratios were initially estimated from the work of Boese (2003) to be in the range of 0.5 to 0.9. These numbers were then adjusted in order to match the observed changes in stored water volumes and ranged from 0.1 to 0.7. The AET/PET ratios were linked to the quality of vegetation observed at each location and range from 0.1 to 0.5 for poor vegetation and 0.5 to 0.7 for good vegetation. Generally, ratios were greater for the south slope than for the north.

The results of the water balances are shown in Figure 5-19 through Figure 5-30. In the figures "PPT" denotes Precipitation, "DP" is deep percolation, and "Balance" is the calculated storage based on Equation 5.1. It should be noted that field change in storage over the winter was not calculated as the sensors did not function properly. Therefore, differences between the calculated and measured change in storage over the winter could be misleading. The pattern of the cumulative water volume during nonfreezing conditions is a better indicator of the agreement between the calculated daily water balance and the field measured storage.

Runoff and interflow were not included in the water balance calculations as the data was unreliable and the values were expected to be minimal. Any interflow or runoff that occurs will be shown lumped together with net percolation.

5.2.1. TP1N

The water balance for TP1N is shown in Figure 5-19, Figure 5-20 and Figure 5-21 for the upslope, midslope and downslope slope locations respectively. All TP1N locations show the same PET and precipitation. However, all other water balance components are different as a result of manipulating AET/PET ratios, percolation rates and different storages measured in the profile. The AET/PET ratios and percolation rates used for TP1N are summarized in Table 5-2.

The AET/PET ratios applied reflect the vegetative properties at each location in each time. For example, in 2004 there was very little if any vegetation at any locations, and 2004 showed the lowest AET/PET ratio. Percolation rates were applied in order to best match the change in storage data. However, trends can be derived from these as well. Generally, when the AET/PET values were lower, that is, when vegetation was less established, percolation rates were higher. This is because water that enters the test plot was neither removed due to plant transpiration, nor drawn to the surface because of suction caused by vegetative transpiration demand, and was therefore free to percolate through the cover with little resistance. It should be noted that the rate of percolation was primarily dependant on the hydraulic gradient and conductivity of the soil near the base of the cover rather than on the total amount of water available. The volume of percolation was dependant on the percolation rate and the time periods percolation was applied (based on available water and hydraulic gradient as described in Section 5.1.3).

Table 5-2 AET/PET ratios and percolation rates for TP1N

		AET/PET	Vegetation	Percolation (mm/day)
Upslope	2004	0.50	Poor	0.50
	2005	0.60	Good	0.20
	2006	0.60	Good	0.20
Midslope	2004	0.50	Poor	1.00
	2005	0.65	Good	0.70
	2006	0.70	Good	0.20
Downslope	2004	0.40	Poor	0.50
	2005	0.50	Poor	1.00
	2006	0.40	Poor	0.70

The values for each component of the water balance over the entire monitoring period are summarized in Table 5-3. Negative values for change in storage and calculated balance indicate that the cover was drier than initial placement. A number of trends are evident in both the water balance figures and the summary values. At both the upslope and midslope locations, AET was approximately equal to precipitation. As the vegetation was very poor at the lower slope location, precipitation exceeded AET. The upslope location showed the least amount of net percolation, the greatest was at the downslope location. The calculated balance was similar at both the upslope and downslope locations as the increased AET at the upslope was matched by the

increased net percolation at the downslope location. As the field change in storage was not calculated over the winter, the pattern of the cumulative water volume during nonfreezing conditions is a better indicator of the agreement between the calculated daily water balance. For example, at the lower slope location at the end of 2005, the storage nearly matched the balance; however, the increases and decreases through 2005 were much more varied indicating a poor match. At the same location in 2006 the values of storage and balance differed significantly, although the shape of each component over time is very similar with similar increases and decreases at the same time indicating a very good match.

The volume of water stored in the covers as estimated from the Diviner 2000® measurements differ somewhat from those estimated from the automated measurements. However the differences probably indicate nothing more than spatial differences or can be attributed to sensor accuracy.

Table 5-3 TP1N Water Balance Components for Each Growing Season(mm)

	2004			2005			2006			Total		
Slope Location	**Down slope**	**Mid slope**	**Up slope**	**Down slope**	**Mid slope**	**Up slope**	**Down slope**	**Mid slope**	**Up slope**	**Down slope**	**Mid slope**	**Up slope**
PPT	148	148	148	269	269	269	247	247	247	664	664	664
PET	252	252	252	393	393	393	469	469	469	1114	1114	1114
AET	101	126	126	197	255	236	188	329	282	485	710	643
NP	35	71	30	113	49	30	29	14	28	177	134	87
ΔS	-54	-108	-29	-17	-24	-12	41	-15	12	-30	-147	-29
Balance	12	-49	-7	-41	-36	3	30	-96	-63	2	-180	-67

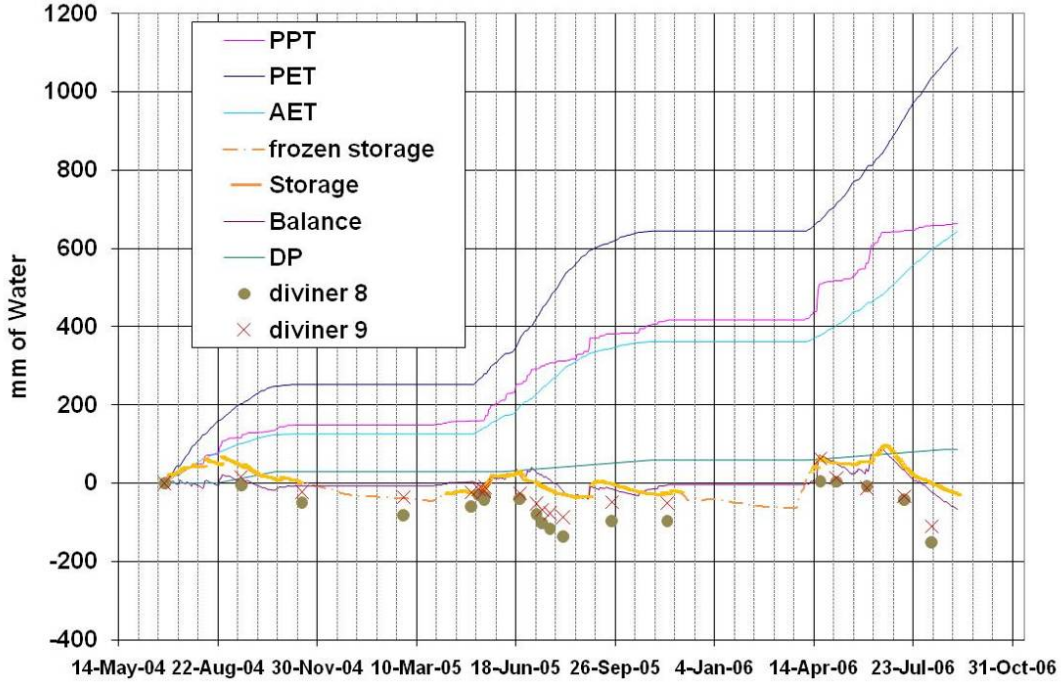

Figure 5-19 TP1N upper water balance

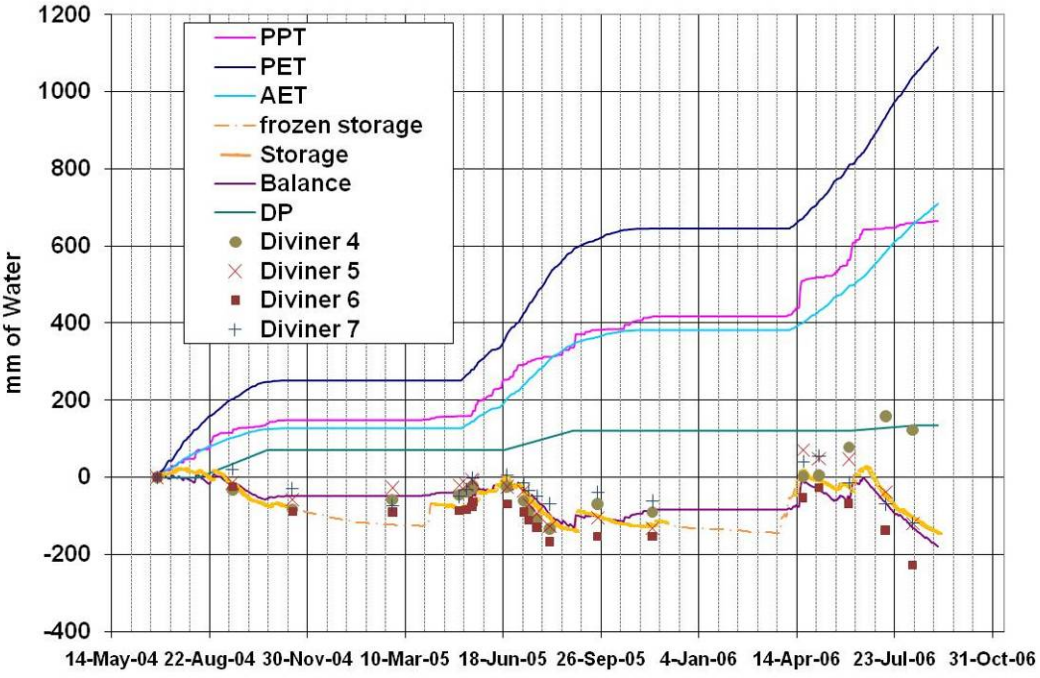

Figure 5-20 TP1N midslope water balance

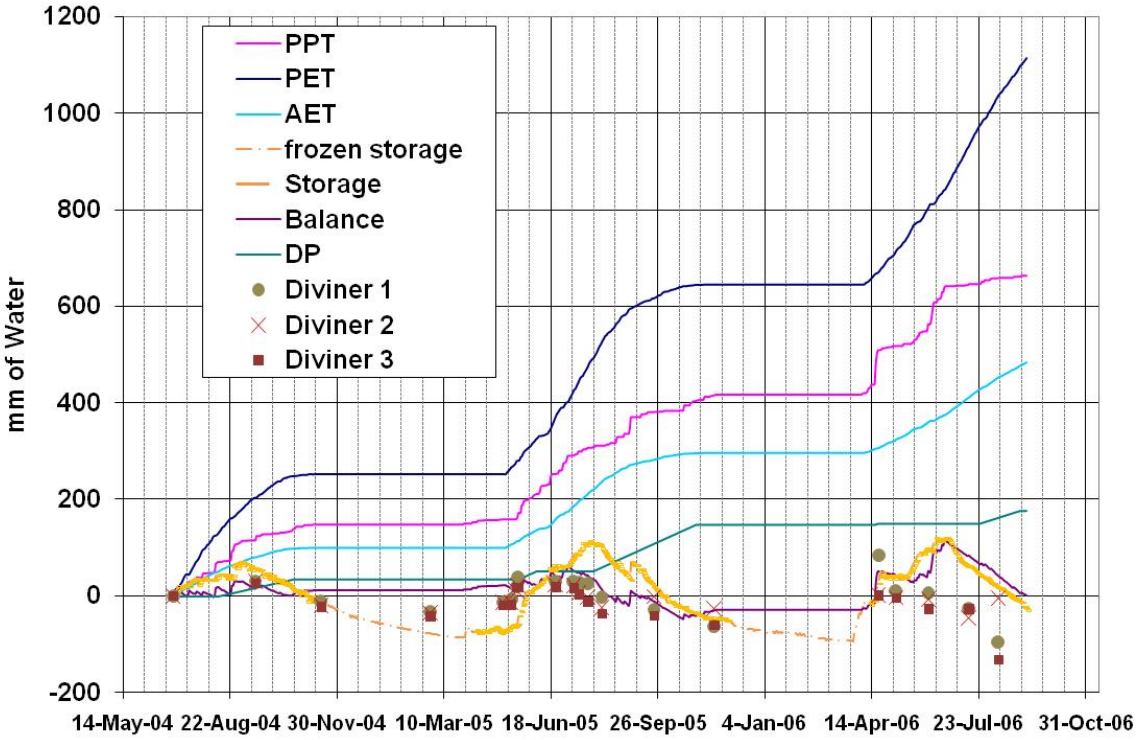

Figure 5-21 TP1N lower water balance

5.2.2. TP2N

The water balances for TP2N are shown in Figure 5-22, Figure 5-23, and Figure 5-24 for the upper, mid and lower slope locations, respectively. The AET/PET ratios and percolation rates used for TP2N are summarized in Table 5-4.

Table 5-4 AET/PET ratios and percolation rates for TP2N

		AET/PET	Vegetation	Percolation (mm/day)
upper	2004	0.50	Poor	0.00
	2005	0.60	Good	0.00
	2006	0.60	Good	0.00
Mid	2004	0.40	Poor	0.80
	2005	0.70	Good	1.00
	2006	0.50	Good	1.00
Lower	2004	0.10	Poor	2.00
	2005	0.40	Poor	3.00
	2006	0.40	Poor	3.00

The values for each component of the water balance after the entire monitoring period are summarized in Table 5-5. Negative values for change in storage and calculated balance indicate that the cover was drier than initial placement.

The estimated values of AET at both the upslope and midslope locations were approximately equal to precipitation meaning that transpiration was utilizing all available water entering the system. The vegetation was very poor at the lower location with the result that the AET was less than precipitation. Again, the upslope experienced the least amount of net percolation and the downslope experienced the most. The calculated water balance showed that the upslope location was wetter than it was at placement and the midslope and downslope locations were drier. This is counter-intuitive as the vegetation was "good" at the upslope yet it showed a net gain in water, whereas the downslope had poor vegetation yet it showed a net loss. This is because the water balance on TP2N was primarily driven by percolation as opposed to AET with percolation ranging from 56% of precipitation at the downslope location to 15% at the upslope. There is a good match at all locations between measured storage and calculated balance indicating that the water balance is providing a good representation of the various processes. The Diviner storage matched the automated storage more closely on TP2N than TP1N, even though the test plot was twice as long, and therefore was expected to have more differences due to spatial differences.

Table 5-5 TP2N Water Balance Components (mm)

	2004			2005			2006			Total		
Slope Location	**Down slope**	**Mid slope**	**Up slope**	**Down slope**	**Mid slope**	**Up slope**	**Down slope**	**Mid slope**	**Up slope**	**Down slope**	**Mid slope**	**Up slope**
PPT	148	148	148	269	269	269	247	247	247	664	664	664
PET	252	252	252	393	393	393	469	469	469	1114	1114	1114
AET	25	101	126	157	275	236	188	235	188	370	611	550
NP	150	38	0	285	93	0	189	75	0	624	206	0
ΔS	-138	-39	-28	-60	-83	39	-55	-5	86	-253	-127	98
Balance	-27	9	22	-173	-99	33	-130	-63	59	-331	-153	114

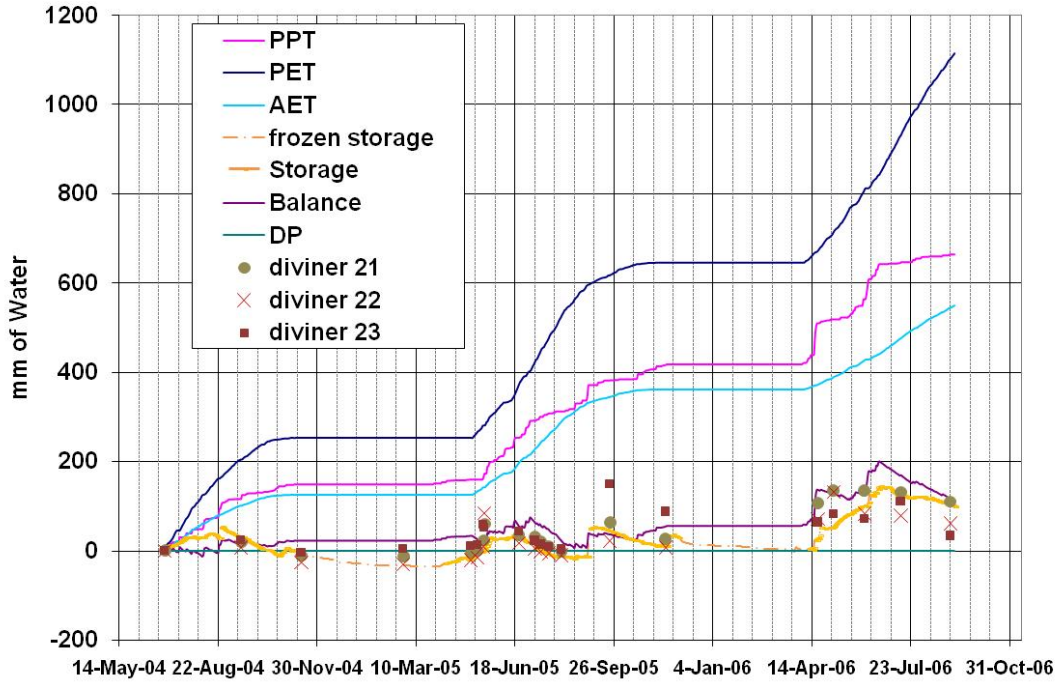

Figure 5-22 TP2N upslope water balance

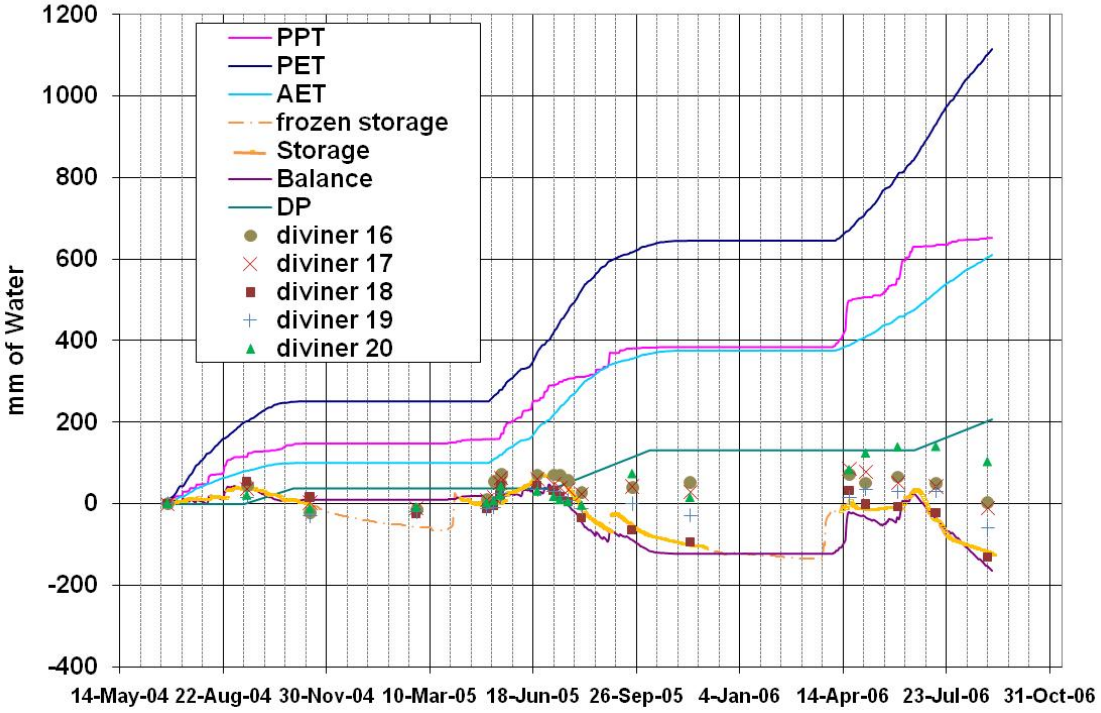

Figure 5-23 TP2N midslope water balance

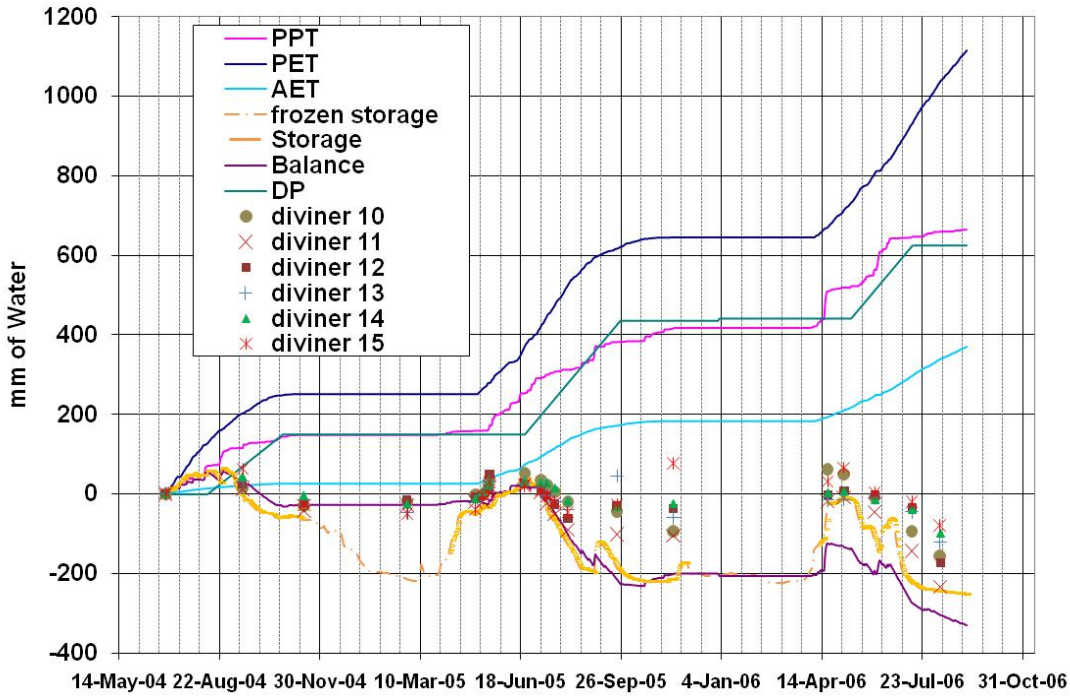

Figure 5-24 TP2N downslope water balance

5.2.3. TP1S

The water balances for TP1S are shown in Figure 5-25, Figure 5-26 and Figure 5-27 for the upslope, midslope and downslope locations, respectively. The AET/PET ratios and percolation rates used for TP1S are summarized in Table 5-6.

The values for each component of the water balance for the entire monitoring period are summarized in Table 5-7. Negative values for change in storage indicate that the cover was drier than initial placement. It should be noted that there was a problem in comparing the different locations since the midslope location water content sensors were offline for 9 months and the upslope for 4 months. Because of this, absolute values of each water balance component were not used;. Instead, the general shape of the water balance was analyzed during periods when the sensors were functioning properly.

Table 5-6 AET/PET ratios and percolation rates for TP1S

		AET/PET	Vegetation	Percolation (mm/day)
upslope	2004	0.20	Poor	0.6
	2005	0.30	Poor	0.8
	2006	0.40	Poor	0.4
midslope	2004	0.30	Poor	1.5
	2005	0.65	Good	0.0
	2006	0.55	Good	0.0
downslope	2004	0.10	Poor	2.0
	2005	0.40	Poor	3.0
	2006	0.40	Poor	3.0

The upslope location showed good correlation between the measured and calculated stored water volumes. The precipitation at this location was approximately 200 mm greater than the AET, yet the change in storage was nearly zero. The excess water entering the system was lost to deep percolation or perhaps runoff. The AET was lower due to the poor vegetation at this location. The midslope water content sensors were functioning properly in 2004 and 2006 and the measured and estimated changes in storage were in good agreement. All of the net percolation at this location (123 mm) occurred in 2004 due to the poor vegetation at this time. Though the automated water sensors located downslope did not provide accurate data, the Diviner readings can still be trusted and the calculated balance was adjusted to match the Diviner readings instead of the automated readings.

Table 5-7 TP1S Water Balance Components (mm)

	2004			2005			2006			Total		
Slope Location	Down slope[1]	Mid slope	Up slope	Down slope[1]	Mid slope[2]	Up slope	Down slope[1]	Mid slope	Up Slope[3]	Down slope[1]	Mid slope	Up slope
PPT	148	148	148	269	269	269	247	247	247	664	664	664
PET	267	267	267	599	599	599	531	531	531	1398	1398	1398
AET	53	80	53	360	390	180	318	292	212	732	762	446
NP	89	123	43	0	0	0	0	0	0	89	123	43
ΔS	-43	-123	-47	17	-71	18	60	-45	25	35	-239	-3
Balance	6	-55	52	-91	-121	89	-72	-45	34	-156	-221	175

[1] water content unreliable at this location
[2] water content sensors offline for 9 months
[3] water content sensors offline for 4 months

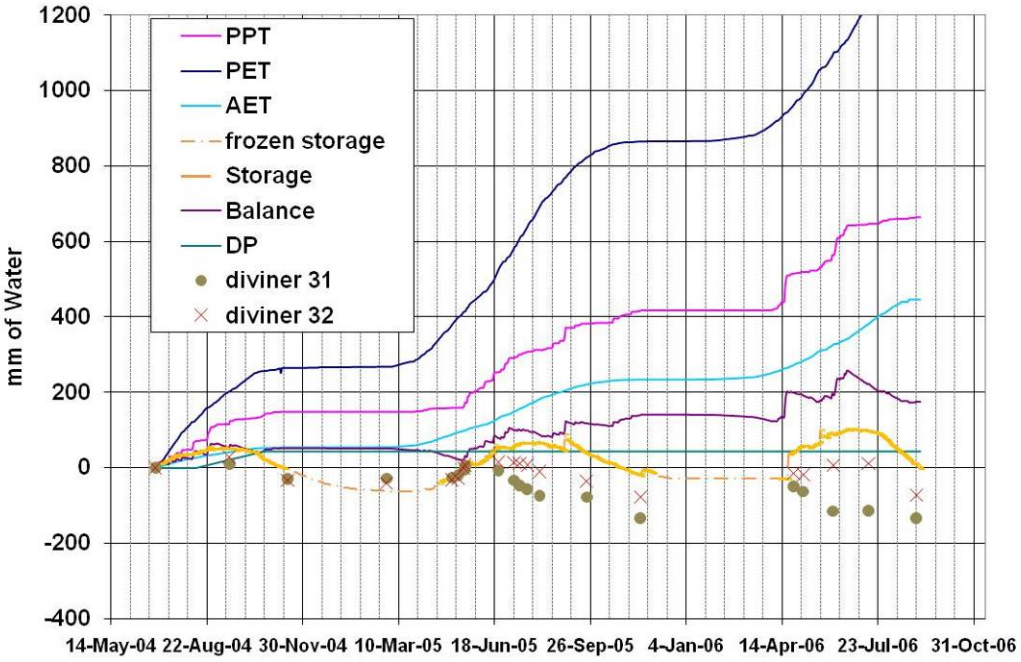

Figure 5-25 TP1S upslope water balance

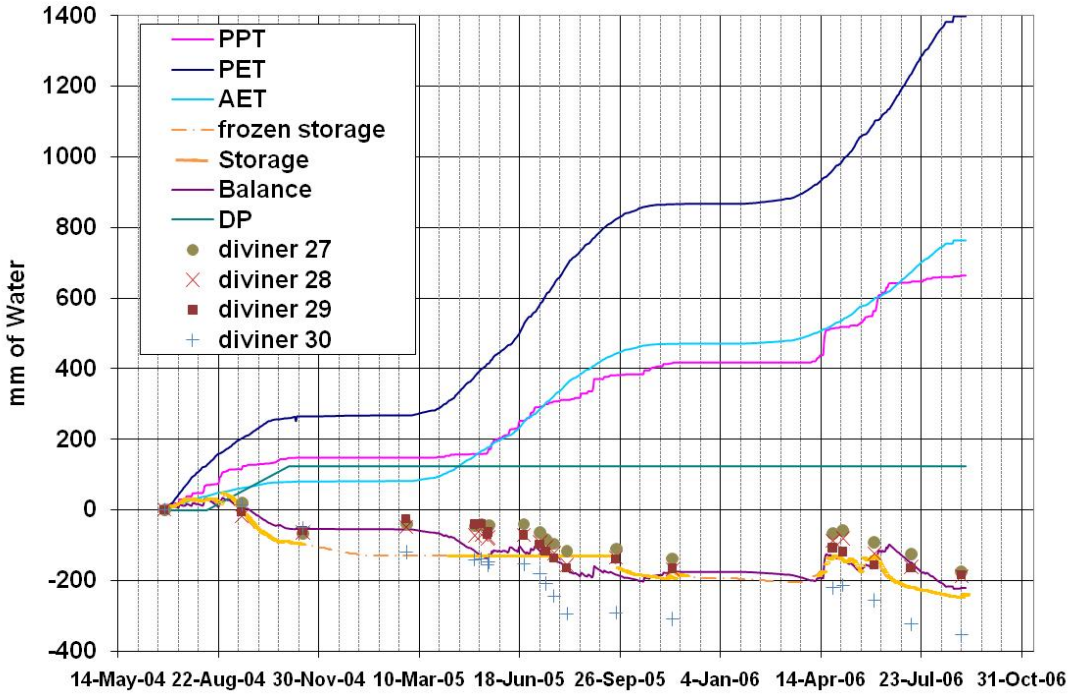

Figure 5-26 TP1S midslope water balance

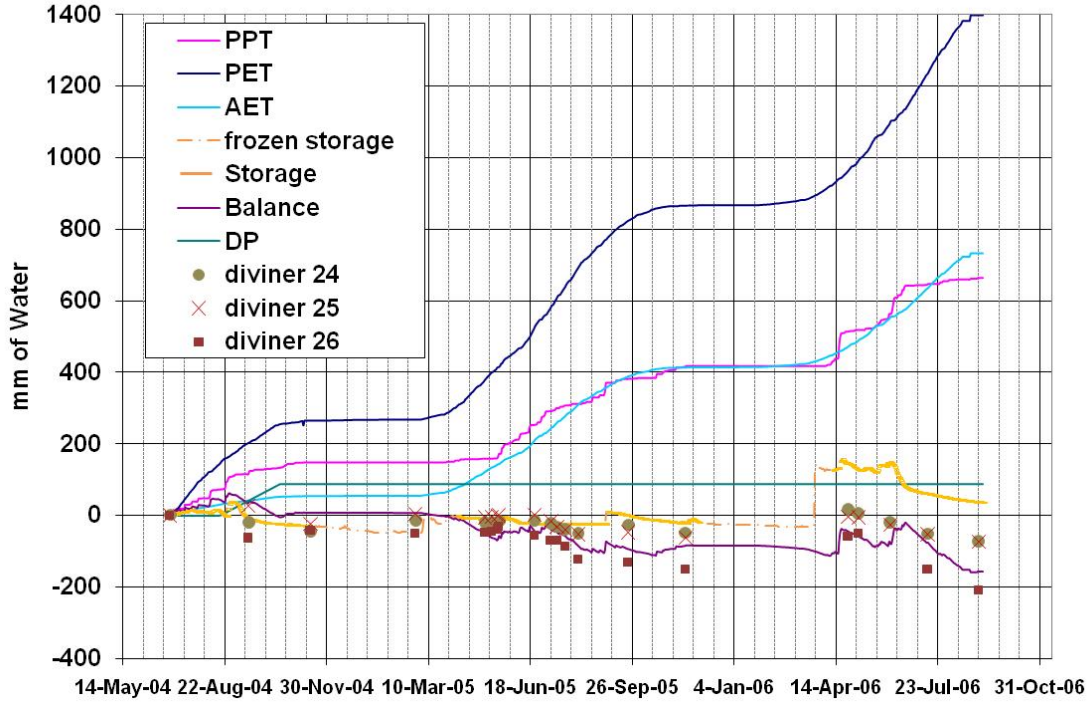

Figure 5-27 TP1S lower water balance

5.2.4. TP2S

TP2S water balances are shown in Figure 5-28, Figure 5-29, and Figure 5-30 for the upslope, midslope and downslope locations respectively. The AET/PET ratios and percolation rates used for TP2S are summarized in Table 5-8. The AET/PET ratios are based on observed vegetation conditions at each location in each year. In 2004 there was little to no vegetation at all locations. Vegetation growth improved greatly in 2005 and 2006; however, the midslope location showed that the AET/PET ratios decrease each year and each location had a lower AET/PET ratio in 2006 than in 2005. Vegetation growth did occur; however, water consumption may have been less efficient due to the very low water contents (higher moisture stress) in 2005 and 2006.

Percolation on this test plot was nearly nonexistent. The cover was very dry and one of the criteria for percolation is that the base must be saturated.

Table 5-8 AET/PET ratios and percolation rates for TP2S

		AET/PET	Vegetation	Percolation (mm/day)
upslope	2004	0.4	Poor	0.5
	2005	0.5	Poor	0
	2006	0.35	Poor	0
midslope	2004	0.5	Poor	0
	2005	0.6	Good	0
	2006	0.5	Good	0
downslope	2004	0.4	Poor	1
	2005	0.6	Good	0
	2006	0.5	Good	3

The values for each component of the water balance over the entire monitoring period are summarized in Table 5-9. Negative values for change in storage and calculated balance indicate that the cover was drier than initial placement. The upslope location showed very little change in water storage throughout the monitoring period. This is because this location was very dry and the vegetation was poor and consequently there is little AET. The midslope and downslope locations were also very dry; however, the vegetation here was good, pulling more of the water out of the system as AET than at the upslope location. There was generally a good match between calculated and measured storage; however, the response of measured water storage to precipitation events was less than calculated storage. This may in part be due to the precipitation being lost to interception by vegetation, or the result of runoff. There was a poor match at TP2S downslope location in 2006 as water appeared to be leaving the cover in the measured storage, even though the calculated balance does not reflect this. It is possible that water was leaving the cover laterally at a depth above the base, or that water was perhaps leaving via preferential flow paths. No deep percolation was calculated as the base of the cover was not near saturation.

Table 5-9 TP2S Water Balance Components (mm)

	2004			2005			2006			Total		
Slope Location	**Down slope**	**Mid slope**	**upslope**	**down slope**	**mid slope**	**upslope**	**down slope**	**mid slope**	**upslope**	**down slope**	**mid slope**	**upslope**
PPT	148	148	148	269	269	269	247	247	247	664	664	664
PET	267	267	267	599	599	599	531	531	531	1398	1398	1398
AET	107	134	107	360	360	300	265	265	186	732	759	592
NP	93	0	39	0	0	0	0	0	0	93	0	39
ΔS	-52	-67	-22	-2	-58	10	-53	-6	31	-107	-132	19
Balance	-52	15	2	-91	-91	-31	-19	-19	61	-161	-95	32

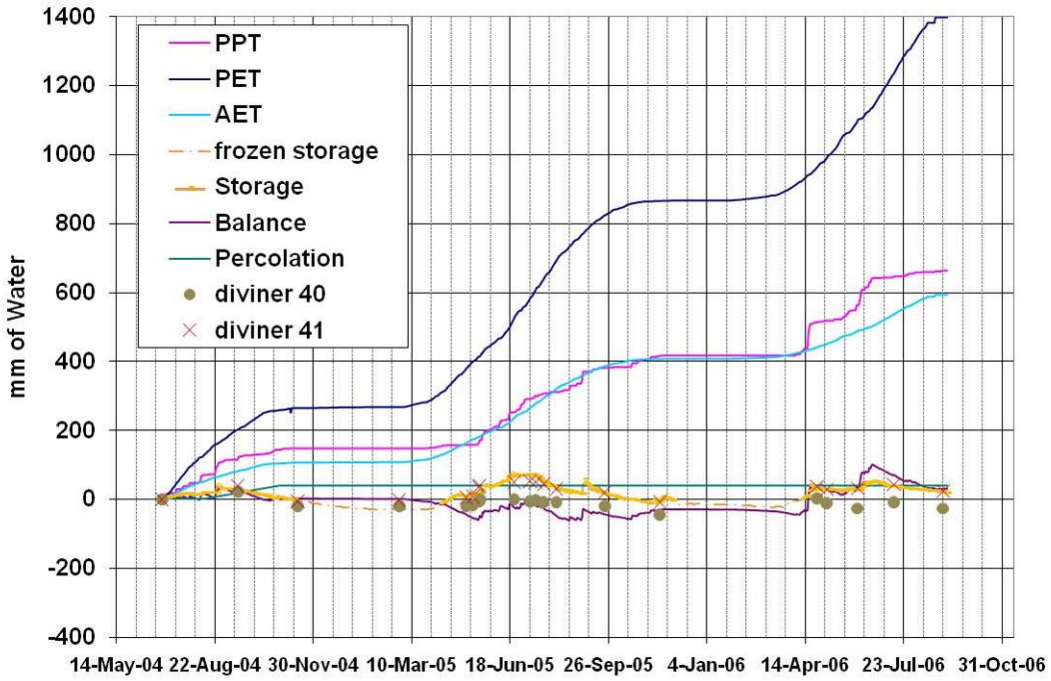

Figure 5-28 TP2S upslope water balance

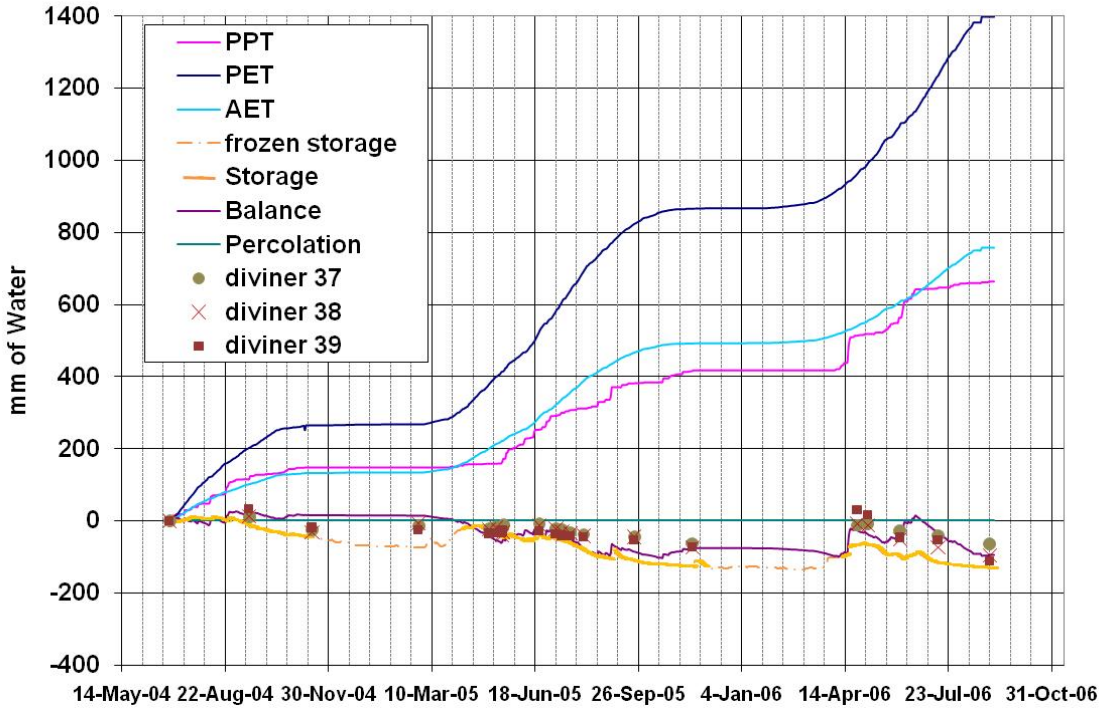

Figure 5-29 TP2S midslope water balance

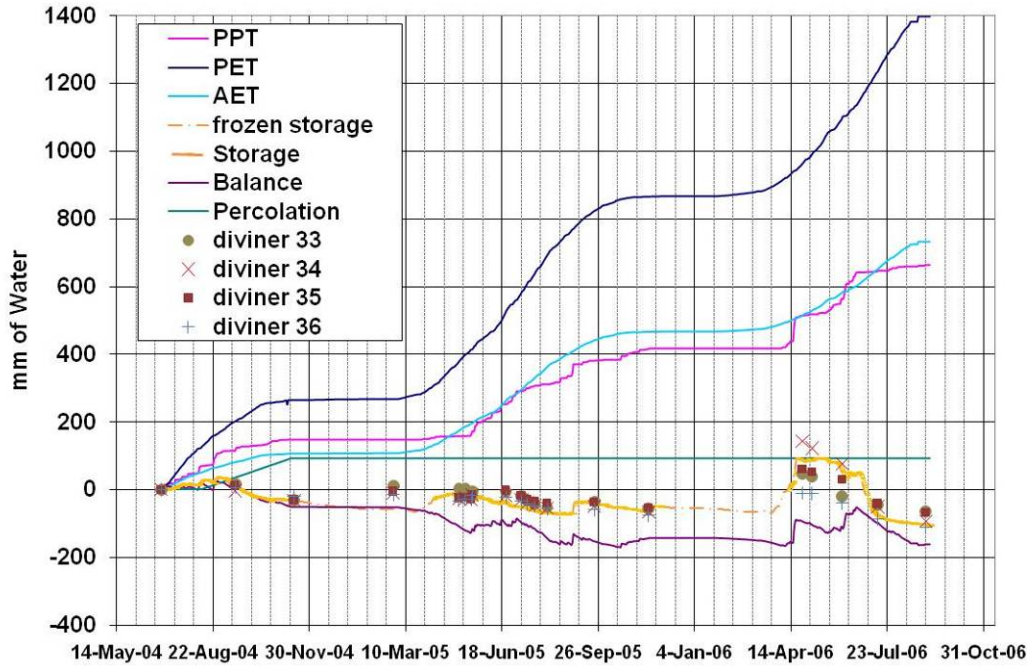

Figure 5-30 TP2S downslope water balance

5.2.5. Comparison of all Test Plots

The water balances can be compared on the basis of slope aspect and design. Both test plots on the north slope showed the greatest net percolation at the downslope location and the least at the upslope location. The downslope location also showed the least amount of AET on the north test plot as the vegetation was poorest at this location. The south test plots had higher average AET than the north test plot. This is because the PET was greater on the south slope and also, the vegetation was very good at most locations on the south slope. Net percolation was generally greater on the north slope than on the south slope. This was primarily because the south slope is very dry, particularly at the base.

Both the store-and-release type covers showed similar magnitudes of net percolation; however, the responses at the upslope and downslope were reversed for the different slopes. This was attributed to the different vegetation at these locations; the vegetation on the lower northern slope was similar to that at the upper southern slope and vice versa. The north capillary break cover showed much more percolation at the midslope and downslope locations compared with the

south capillary break cover. This is again due to the fact that the south slope was much drier than the north slope. Therefore it can be seen that slope aspect and vegetation play more significant roles than that played by cover type.

The average annual net percolation for each test plot is summarized below in

Table 5-10. It can be seen that the north capillary break cover had the greatest average net percolation while the south capillary break had the least. Capillary break was not maintained on TP2N on various occasions when water percolated into the sand layer. The south slope does not show any clear failures as the sand layer remained in a drained condition throughout the monitoring period, resulting in the low average net percolation.

Table 5-10 Net Percolation Summary

Test Plot	Average Net Percolation (mm)
TP1N	44.2
TP2N	92.2
TP1S	28.3
TP2S	14.7

Due to the failure of the north capillary break test plot and the associated large amount of net percolation, it is suggested that the store-and-release test plots were functioning better than the capillary break test plots. Both covers on the south slope provided very little net percolation because they were very dry, so cover design plays less of a role. Net percolation may still be occurring through preferential flow or there was possibly some loss of water to lateral flow. The capillary break cover showed large differences in performance based on slope aspect and subsequently net radiation, while the store-and-release cover showed little difference over both covers. Because of the discussed difficulties in calculating the water balance for the south covers, the net percolation results for the north covers were assumed to be more trustworthy and representative of the comparison in performance between the two designs. In the Year Three Performance Monitoring Report (GAL and OKC, 2008), the recommendation was to implement the store-and-release cover as part of the final design, rather than the capillary break cover based on cover performance, in particular, net percolation.

CHAPTER 6
CONCLUSIONS AND RECOMMENDATIONS

The overall objective of this project was to evaluate the preliminary performance of the four test plots on the City of Regina landfill with regards to net percolation, gas flux, water balance and vegetation. To meet this overall objective three specific objectives were identified:

- Evaluate the performance and integrity of the monitoring scheme.
- Characterize the properties of the soil covers on the four test plots.
- Develop a preliminary water balance using the monitoring field data.

The fulfillment of these objectives is described in the following sections.

6.1. Summary

6.1.1. Evaluation of the Monitoring Scheme

Installation of most of the instrumentation for this project was outside the scope of the thesis. However, proper installation and accurate calibration is critical to ensuring useable data. Regular maintenance is also important to prevent and promptly repair malfunctioning instrumentation. As was seen in this project, various problems occurred with nearly every type of monitoring. A summary of some of these difficulties is provided below:

The rainfall tipping bucket installed at the site did not appear to be recording precipitation events accurately. The results from the Environment Canada weather station at the Regina Airport were compared to those recorded on the test plot and the difference was approximately 21% less on site. Despite any spatial variability, it was believed that the Environment Canada precipitation was more accurate and was therefore used in the interpretations made in this study. It is unclear what caused erroneous readings from the on site tipping bucket.

Net radiation was measured on both the south and north slopes. The net radiometer on the north slope was not functioning between November 2005 and April 2006, likely due to interference from snow or debris. The net radiometer on the south slope was not functioning

from August 2006 to the end of monitoring due to damage from wildlife. The overall downtime for both sensors was 12%.

Runoff collection on all test plots proved to be unreliable. There were various problems including debris blocking the runoff channel interfering with the sonic depth probe. The channels also shifted over time, causing them to become more shallow which allowed runoff to overflow the collection channel. Holes were present in the channel lining allowing water to seep below the liner and therefore preventing all runoff from being measured. The temperature sensor used to correct the weir depth malfunctioned during the first year of monitoring. The heaters in the runoff huts were not turned on before runoff began therefore runoff was frozen in the collection channel leading to false readings.

Suction sensors failed on TP1S between April 20 and May 16, 2006. This affected both suction readings and temperature readings during this period. The cause is believed to be an error with the datalogger which was corrected after the datalogger program was reloaded. It was also noted when comparing lab and field SWCCs that field water content and suction values were often reading low.

Manual temperature readings were unavailable at the upslope location on TP1S as the sensors were pulled from the ground repeatedly, presumably by wildlife.

Automated water content sensors on the TP1S upslope, midslope and downslope all had errors. The upslope location was broken between December 28, 2005 and April 20, 2006. The midslope location was broken between January 27 and September 21, 2005. The problem was believed to be problems with the SDI-12 interface board that controls the readings. The board was replaced in both situations and the problems were resolved. The TP1S downslope water content sensors between 55 cm and 155 cm were not responding appropriately to atmospheric conditions, showing very low water contents until mid March 2006 when there was a sudden increase. This may be attributed to poor contact between the PVC access tube and the surrounding soil between these depths. The increase in March may be from sediment shifting or perhaps from settlement filling the gap between the sensor tube and the soil. However the readings were still not comparable with those measured at adjacent locations and are not used in analysis. Overall on this test plot, only 50% of sensors were working on average.

Manual Diviner 2000® water content access tubes were installed on each test plot on the right edge to test for any possible edge effects. Readings in these locations did not respond

appropriately to atmospheric conditions. Readings were very dry, indicating poor contact with surrounding soil. This is likely due to poor installation techniques as the proper installation equipment was not available.

Although there were several problems, the overall performance of the monitoring scheme was good. Problems with automated water content sensors, suction sensors and net radiometers were only temporary and were easily fixed shortly after they were detected. The reason for the difficulties with the rain gauge is still unknown but may be due to some kind of instrument defect. The problems with runoff measurement are perhaps the most troublesome and difficult to overcome. More care and human intervention may have prevented the problems such as not having the monitoring hut heaters turned on in time and not having regular daily maintenance to clean out the debris. The holes in the liner could be patched but the deformation due to settlement and movement of the entire test plot cannot be prevented. Perhaps annual reshaping of the channel is necessary to ensure all runoff water is captured, or perhaps a less flexible structure should be installed such as a half culvert to collect and transport runoff.

6.1.2. Estimation of the Soil Cover Properties

Various soil properties were measured or calculated for the soil covers. Although the water content and hydraulic conductivity functions were not dissimilar to those presented by GAL and OKC (2005(b)) the results from the undisturbed samples and the interpretation of monitoring data does provide more reliable estimates of these important properties.

One of the most apparent differences in material properties from those used in the initial design was the high level of compaction of the test plots. The plots were supposed to be constructed of non-compacted till. However, based on density testing done on *in situ* samples, the till is compacted to approximately 98% of its maximum density based on compaction tests by GAL and OKC, (2005(b)). Compaction at this level will impede the establishment of vegetation by restricting root growth and promote the development of preferential flow through macrostructure (e.g. fractures) created by wet/dry and freeze/thaw cycling.

The degree of compaction also controls the porosity of the cover, and thus the saturated water content. This results in moisture retention curves that have a lower saturated water content than those used in the initial design. The values of saturated hydraulic conductivity were also slightly lower than those used by Golder in the preliminary modelling. Available water holding capacity

is also affected by the increased compaction. The amount of water the covers can store is decreased as compared to what would have been possible with less compaction. This may cause more net percolation as the covers become saturated with less water.

6.1.3. Preliminary Water Balance

Slope aspect and vegetation had a large influence over the the water balance of the covers. Test plots on the south were much drier than those on the north. This was generally due to PET being greater on the south slope due to increased net radiation and higher AET/PET ratios as a result of better vegetation.

The test plots on the north slope showed the greatest net percolation at the downslope location and the least at the upslope location. The downslope locations also showed the least amount of AET as the vegetation was poorest at this location. The south test plots had higher average AET values than the north test plot. This is because the PET was greater on the south slope and the vegetation was very good at most locations on the south slope. Net percolation was generally greater on the north slopes due primarily to the fact that the south slope was very dry, particularly at the base.

Both the store-and-release type covers showed similar magnitudes of net percolation, however the upslope and downslope responses were reversed on the different slopes. This was attributed to the different vegetation at these locations; the downslope on the north was similar to the upslope on the south and vice versa. The north capillary break showed much more percolation at the midslope and downslope locations than the south. This was again due to the fact that the south slope was much drier than the north. Therefore it can be seen that slope aspect had more influence on cover performance than did the different cover designs.

The net percolation was greater for the capillary break test plots than the store-and-release test plots on the north slope. This was primarily because the north capillary break test plot failed on numerous occasions and allowed a large amount of net percolation. Both covers on the south slope provide very little net percolation due to their very dry condition, irrespective of cover design. Net percolation may still have been occurring through preferential flow and there may have been some loss of water to lateral flow. The capillary break cover showed a large difference in performance based on slope aspect and subsequently net radiation, while the store-and-release covers performed similarly over both slopes. Because of the discussed difficulties

estimating net percolation for the south covers, the net percolation values for the north covers were assumed to be more trustworthy and representative of the comparison in performance between the two designs.

6.2. Conclusions

The main conclusions drawn with respect to the objectives outlined for the project are as follows:

- The monitoring scheme had a few significant flaws. The runoff collection system did not accurately capture and record runoff on all test plots. Also, the interflow collection system was designed so that it only would collect interflow before it broke through into the sand layer, where substantial interflow could not be collected.
- A number of key physical properties of the soil were measured and canbe used as a baseline for future studies. The main finding was that bulk density of the till was significantly over compacted in a manner that would affect the cover performance .
- The water balances calculated for the test plot indicated that there was no significant difference in performance in terms of increased storage or decreased net percolation between the capillary break and store-and-release covers. In contrast, the different slope aspects resulted in large differences in both water storage and net percolation.

6.3. Recommendations

The following recommendations are provided to improve operation of the COR landfill test plot instrumentation:

- Repair the runoff collection system to ensure accurate collection and recording of runoff from each test plot. Provide regular maintenance and monitoring during the snowmelt period to keep debris out of the collection channel and weir box.
- An analyses of slope deformation (e.g. settlement and/or stability) was not included in the scope of this thesis, however it was noted that movement was occurring on the test plots. It is recommended that an evaluation of the geotechnical stability of the covers be undertaken in future work on the site, including the incorporation of deformation monitoring as part of the cover monitoring system.

- Reinstall EnviroSCAN® and Diviner 2000 ® access tubes at locations where poor soil contact is suspected. Use the data from Diviner tubes installed on the right side of each test plot to investigate possibilities of edge effects.
- Conduct additional testing to help characterize the evolution of material properties with time - particularly hydraulic conductivity, density, gas composition, root mass density and biomass.
- Further characterize the vegetation on each test plot in order to determine species and likely transpirative demands.
- Consider reconstructing a portion of the covers with lower levels of compaction and more control over topsoil placement and vegetation to highlight the effect of compaction on cover performance. This could be done through mechanical disturbance of the upper one meter of the covers followed by replacement of the topsoil and reseeding.
- Undertake *in situ* testing of the density and *in situ* hydraulic conductivity of the soil near the base of the covers, and perhaps the temporary cover placed by the COR above the waste to verify the presence of a lower compacted layer which is limiting downward percolation on the north covers.
- Review and redesign the interflow collection system to verify whether interflow within the covers is actually occurring. Consider installation of an interflow capture system on both the store-and-release and capillary break covers.
- Saturated conditions at the base of the covers, particularly on the north slope, should provide a barrier to gas fluxes. This could be investigated by carrying out a proper gas survey right into the waste.
- Final cover placement should have tighter controls on the placement density of the till and more QA/QC. Future construction should also include tighter control on the vegetation placement and QA/QC on growth should take place to ensure that plants are growing and removing water effectively.
- Future work should be more multidisciplinary. Designers should consult geotechnical engineers, plant biologists, soil scientists as well as the contractors who will be

performing the work as each group will have different insights beneficial to the final design.

The following recommendations are provided for future research:

- Investigate the geotechnical behavior of covered slopes (e.g. deformation and stability). The south slope was very steep and showed some evidence of cracking and slumping. This has the potential to create preferential flow paths, as well as cause problems with instrumentation and runoff collection. The steepness of the slopes may cause movement of the cover, as well as settlement of the waste.
- A numerical model of moisture dynamics within the cover should be developed and be calibrated to the field measurements of water content and suction. The calibrated model can then be used to predict long-term performance of the cover under various climate scenarios. Additionally, the model can be used to fine-tune elements of the cover design such a selection of an optimal cover thickness for each slope aspect.
- Further research into the end receptors and maximum allowable net percolation rate and leachate composition is warranted. This should be balanced with the contaminating life of the landfill and the rate of decomposition.
- The net percolation data obtained from this site should be compared to other sites (e.g. landfills and covered mine waste) with similar materials, climate and/or monitoring systems.

REFERENCES

Abu-Hamdeh, N.H., and Reeder, R.C.. 2000. Soil Thermal Conductivity: Effects of Density, Moisture, Salt Concentration, and Organic Matter. Soil Science Society of America Journal. Vol. 64: 1285-1290.

Albright, W.H., Benson, C.H., Gee, G.W., Roesler, A.C., Abichou, T., Apiwantragoon, P., Lyles, B.F., Rock, S.A. 2004. Field Water Balance of Landfill Final Covers. Journal of Environmental Quality, 33: 2317-2332.

Agilent Technologies Inc. 2000. Agilent G2890A and G2891A Series Micro GCs, M Series User's Manual. Agilent Technologies, Inc. 2850 Centerville Road. Wilmington, DE 19808-1

Agriculture Canada. 1992. Land Suitability Rating System for Spring-Seeded Small Grains, 1992 Working Document. A technical report prepared by Agronomics Interpretations Working Group submitted to Expert Committee on Soil Survey.

American Society for Testing and Materials (ASTM). 1990. Standard test method for particle size analysis of soils (D422-63; reapproved 1990). In 1996 Annual Book of ASTM Standards, Vol. 4.08. ASTM, Philadelphia, Pa. pp 10-16.

American Society for Testing and Materials (ASTM). 1991. Standard guide for measuring matric potential in the vadose zone using tensiometers (D3404-91). In 1996 Annual Book of ASTM Standards, Volume 4.08. ASTM, Philadelphia, Pa., pp. 338-347.

American Society for Testing and Materials (ASTM). 1993. Standard classification of soils for engineering purposes (Unified Soil Classification System) (D2487-93). In 1995 Annual Book of ASTM Standards, Vol 4.08. ASTM, Philadelphia, Pa., pp 217-226.

American Society for Testing and Materials (ASTM). 2003..Standard test method for the determination of the soil water chararcteristic curve for desorption using a hanging column, pressure extractor, chilled mirror hygrometer, and/or centrifuge (D6836 - 02(2008)e1) In 2008 Annual Book of ASTM Standards, Vol. 4.09. ASTM, Philadelphia, Pa.

Anderson, S.P., Dietrich, W.E., Montgomery, D.R., Torres, R., Conrad, M.E. and Loague, K. 1997. Subsurface flow paths in a steep, unchanneled catchment. Water Resources Research. Vol. 33, no. 12: 2637-2653.

Ayres, B.K. 1998. Field Monitoring of Soil-Atmosphere Fluxes through Uranium Mill Tailings and Natural Surface Soils at Cluff Lake, Saskatchewan. M.Sc. Thesis, University of Saskatchewan, Saskatoon, Saskatchewan, Canada.

Barbour, S.L., Boese, C., Stolte, B., 2001. Water Balance for Reclamation Covers on Oilsands Mining Overburden Piles. 2001 Canadian Geotechnical Conference, Calgary, Canadian Geotechnical Society, pp 313-319.

Barbour, S.L., Chanasyk, D., Hendry, J., Leskiw, L., Macyk, T., Mendoza, C., Naeth, A., Nichol, C., OKane, M., Purdy, B., Qualizza, C., Quideau, S. and Welham, C. (2007). Soil Capping Research in the Athabasca Oil Sands Region Volume 1: Technology Synthesis, DRAFT, Syncrude Canada Ltd., March, (175 pages).

Beeri, O., Phillips, R., Hendrickson, J., Frank, A., and Kronberg, S. 2007. Estimating forage quantity and quality using aerial hyperspectral imagery for northern mixed-grass prairie. Remote Sensing of Environment. Vol 110. pp 216-225.

Bendz, D., and Bengtsson, L. 1996. Evaporation from an active, uncovered landfill. Journal of Hydrology. Vol. 182. pp 143-155

Benson, C.H., Bosscher, P.J., Lane, D.T. and Pliska, R.J. 1994. Monitoring system for hydrologic evaluation of landfill covers. Geotechnical Testing Journal. 17: 138-149.

Berger, J., Fornes, L.V., Ott, C., Jager, J., Wawra, B. and Zanke, U. 2005. Methane oxidation in a landfill cover with capillary barrier. Waste Management. Vol. 25, pp 369-373.

Blight, G.E., and Fourie, A.B. 2005. Experimental Landfill Caps for Seim-Arid and Arid Climates. Waste Management and Research, Vol. 23, pp 113-125.

Boese, C.D. 2003. The Design and Installation of a Field Instrumentation Program for the Evaluation of Soil-Atmosphere Water Fluxes in a Vegetated Cover over Saline/Sodic Shale Overburden. M.Sc. Thesis, University of Saskatchewan, Saskatoon, Saskatchewan, Canada.

Bosch, D.D., Hubbard, R.K., West, L.T. and Lowrance, R.R. 1994. Subsurface flow patterns in a Riparian Buffer System. American Society of Agricultural Engineers. 37(6): 1783-1790.

Bussiere B., Aubertin M., & Chapuis R.. 2003. Canadian Geotechnical Journal. Vol. 40, pp 512-535.

Bras, R.L. 1990. Hydrology: An introduction to Hydrologic Science. Addison-Wesley Publishing Company, Inc., Reading, Mass.

Campbell Scientific (Canada) Corporation. 1994. CR10 Measurement and Control Module Operator’s Manual.

Curtis, A.A. and Johnson, C.D. 1987. Monitoring unsaturated soil water conditions in groundwater recharge studies. In Proceedings, International Conference on Measurement of Soil and Plant Water Status, Logan, Utah, 1987. pp. 267-274.

Dwyer, S.F.. 1995. Alternative landfill cover demonstration. Geotechnical Special Publication. n.53. p 19-34

Dwyer, S.F. 1998. Alternative Landfill Covers Pass the Test. Civil Engineering. vol. 68. iss 9.

Feng, M. 1999. The Effects of Capillary Hysteresis on the Measurement of Matric Suction Using Thermal Conductivity Sensors. M.Sc. Thesis, University of Saskatchewan, Saskatoon, Saskatchewan, Canada.

Flerchinger, G.N., Cooley, K.R., Hanson, C.L. and Seyfried, M.S. 1998. A uniform versus an aggregated water balance of a semi-arid watershed. Hydrological Processes. 12:331-342.

Fredlund, D.G., Gan, J.K-M. and H. Rahardjo. 1991. Measuring negative pore-water pressures in a freezing environment. Transportation Research Record 1307: 291-299.

Fredlund, D.G. and Rahardjo, H. 1993. Soil Mechanics for Unsaturated Soils. John Wiley & Sons, Inc., New York, NY.

GAL 2003. Final Cover Evaluation Study – Fleet Street Landfill. Stage 2 Proposal.

Gardner, W.R., and Kirkham, D. 1952. Determination of soil moisture by neutron scattering. Soil Science 73: 391-401.

Gartung, E. 1996. Landfill liners and covers. Proceedings of the 1996 1st European Geosynthetics Conference. P. 55

GeoAnalysis 2000 Ltd. 2001. SoilCover Version 5.2 User's Manual.

Geo-Slope Internation Ltd. 2003. VADOSE/W On-Line Help Version 1.16

Golder Associates Ltd. and O'Kane Consultants Inc. (GAL and OKC). 2005(a). Field Performance Monitoring Reference Manual for the City of Regina Fleet Street Landfill Final Cover Trials. Report #705-01 submitted to City of Regina, January, 2005.

Golder Associates Ltd. and O'Kane Consultants Inc. (GAL and OKC). 2005(b). Fleet Street Landfill final cover evaluation study – design and construction report. Report submitted to City of Regina, January, 2005.

Golder Associates Ltd. and O'Kane Consultants Inc. (GAL and OKC). 2008. City of Regina – Fleet Street Landfill Test Cover Program, Year Three Performance Monitoring Report.

November 2006 to October 2007. Prepared for City of Regina Engineering and Works. January 2008.

Granger, R.J. 1989. An Examination of the Concept of Potential Evaporation. Journal of Hydrology, 111: 9-19.

Gray, D.M. 1970. Handbook on the Principles of Hydrology. Canadian National Committee for the International Hydrological Decade.

Hauser, V.L, Weand, B.L., Gill, M.D. 2001. Natural Covers for Landfills and Buried Waste. Journal of Environmental Engineering, 127, no. 9, p. 769-775.

Hewlett, J.D. 1982. Principles of Forest hydrology. Univ. of Georgia Press, Athens, GA.

Hutchinson, D.G. and Moore, R.D. 2000. Throughflow variability on a forested hillslope underlain by compacted glacial till. Hydrological Processes. 14: 1751-1766.

Jordan, J.P. 1994. Spatial and temporal variability of stormflow generation processes on a Swiss catchment. Journal of Hydrology. 153: 357-382.

Kampf, M., Holfelder, T. and Montenegro, H. 2001. Material Selection Capillary Barriers. Proceeding Sardinia 2001, Eighth International Waste Management and Landfill Symposium. Vol. 3, pp 325-334

Khire, M.V., and Haydar M. M. 2007. Leachate Recirculation in Bioreactor Landfills Using Geocomposite Drainage Material. Journal of Geotechnical and Geoenvironmental Engineering. 133: 166-174.

Khire, M.V., Benson, C.H., and Bosscher, P.J. (1997). Water calance modeling of earthen final covers. Journal of Geotechnical and Geoenvironmental Engineering. American Society of Civil Engineering, Vol 123, No 8, pp 744-754

Kim, W-H. and Daniel, D.E.. 1992. Effects of freezing on hydraulic conductivity of compacted clay. Journal of Geotechnical Engineering. 118: 1083-1097.

Lee, N.H. 1999. Evaluation of Cover Materials for a Large Scale Test Facility at Key Lake. M.Sc. Thesis, University of Saskatchewan, Saskatoon, Saskatchewan, Canada.

Look, B.G. and Reeves, I.N. 1992. The application of time domain reflectometry in geotechnical instrumentation. Geotechnical Testing Journal. 15: 277-283.

McCartney, J.S. and Zornberg, J.G. 2006. Decision analysis for design of evapotranspirative landfill covers. Proceedings of the fourth International Conference on Unsaturated Soils. P 694-705

Meiers, G.P. 2002. The use of field measurements of hydraulic conductivity to characterize the performance of reclamation soil covers with time. M.Eng Thesis, University of Saskatchewan.

Meiers, P.G., Barbour, S.L., and Qualizza, V.C., 2006. The use of *in situ* measurements of hydraulic conductivity to provide an understanding of cover system performance over time. Paper presented at the 7th International Conference on Acid Rock Drainage, St. Louis, MO, USA, March 26-29.

Meerdink, J.S., Benson, C.H., and M.V. Khire, 1996. Unsaturated Hydraulic conductivity of Two Compacted Barrier Soils. Journal of Geotechnical Engineering. Amercian Society of Civil Engineers, Vol. 122, No. 7, July, pp. 565-576.

Nyhan, J.W., Schofield, T.G., and Starmer, R.H. 1997. A Water Balance Study of Four Landfill Cover Designs Varying in Slope for Semiarid Regions. Journal of Environmental Quality, Vol. 26: 1385-1392.

O'Kane, M. 1996. Instrumentation and Monitoring of an Engineered Soil Cover System of Acid Generating Mine Waste. M.Sc. Thesis, University of Saskatchewan, Saskatoon, Saskatchewan, Canada.

Othman, M.A., Bonaparte, R., Gross, B.A., and Schmertmann, G.R. 1995. Design of MSW Landfill Final Cover Systems. Proceedings of the 1995 Conference of the Geotechnical Engineering Division of ASCE in Conjunction with the ASCE Convention. San Diego, CA. p 218-257.

Parent, S.-E. and A. Cabral. 2006. Design of Inclined Covers with Capillary Barrier Effect. Geotechnical and Geological Engineering. 24: 689–710

Penman, H.L. 1948. Natural evapotranspiration from open water, bare soil and grass. Proceedings of the Royal Society of London, Series A, 193: 120-146.

Raven, P.H., Evert, R.F., Eichhorn, S.E. 1999. Biology of Plants, 6th Edition. W.H. Freeman and Company/Worth Publishers. New York.

Reid Crowther & Partners Ltd. 1993. Fleet Street Landfill Proposed Closure Plan. Prepared for the City of Regina Municipal Engineering Department.

Saskatchewan Environment and Resource Management (SERM). 1998. Draft Guideline for the Closure and Reclamation of Municipal Waste Disposal Grounds, October 1998.

Shafer, R., Renta-Babb, A., Smith, E., Bandy, J. June 1984. Landfill liners and covers: properties and application to Army landfills. US Army Corps of Engineers, Construction Engineering Research Laboratory. Technical Report N-183.

Soilmoisture Equipment Corporation, 1997. Model 2725AR Jet-fill Tensiometer Operating Instructions. http://www.soilmoisture.com/PDF%20Files/82725a.pdf. December 2006

Smith, C.D. 1995. Hydraulic Structures. University of Saskatchewan Printing Services, Saskatoon, SK.

Soilmoisture Equipment Corp. 2007 www.soilmoisture.com/trace.html

Somasundaram, S., LaFountain, L., and Ananthanathan, J.. 2005. Performance monitoring and model verification for an evapotranspirative landfill cover. Geo-Frontiers 2005. p 3557-3568

Stormont, J.C. 1996. Effectiveness of two capillary barriers on a 10% slope. Geotechnical and Geological Engineering. 14: 243-267.

Strahler, A.N. and Strahler, A.H. 1983. Modern Physical Geography. John Wiley & Sons, Inc., New York, NY.

Topp, G.C., Davis, J.L. and Annan, A.P. 1980. Electromagnetic determination of soil water content: measurements in coaxial transmission lines. Water Resources Research. 16: 574-582.

Van Genuchten, M., 1980. A closed-form equation for predicting the hydraulic conductivity of unsaturated soils. Soil Science Society of America Journal. 44, pp:892-898.

Vesilind, P. A., Worrell, W., and Reinhart, D. R. 2002. *Solid Waste Engineering*. Brooks/Cole, Pacific Grove, Calif.

Weeks, B. and Wilson, G.W. 2006. Prediction of evaporation from soil slopes. Canadian Geotechnical Journal. 23: 815-830.

Wilson, G.W. 1990. Soil evaporative fluxes for geotechnical engineering problems. Ph.D. Thesis, University of Saskatchewan, Saskatoon, Saskatchewan, Canada.

Wilson, G.W., Fredlund, D.G. and Barbour, S.L. 1991. The evaluation of evaporative fluxes from soil surfaces for problems in geotechnical engineering. In Proceedings, 44th Canadian Geotechnical Conference, Vol. 2. September, 29-October, 2. Paper No. 68.

Wilson, G.W., Barbour, S.L. and Fredlund, D.G. 1995. The Prediction of evaporative fluxes from unsaturated soil surfaces. In Proceedings, First International Conference on Unsaturated Soils, Paris, France, September 6-8, 1995.

Woo, M. 1997. A guide for ground based measurement of the arctic snow cover. Climate Research Branch, Atmospheric Environment Service.

Young, M.H., Albright, W., Pohlmann, K.F., Pohll, G., Zachritz, W.H., Zinter, S., Shafer, D.S., Nester, I. and Oyelowo, L. 2006. Incorporating Parametric Uncertainty in the Design of Alternative Landfill Covers in Arid Regions. Vadose Zone Journal. Vol 5, p 742-750.

Zornberg, J.G., LaFountain, L., and Caldwell, J.A. 2003. Analysis and design of evapotranspirative cover for hazardous waste landfill. Journal of Geotechnical and Geoenvironmental Engineering. Vol 129, no. 5, p 427-438.

APPENDIX A
INSTRUMENTATION DETAILS AND METHODS

Data Acquisition System

The DAS consists of the datalogger, a Campbell Scientific Inc. (CSI) CR10X, a Multiplexer, CSI AM 16/32, and a Power Source (a solar panel and battery from CSI). Further details about these components can be found in Boese (2003), Campbell Scientific (1994, 2001). The thermal conductivity sensors and the automated electrical capacitance sensors are connected to the DAS that automatically records *in situ* matric suction, temperature and volumetric water content measurements every two hours. Buried communication wires connect the upslope and downslope sensors to the DAS.

Thermal Conductivity Sensors

A Model 229 thermal conductivity sensor consists of a probe inserted axially into a porous cylinder, which has a diameter of 15 mm and length of 32 mm. The probe consists of a heating element and a thermocouple embedded in a stainless steel tube. The heating element and thermocouple are connected to extension wires embedded in an electrical insulating resin that connects the instrument to the data logger.

Water Content Sensors

The EnviroSCAN® system consists of a number of sensors mounted onto a rail inserted into a PVC access tube and controlled by a SDI-12 logic board. The SDI-12 board is then connected to the datalogger to provide automated measurement of volumetric water content. The Diviner 2000® system consists of a single sensor on a shaft with an automated depth sensor (the probe), PVC access tubes, and a handheld display unit. Insertion of the probe into an access tube provides an immediate profile of soil moisture at regular depth intervals of 10 cm. The handheld display unit gives the operator graphical displays of the data as well as storage of multiple sets of readings and can also be connected to a computer to download the data.

Weather Station

Air temperature and RH are being measured with a Vaisala HMP45CF probe, which has an operating temperature range of -55^{o}C to +55^{o}C and RH range of 0 to 100%. A radiation shield surrounds the air temperature/RH probe to minimize effects of wind and solar radiation on the reading. Net radiation (the algebraic sum of incoming and outgoing all-wave radiation) is being measured with a Kipp & Zonen NR-Lite net radiometer, which is a high-output thermopile sensor mounted approximately 2.0 m above the ground. A second net radiometer and DAS was

installed on the south slope (i.e. TP2S) since net radiation on the south slope was expected to differ from that on the north. An R.M. Young 05103 wind monitor is being used to measure wind speed and direction. Precipitation is recorded with a Texas Electronics TE525WS tipping bucket rain gauge. The resolution of the TE525 tipping bucket is 0.254 mm. In the winter months, a CSI CS705 snowfall adapter containing ethylene glycol is added to melt snowfall and subsequently measure snow water equivalent. Figure 3-8 shows the weather station installed at the site.

The weather station DAS consists of a SCI CR510 datalogger with a 10 W solar panel/rechargeable 12 V battery power source. The recorded data includes the number of tips, up to a frequency of 1-minute intervals, and the time of tipping, although this data is only recorded when a bucket tip occurs. Other data is output into daily summaries including the minimum, maximum and average of air temperature, relative humidity, and wind speed, as well as the time when each reading occurred.

Depthprobe

The Depthprobe is a density-moisture probe that operates by emitting both gamma radiation for measuring density and neutron radiation for measuring moisture content. To determine density, the Cesium-137 source emits gamma radiation into the soil, some of which will pass through the soil and be detected by the Geiger-Mueller detectors in the probe. A soil with high density will give a low count on the Geiger-Mueller detectors as the high density soil absorbs more gamma radiation. To measure moisture content, neutron radiation is emitted from the Americium-241:Beryllium source into the soil. The high-energy neutrons emitted are slowed by colliding with hydrogen atoms in the soil water. The Helium-3 detector identifies the moderated neutrons. A wet soil will give a high count in the Helium-3 detector. The Depthprobe was lowered into predrilled and cased holes; in this case the Diviner 2000® access tubes were used. The Depthprobe is designed to be used with aluminum casing and to be specifically calibrated in that casing. The Depthprobe was not calibrated to the plastic used in the Diviner 2000® access tubes, instead readings were matched with densities from field samples taken at similar locations and depths.

The first step when using the Depthprobe is to measure a standard count at the surface. This provides a reading for the background radiation in the area, ignoring soil density and moisture content. The probe is then inserted to the desired depth and a reading is taken. The output is a

raw count number for both density and water content. The numbers are recorded and the probe was lowered to the next desired depth. In this way readings were taken at seven depths at the bottom, midslope, and upslope location of each test plot.

Guelph Permeameter

The Guelph Permeameter measures saturated hydraulic conductivity. A hole is augered into the soil to the desired depth and then the walls are scarified to reduce the impact of smearing. The instrument is placed into the hole and filled with water. The air tube is then lifted to the desired height to create desired depth of water in the hole. Water height in the GP is recorded at regular time intervals until the rate of infiltration reaches steady state. Two different equations can be used to calculate the saturated hydraulic conductivity; the single height calculation or dual height calculation.

The single height equation is:

$$K_{fs} = (CQ) / (2\pi H^2 + C\pi r^2 + 2\pi(H/\alpha^*))$$

where K_{fs} (L/T) is the field-saturated hydraulic conductivity, α^* (/L) is the ratio of K_{fs} to matric flux potential, H (L) is the constant height of ponded water in the well, r (L) is the radius of the well, C is a dimensionless shape factor, and Q (L^3/T) is the steady-state flow rate from the GP.

The dual height equation is:

$$K_{fs} = 0.0041Q_2\text{-}0.0054Q_1$$

where, K_{fs} (L/T)is the field-saturated hydraulic conductivity, Q_1 (L^3/T) is the first steady-state flow rate from the GP; and Q_2 (L^3/T) is the second steady state flow rate from the *GP*.

The complete procedure for taking measurements and performing calculations with the GP can be found in the Model 2800K Guelph Permeameter manual (Soilmoisture Equipment Corp., 1991) and Meiers (2002).

APPENDIX B
CALIBRATION CURVES FOR INSTRUMENTATION

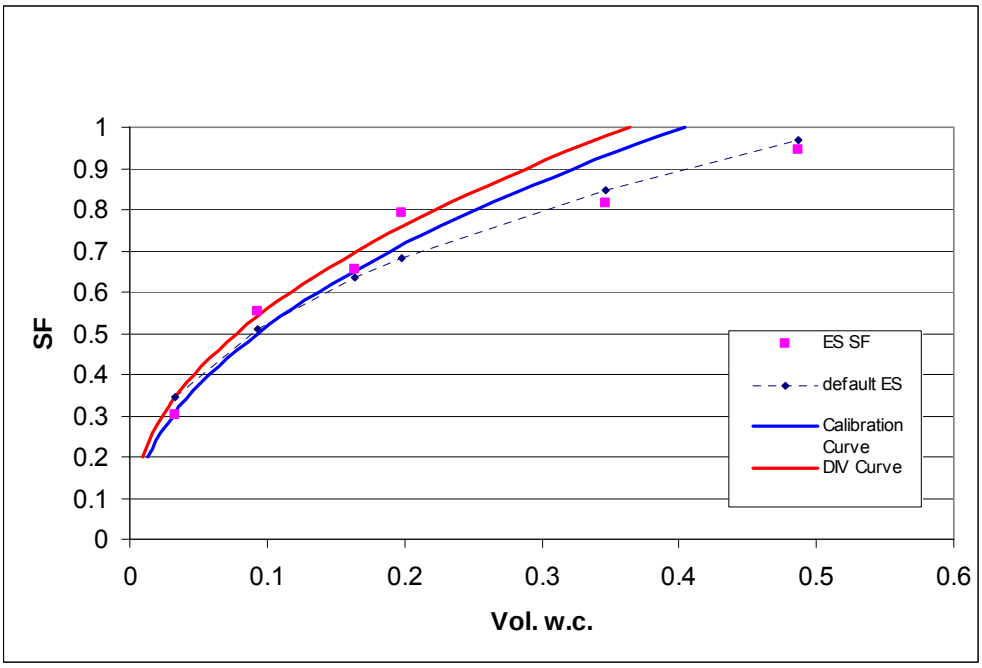

Figure B-1 EnviroSCAN calibration for till

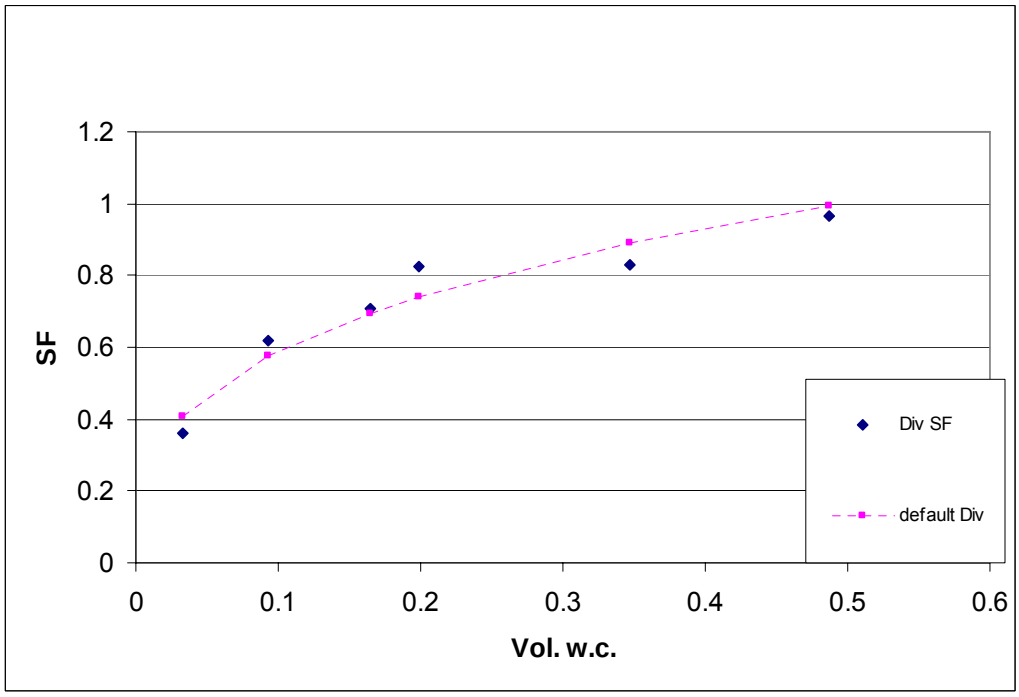

Figure B-2 Diviner Calibration for the till

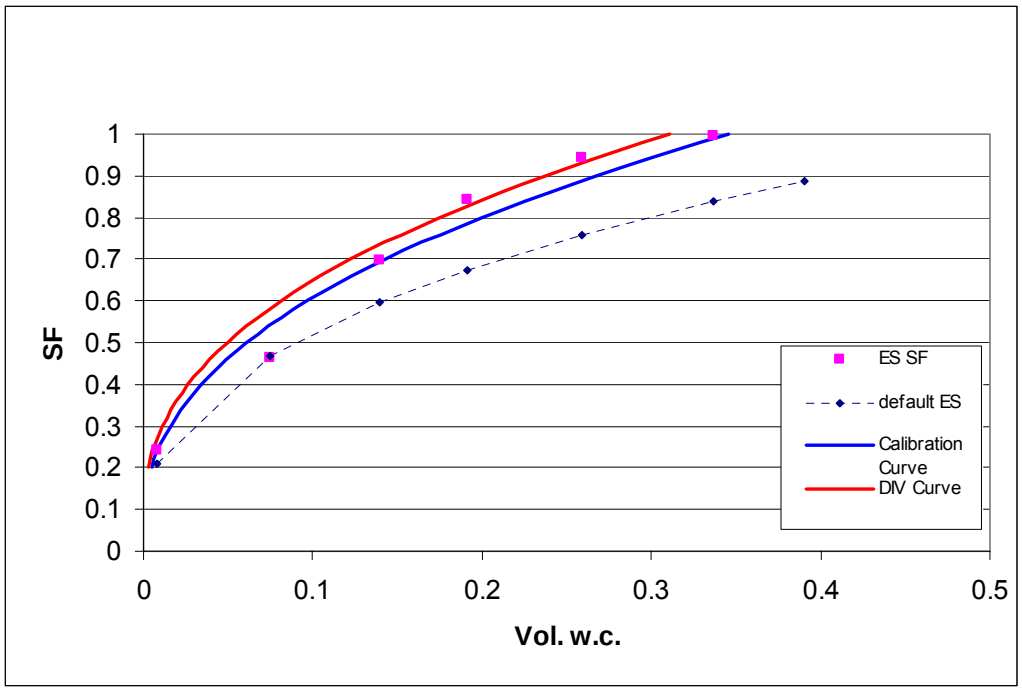

Figure B-3 EnviroSCAN calibration for the top soil

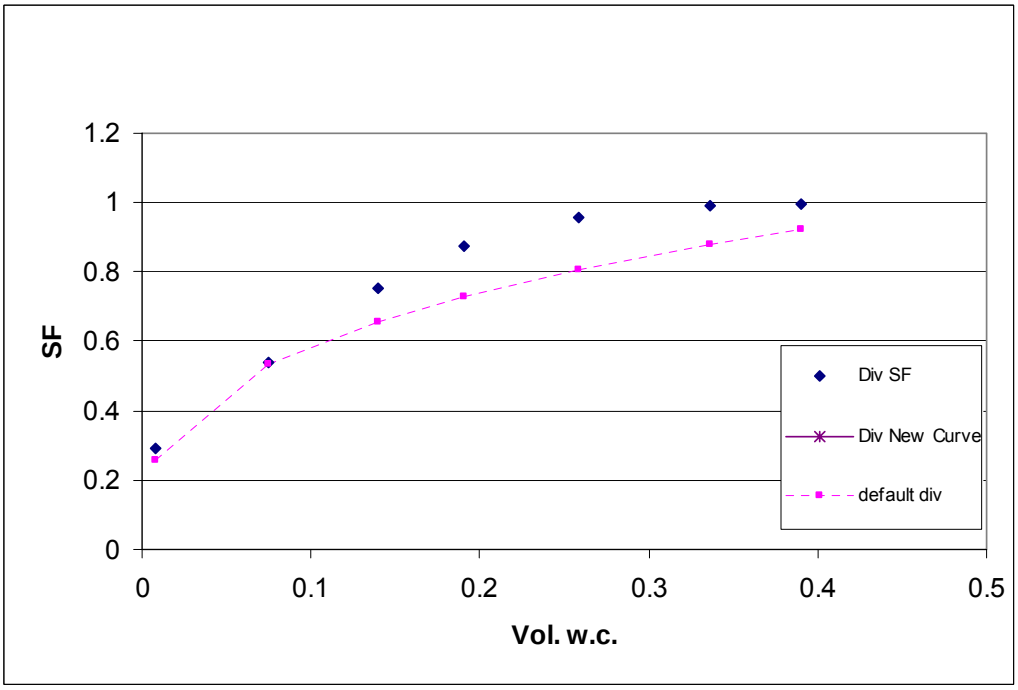

Figure B-4 Diviner Calibration for top soil

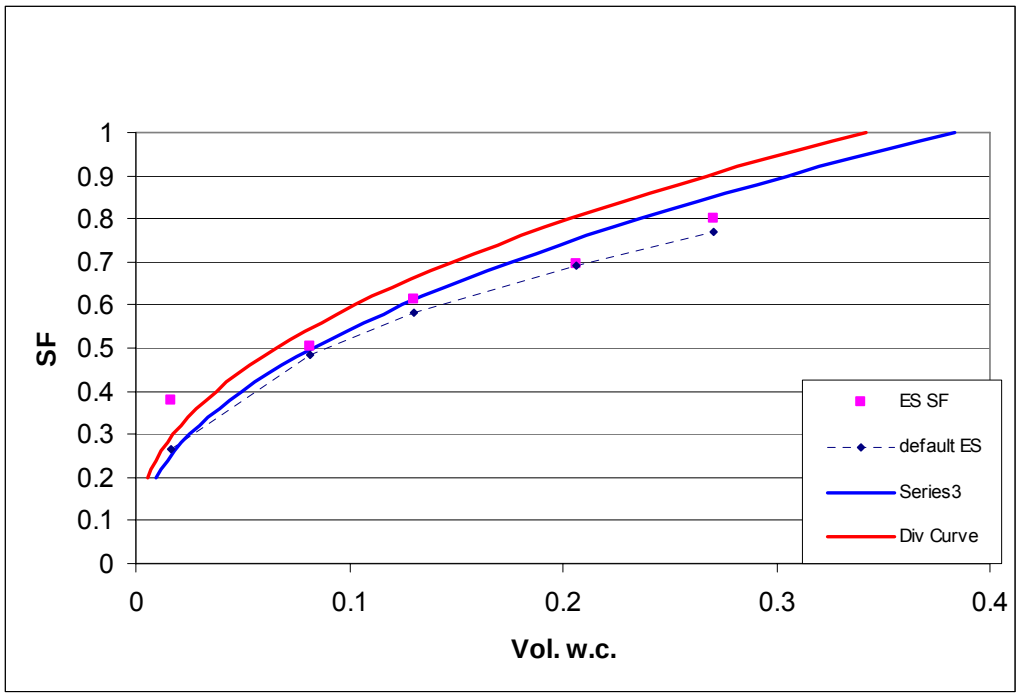

Figure B-5 EnviroSCAN Calibration for sand

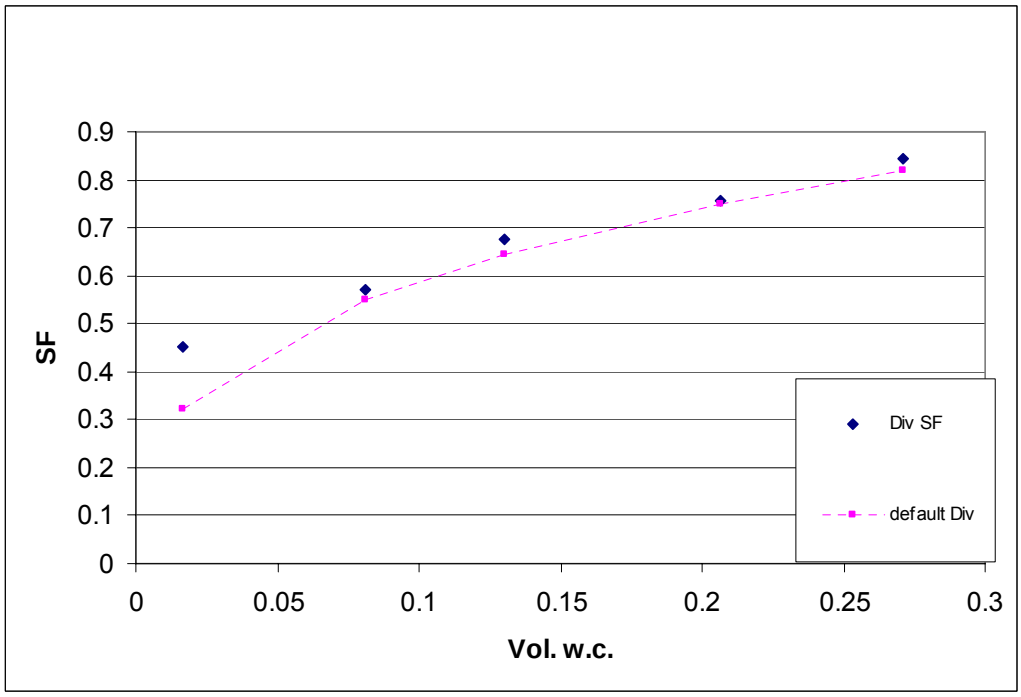

Figure B-6 Diviner Calibration for sand

APPENDIX C
WATER VOLUMES

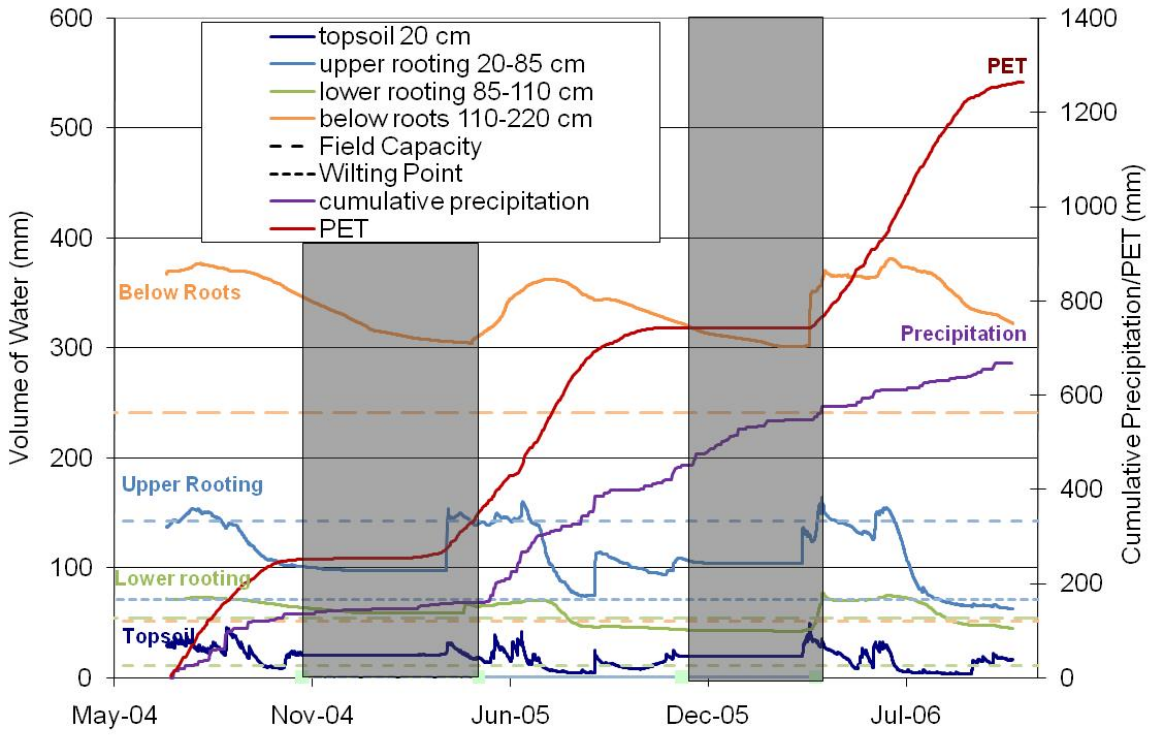

Figure C-1 TP1N midslope water volumes

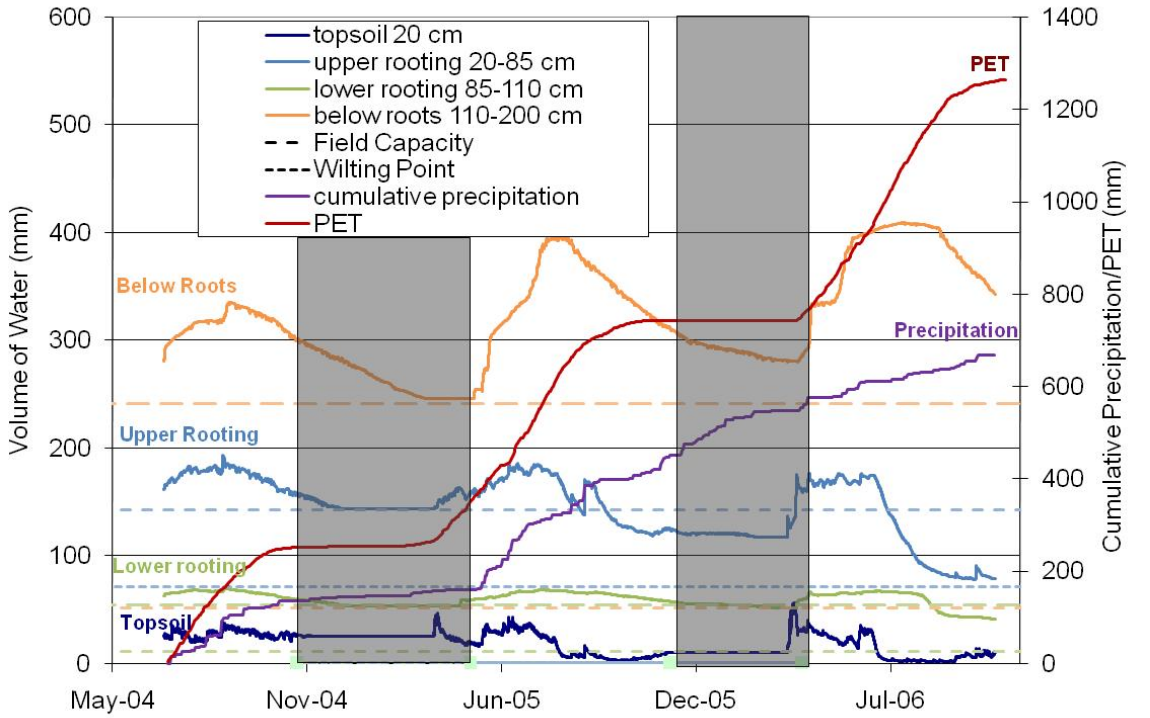

Figure C-2 TP1N lower slope water volumes

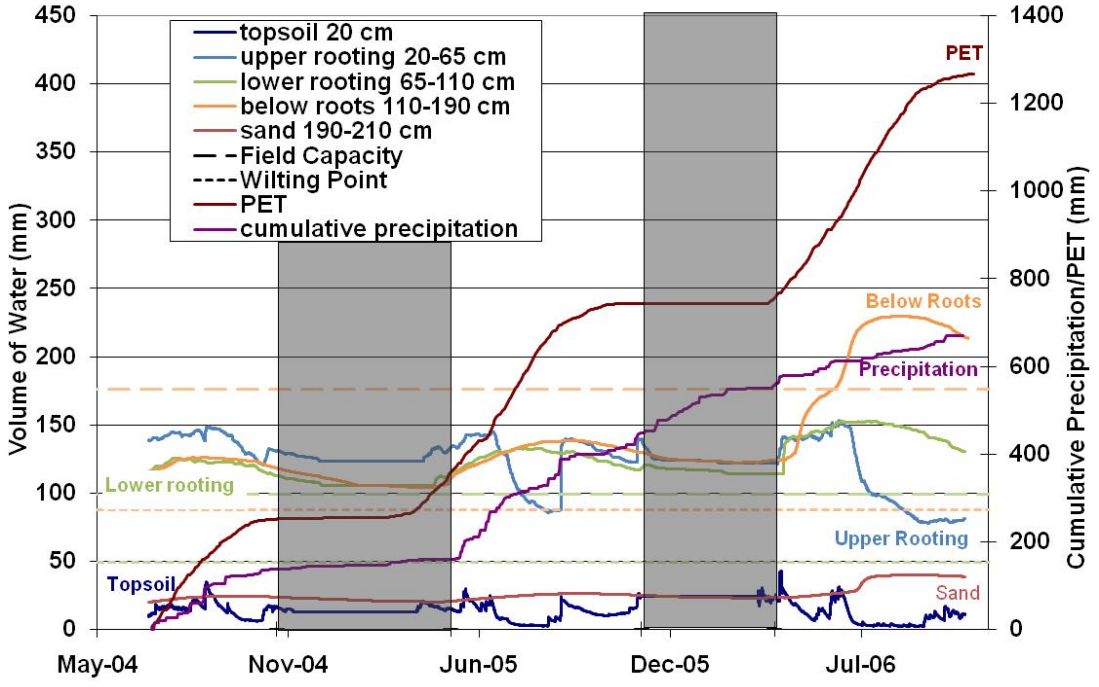

Figure C-3 TP2N upper slope water volumes

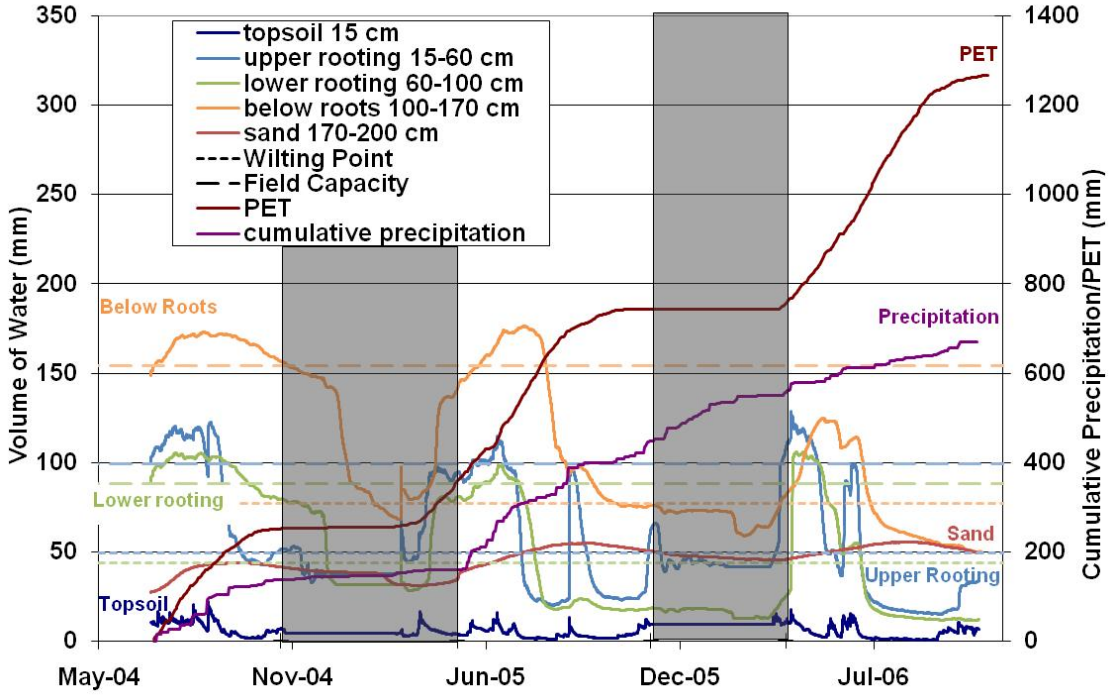

Figure C-4 TP2N lower slope water volumes

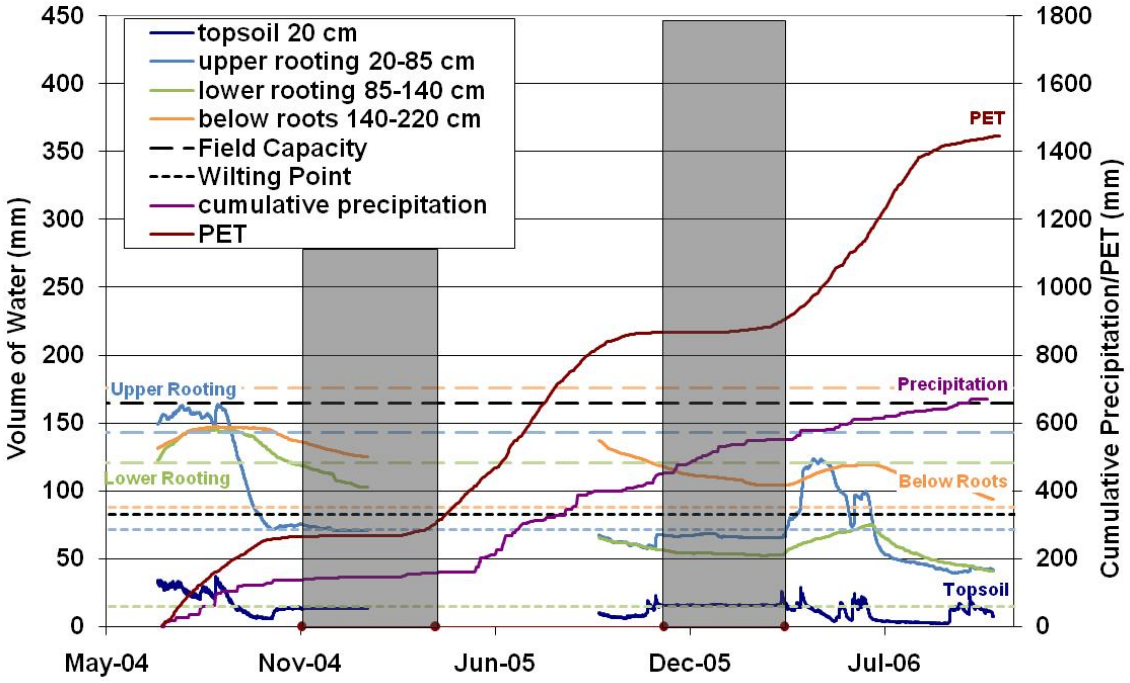

Figure C-5 TP1S mid slope water volumes

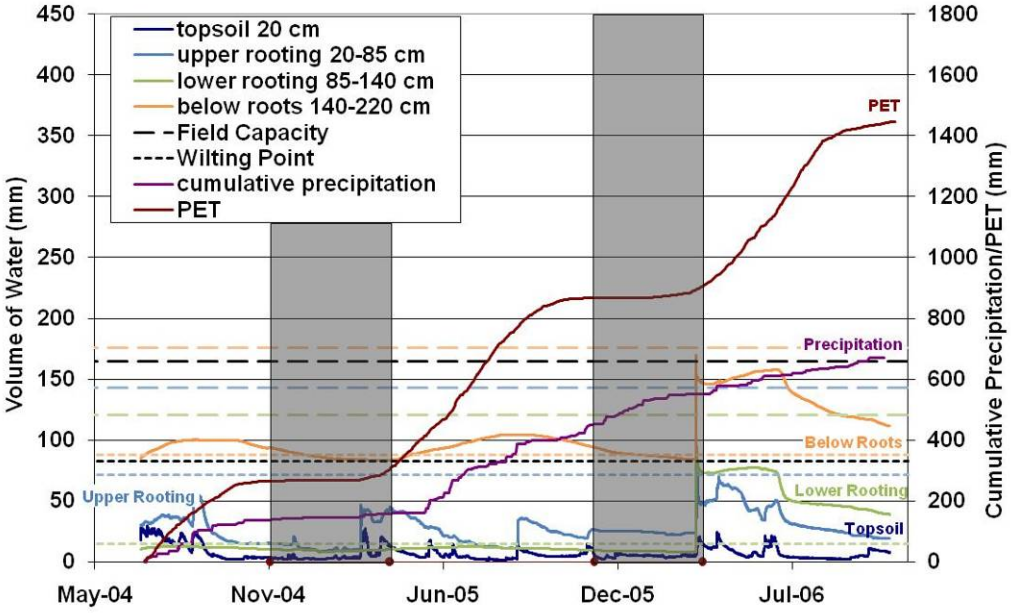

Figure C-6 TP1S lower slope water volumes

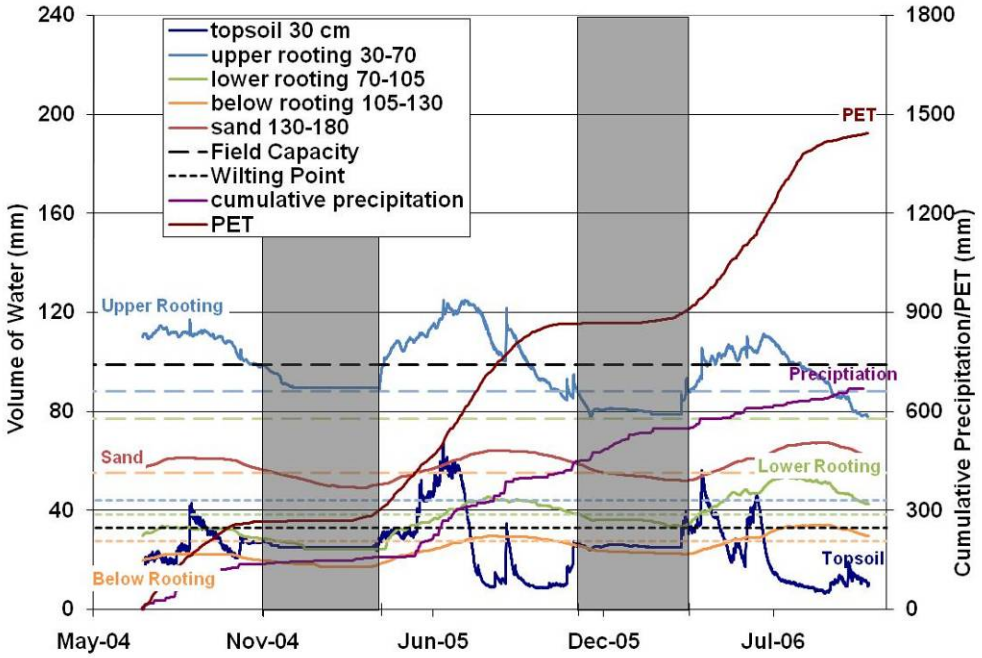

Figure C-7 TP2S upper slope water volumes

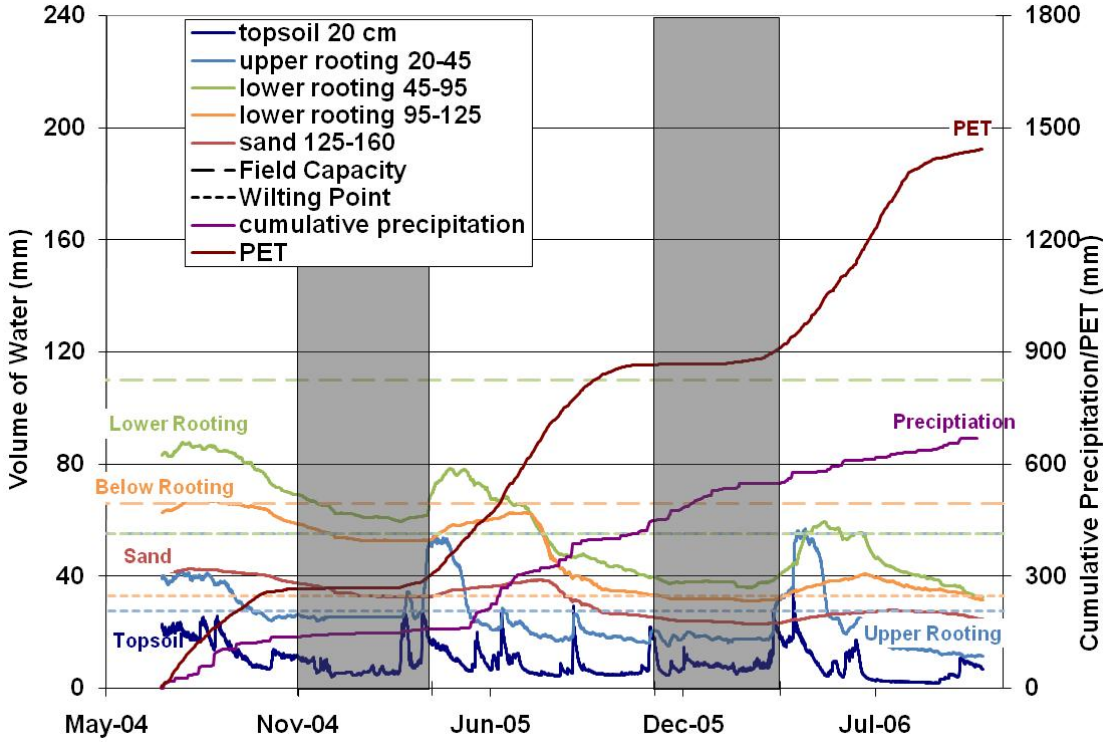

Figure C-8 TP2S mid slope water volumes